Modeling and Analysis of Population Dynamics in Advective Environments

Olga Vassilieva

Thesis submitted to the Faculty of Graduate and Postdoctoral Studies
in partial fulfillment of the requirements for the degree of Doctor of Philosophy in Mathematics [1]

Department of Mathematics and Statistics
Faculty of Science
University of Ottawa

[1]The Ph.D. program is a joint program with Carleton University, administered by the Ottawa-Carleton Institute of Mathematics and Statistics

Abstract

We study diffusion-reaction-advection models describing population dynamics of aquatic organisms subject to a constant drift, with reflecting upstream and outflow downstream boundary conditions. We consider three different models: single logistically growing species, two and three competing species.

In the case of a single population, we determine conditions for existence, uniqueness and stability of non-trivial steady-state solutions. We analyze the dependence of such solutions on advection speed, growth rate and length of the habitat. Such analysis offers a possible explanation of the "drift paradox" in our context. We also introduce a spatially implicit ODE (nonspatial approximation) model which captures the essential behavior of the original PDE model.

In the case of two competing species, we use a diffusion-advection version of the Lotka-Volterra competition model. Combining numerical and analytical techniques, in both the spatial and nonspatial approximation settings, we describe the effect of advection on competitive outcomes.

Finally, in the case of three species, we use the nonspatial approximation approach to analyze and classify the possible scenarios as we change the flow speed in the habitat.

Acknowledgements

First and foremost, I would like to thank my Ph.D. thesis advisor Dr. Frithjof Lutscher for continuous support of my Ph.D study and research, for his guidance, motivation and enthusiasm. I am also grateful to the thesis committee members, Dr. Lucy Campbell, Dr. Victor LeBlanc, Dr. Robert Smith, and Dr. Gail Wolkowicz, for their careful reading of my thesis and their helpful suggestions, and to all my fellow Mathematical Biology students at the University of Ottawa for the interesting discussions during our group meetings.

I would like to express my gratitude to my undergraduate diploma thesis advisor Dr. Vladimir Gusev and my M.S. advisor Dr. Mark Alber for introducing me to the exciting field of Mathematical Biology.

I gratefully acknowledge the financial support from the Department of Mathematics and Statistics, as well as the support provided by the funding from the Ontario Ministry of Research and Innovation in the form of an Early Researcher Award for research on "The effects of temporal and spatial variability on river ecosystems" to Dr. Lutscher.

Finally, I am grateful to my husband Yevgeniy for his support, encouragement and patience during my graduate studies.

Dedication

To my grandmother Nadezhda, my mother Natalia, my husband Yevgeniy and my daughter Valeria.

Contents

List of Figures

Chapter 1

Introduction

1.1 Biological motivation

Mathematical biology studies biological processes using techniques of applied mathematics. A model in mathematical biology is described by a system of equations (for example, Ordinary Differential Equations or Partial Differential Equations). Solving such a system (analytically or numerically) allows one to predict the behavior of the model over time, or to make inferences about biological processes.

In this work, we study several models of population dynamics in ecosystems that are characterized by unidirectional flow such as streams, rivers or canals. Such ecosystems are especially vulnerable to changes in the flow speed, which may cause an ecological imbalance, eventually breaking food chains in the entire ecosystem. For example, human activities and erosion may change the channel geometry and increase or decrease the flow speed. Examples of such changes include efforts to contain floodwaters[1], building of dams, diverting water for agricultural use etc. The main motivation for my work is to understand the possible population dynamics consequences of changes in flow speed in such habitats.

[1] see http://www.waterencyclopedia.com/Re-St/Stream-Channel-Development.html

We focus on three ecological settings: single species, two and three competitors. Our goal, in the case of a single species, is to give a mathematical explanation of the mechanisms behind the "drift paradox" [34], [50] (persistence of populations in advective habitats), in a specific reaction-diffusion-advection model. Our model involves the logistic growth term, which describes a more realistic situation than the linear growth term case considered in [47]. The non-linear approach is especially important in describing the long-term dynamics of river populations. In the case of two and three species, we are mainly interested in the effect of advection on the competitive outcome. We achieve our goals by analyzing systems of reaction-diffusion equations originating in the Lotka-Volterra competition model.

Since we are dealing with an aquatic habitat with biased water movement, we assume that in all three models there is a "source" such as a waterfall or a dam, which serves as a "reflecting" upstream boundary. We also assume the existence of a downstream boundary characterized by the absence of change of population density (e.g. river flows into a freshwater lake). The populations are assumed to grow logistically (in the absence of competitors). In competition models, growth rates of different competitors are different as well (otherwise, the affect of advection will not be seen). In addition to unidirectional advective movement, the organisms also diffuse within the habitat. In the case of competition, we assume that the species have equal diffusivity and they are subject to the same "effective advection" (average advection speed affecting the organism over its lifespan, e.g. zero advection while in refugia or on benthos, and full advection when in the drift).

1.2 Population growth models

We begin by reviewing some basic population growth models, which view the population as a quantity depending on time, without taking into consideration its spatial distribution. The simplest models deal with a single species, whose growth dynam-

ics are determined by the current size of the population. These models include the exponential growth model (suitable for bacteria populations in ideal conditions) and logistic model (which takes into account the carrying capacity). Next we consider the Lotka-Volterra model describing the competition of two species, and its generalization to the case of three species.

1.2.1 Exponential growth

Let us represent the number of individuals in the population at time t by $y(t)$. Consider the following simplest model where the rate of change of y is proportional to the current value of y. Namely

$$\frac{dy}{dt} = ry, \tag{1.2.1}$$

where r is the net per capita growth rate, the difference between the birth and the death rate. It corresponds to the growth rate in the absence of any limiting factors. If, in addition to (1.2.1), we have an initial condition $y(0) = y_0$, then model (1.2.1) possesses the solution $y(t) = y_0 e^{rt}$.

In many cases, this model gives a reasonable and accurate solution for limited periods of time. If $r > 0$, zero is an unstable equilibrium and the population exhibits unbounded growth. If $r < 0$, the equilibrium state is asymptotically stable and small perturbations lead back to it. Namely, the population goes extinct.

1.2.2 Logistic model

Due to a variety of reasons (e.g.limited food supplies or space), an increase in the population may be accompanied by a decrease in birth rate, or increase in death rate, or both. Therefore, the exponential model above is unrealistic for large times. Instead, we consider a model that has a non-constant intrinsic growth rate, depending

on population size. That is, we replace the constant r with a function $h(y)$:

$$\frac{dy}{dt} = h(y)y,$$

where $h(y)$ is the per capita growth rate. Assume that $h(y)$ satisfies the following: $h(y) \approx r > 0$, when y is small and $h'(y) < 0$ when y is sufficiently large.

For example, $h(y) = r - ay$ satisfies these properties and allows us to handle limited growth of the population in the most natural way. Therefore, the logistic growth model is presented by the following equation:

$$\frac{dy}{dt} = (r - ay)y. \tag{1.2.2}$$

This equation was first studied by Pierre F. Verhulst in 1838 (see [25]). It can be rewritten in an equivalent form

$$\frac{dy}{dt} = (r - ay)y = ry\left(1 - \frac{a}{r}y\right) = ry\left(1 - \frac{y}{K}\right), \tag{1.2.3}$$

where $\frac{r}{a} = K$ is called the environmental carrying capacity. Here $\frac{dy}{dt} > 0$ for $0 < y < K$, and $\frac{dy}{dt} < 0$ for $y > K$. Equation (1.2.3) has the explicit solution

$$y(t) = \frac{Ky_0e^{rt}}{K + y_0(e^{rt} - 1)}.$$

For a solution to be biologically relevant (non-negative), we must have $y_0 \geq 0$. If $y_0 > 0$, then $\lim_{t\to\infty} y(t) = K$, i.e. K is the limiting value of y (it is the size at which the population birth rate is equal to its death rate).

We can gain insight into the qualitative behavior of our model without using the explicit solution, by studying steady states and their stability via linearization. Equation (1.2.3) has two equilibria $y_1^* = 0$ and $y_2^* = K$ which correspond to zero growth rates of the population.

Near y_1^*, $\frac{dy}{dt} \approx ry$. Near y_2^*, we introduce a new variable $x = y - K$, which gives us

the difference between the population density and carrying capacity.
In terms of the new variable, equation (1.2.3) can be rewritten as

$$\frac{dx}{dt} = -rx - \frac{rx^2}{K}.$$

If y is close to K, x is close to zero and the linearization gives us

$$\frac{dx}{dt} = -rx.$$

For $r > 0$, the equilibrium $y_1^* = 0$ is unstable and y_2^* is asymptotically stable. Therefore, for a positive intrinsic growth rate, solutions to (1.2.3) are combinations of exponential growth close to zero and exponential decay close to the carrying capacity.

1.2.3 Lotka-Volterra model: two competitors

We will now look at the classical competition model due to Lotka [28] and Volterra [49]. In this subsection, we follow [25]. Let us consider two species with population sizes Y_1 and Y_2 that compete with each other over some resource or space in the environment. In the absence of its competitor, each population grows logistically. We assume that each species has its own intrinsic growth rate and its own carrying capacity.

As a result of competitive interaction, we expect a decrease in the per capita growth rates for the two species. We introduce the competition coefficients α_{12} and α_{21} that describe the influence of the first population on the second one and vice versa. Under these assumptions, the Lotka-Volterra competition model takes the following form:

$$\begin{cases} \frac{dY_1}{dT} = r_1 Y_1 (1 - \frac{Y_1 + \alpha_{21} Y_2}{K_1}), \\ \frac{dY_2}{dT} = r_2 Y_2 (1 - \frac{Y_2 + \alpha_{12} Y_1}{K_2}). \end{cases} \tag{1.2.4}$$

We rescale the system by setting $T = \frac{t}{r_1}$, $Y_1 = y_1K_1$, $Y_2 = y_2K_2$, $\alpha_{21} = a$, $\alpha_{12} = b$, $s = \frac{r_2}{r_1}$.

The original system becomes

$$\begin{cases} \frac{dy_1}{dt} = y_1(1 - y_1 - ay_2) = y_1 - y_1^2 - ay_1y_2, \\ \frac{dy_2}{dt} = sy_2(1 - y_2 - by_1) = sy_2 - sy_2^2 - sby_1y_2. \end{cases} \tag{1.2.5}$$

There are four steady states that correspond to (1.2.5). Namely, they are $(0, 0)$, $(1, 0)$, $(0, 1)$ and the coexistence state

$$(y_1^*, y_2^*) = \left(\frac{a-1}{ab-1}, \frac{b-1}{ab-1}\right).$$

The last equilibrium has biological meaning only if $a, b > 1$ or $0 < a, b < 1$. Note that orbits of biologically relevant solutions must be contained in $\mathbb{R}^2_+$. Let us study the linearization of system (1.2.5) that is given by the Jacobian matrix J:

$$\frac{d}{dt}\begin{pmatrix} y_1 \\ y_2 \end{pmatrix} = J\begin{pmatrix} y_1 \\ y_2 \end{pmatrix} = \begin{pmatrix} 1 - 2y_1 - ay_2 & -ay_1 \\ -bsy_2 & s(1 - 2y_2 - by_1) \end{pmatrix}\begin{pmatrix} y_1 \\ y_2 \end{pmatrix}.$$

At the zero state, we have

$$J(0, 0) = \begin{pmatrix} 1 & 0 \\ 0 & s \end{pmatrix},$$

and $\det J(0, 0) = s > 0$. Since the trace of $J(0, 0)$ is positive, the steady state $(0, 0)$ is always an unstable node.

Next, at $(1, 0)$ we see

$$J(1, 0) = \begin{pmatrix} -1 & -a \\ 0 & s(1 - b) \end{pmatrix},$$

and $\det J(1, 0) = s(b - 1) > 0$ iff $b > 1$. Also, when $b > 1$ the trace of $J(1, 0)$ is negative. Therefore, the steady state $(1, 0)$ is a stable node for $b > 1$, and a saddle

point for $b < 1$.

Now,

$$J(0,1) = \begin{pmatrix} 1-a & 0 \\ -bs & -s \end{pmatrix}.$$

Similarly, the steady state $(0,1)$ is a stable node if $a > 1$ and a saddle point if $a < 1$.

Finally,

$$J(y_1^*, y_2^*) = \begin{pmatrix} -y_1^* & -ay_1^* \\ -sby_2^* & -sy_2^* \end{pmatrix},$$

$\det J(y_1^*, y_2^*) = sy_1^* y_2^*(1-ab)$. Consequently, the coexistence steady state is unstable (saddle point) if $ab > 1$ and stable if $ab < 1$. As it is seen, the competitive outcome depends entirely on the values of the competition coefficients. Let us treat all four cases separately.

Case 1, (competitive exclusion by the second competitor, $b > 1$ and $a < 1$)

The equilibrium $(1,0)$ is stable, $(0,1)$ is unstable and the coexistence equilibrium is not biologically meaningful. The first species has a significant effect on the second, while Species 2 has only a minor effect on its competitor. Thus, y_1 excludes y_2.

Case 2, (competitive exclusion by the first competitor, $a > 1$ and $b < 1$)

The competitive outcome is reversed. The second species approaches its carrying capacity (1 in non-dimensional case) and its competitor goes extinct.

Case 3, (coexistence, $a, b < 1$)

Both species have relatively small effects on each other. Both single species steady states are unstable saddle points. On the other hand, the coexistence state becomes a stable node. When the interspecific coefficients are small then coexistence for two species is possible.

Case 4, (founder control, $a, b > 1$)

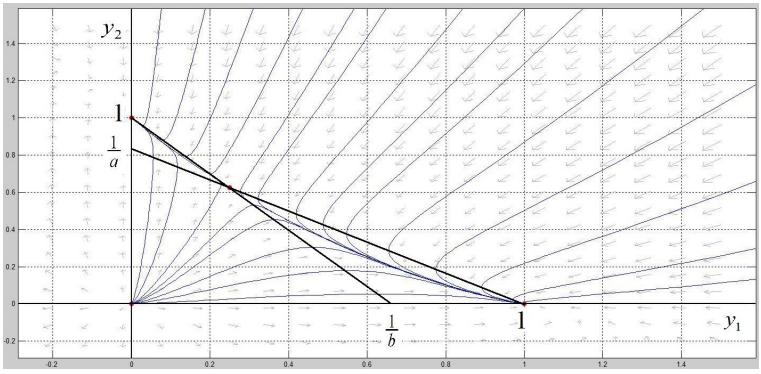

Figure 1.1: Phase plane portrait for the founder control outcome.

Using the above argument, we conclude that both single species steady states are stable and the coexistence equilibrium is positive, but unstable. System (1.2.5) has $y_1 = 0$, $y_2 = \frac{1-y_1}{a}$ as y_1-nullclines, and $y_2 = 0$, $y_2 = 1 - by_1$ as y_2-nullclines. Below the line given by the equation $y_2 = \frac{1-y_1}{a}$, y_1 increases, and above this line y_1 decreases. Also, y_2 increases below $y_2 = 1 - by_1$ and decreases above it. The situation is summarized in Figure 1.1. In this case, the interspecific effects are quite large. As a result, we observe exclusion of one or the other species. Depending on initial conditions, either the first or the second competitor will be the winner. This situation is called founder control.

Using the Bendixson-Dulac negative criterion, we show that there are no solutions with limit cycles.

Theorem (Bendixson-Dulac Criterion) *(in [25], page 125)*
Let B be a smooth function on a simply connected domain $D \subset \mathbb{R}^2$ and let

$$\left\{ \begin{array}{l} \dot{x} = F(x,y) \\ \dot{y} = G(x,y) \end{array} \right.$$

be a differentiable dynamical system on D. If the divergence

$$\nabla \cdot (BF, BG) = \frac{\partial (BF)}{\partial x} + \frac{\partial (BG)}{\partial y}$$

does not change sign in D, and is not identically zero, then the system cannot have a periodic orbit in D.

Note: There is no algorithm to find such a function B. In the case of the Lotka-Volterra competition model, the following function can be used: $B(y_1, y_2) = \frac{1}{y_1 y_2}$. Thus,

$$\frac{\partial(By_1)}{\partial y_1} + \frac{\partial(By_2)}{\partial y_2} = \frac{\partial}{\partial y_1}\left(\frac{1 - y_1 - ay_2}{y_2}\right) + \frac{\partial}{\partial y_2}\left(\frac{s(1 - y_2 - by_1)}{y_1}\right) = -\frac{1}{y_2} - \frac{s}{y_1} < 0.$$

The divergence does not change sign in the first quadrant. Therefore, there are no closed orbits within this area.

1.2.4 Lotka-Volterra model: three competitors

We consider the dynamics of three competing species, with population sizes represented by $y_1(t)$, $y_2(t)$ and $y_3(t)$. The equations of the Lotka-Volterra model read:

$$\begin{cases} \dfrac{dy_1}{dt} = y_1(r_1 - a_{11}y_1 - a_{12}y_2 - a_{13}y_3), \\ \dfrac{dy_2}{dt} = y_2(r_2 - a_{21}y_1 - a_{22}y_2 - a_{23}y_3), \\ \dfrac{dy_3}{dt} = y_3(r_3 - a_{31}y_1 - a_{32}y_2 - a_{33}y_3), \end{cases} \tag{1.2.6}$$

where $r_i > 0$ are the respective intrinsic growth rates, and $a_{ij} > 0$ are the inter- and intraspecific coefficients. Orbits of biologically meaningful solutions must be contained in $\mathbb{R}^3_+$. Note that the system has at least four fixed points: one unpopulated fixed point $(0, 0, 0)$ and three single-species fixed points $F_1 = (\frac{r_1}{a_{11}}, 0, 0)$, $F_2 = (0, \frac{r_2}{a_{22}}, 0)$, $F_3 = (0, 0, \frac{r_3}{a_{33}})$.

We will need the following definitions given in [19].

Definition 1.2.1 *The solutions of (1.2.6) are called uniformly bounded if there exists $D > 0$ such that for any solution $\bar{y}(t) = (y_1(t), y_2(t), y_3(t))$ of (1.2.6) with $y_i(0) > 0$*

for all $i \leq 3$, we have:

$$\limsup_{t\to\infty} y_i(t) \leq D.$$

Definition 1.2.2 *Matrix $A = (a_{ij})$ is called a B-matrix if for any $\bar{r} \in \mathbb{R}^3$, the solutions of (1.2.6) are uniformly bounded.*

By Theorem 15.2.4 of [19], uniform boundedness is equivalent (in our notation) to the property that for all $\bar{y} \in \mathbb{R}^3$ such that $\bar{y} \geq \bar{0}$ and $\bar{y} \neq \bar{0}$, there exists $i \leq 3$ such that $y_i > 0$ and $(A\bar{y})_i > 0$. This is obviously true if all a_{ij} are positive, as we assume. Thus, in our case, solutions are always uniformly bounded.

Definition 1.2.3 *System (1.2.6) is called persistent if for any solution $\bar{y}(t)$ of (1.2.6) such that $y_i(0) > 0$ for all $i \leq 3$, we have:*

$$\limsup_{t\to\infty} y_i(t) > 0.$$

Equivalently, for any solution with non-zero initial populations, none of the populations approaches zero as $t \to \infty$.

The persistence condition defined above still allows populations to become arbitrarily small periodically. The next definition excludes this behavior.

Definition 1.2.4 *System (1.2.6) is called permanent if its solutions are uniformly bounded and there exists $\delta > 0$, such that for any solution $\bar{y}(t)$ of (1.2.6) with $y_i(0) > 0$ for all $i \leq 3$, we have:*

$$\liminf_{t\to\infty} y_i(t) > \delta.$$

The above definition means that for any solution with non-zero initial populations, each population will eventually stay above δ (and δ does not depend on the particular solution). Thus, permanence is stronger than persistence.

In the analysis of the behavior of the three species system (1.2.6), we will need to refer to its two-species subsystems. If the third species is missing, the corresponding two-species subsystem

$$\begin{cases} \dfrac{dy_1}{dt} = y_1(r_1 - a_{11}y_1 - a_{12}y_2), \\ \dfrac{dy_2}{dt} = y_2(r_2 - a_{21}y_1 - a_{22}y_2) \end{cases} \tag{1.2.7}$$

has four possible equilibria: the unpopulated state $(0,0)$, the two monocultural (exclusion) states $(\frac{r_1}{a_{11}},0)$ and $(0,\frac{r_2}{a_{22}})$, and the coexistence state given by $A^{-1}\bar{r}$, where $A=(a_{ij})$ and $\bar{r}=(r_1,r_2)^T$. The unpopulated state $(0,0)$ is always unstable. Depending on the value of the parameters, there are four (biologically relevant) possible outcomes (compare with the previous subsection) :

- stable coexistence, if $r_1 > \frac{a_{12}r_2}{a_{22}}$ and $r_2 > \frac{a_{21}r_1}{a_{11}}$;
- competitive exclusion by first species, if $r_1 > \frac{a_{12}r_2}{a_{22}}$ and $r_2 < \frac{a_{21}r_1}{a_{11}}$;
- competitive exclusion by second species, if $r_1 < \frac{a_{12}r_2}{a_{22}}$ and $r_2 > \frac{a_{21}r_1}{a_{11}}$;
- founder control, if $r_1 < \frac{a_{12}r_2}{a_{22}}$ and $r_2 < \frac{a_{21}r_1}{a_{11}}$.

Note that, just as in the case of (1.2.6), solutions of (1.2.7) are uniformly bounded.

We say that system (1.2.6) admits a *heteroclinic cycle* if each of its two-species subsystems has a competitive exclusion outcome, and there is a cyclic arrangement of winners and losers, i.e. in the absence of species i, species $i-1$ will outcompete species $i-2$ (indices are counted modulo 3). Thus, there are orbits in the three coordinate planes in $y_1y_2y_3$-space, with the ith orbit having α-limit F_i and ω-limit F_{i+1} (indices modulo 3). In terms of the coefficients of system (1.2.6) this means

$$\frac{r_1}{r_2} < \frac{a_{12}}{a_{22}}, \frac{a_{11}}{a_{21}}; \quad \frac{r_2}{r_3} < \frac{a_{23}}{a_{33}}, \frac{a_{22}}{a_{32}}; \quad \frac{r_3}{r_1} < \frac{a_{31}}{a_{11}}, \frac{a_{33}}{a_{13}}.$$

The following criteria of persistence and permanence are proved in [19].

Theorem 1.2.5 *(in [19], page 206)*

System (1.2.6) is persistent (and uniformly bounded) iff

1. *it has an interior fixed point* $\bar{y}^*$*;*

2. $\det(A) > 0$*;*

3. *none of the two-species subsystems of (1.2.6) has the founder control outcome.*

Remark 1.2.6 Note that the system

$$\begin{cases} \dfrac{dy_1}{dt} = y_1(r_1 - a_{11}y_1 - a_{12}y_2), \\ \dfrac{dy_2}{dt} = y_2(r_2 - a_{21}y_1 - a_{22}y_2) \end{cases} \tag{1.2.8}$$

is in the founder control situation exactly when

$$\frac{a_{11}}{a_{21}} < \frac{r_1}{r_2} < \frac{a_{12}}{a_{22}}.$$

This inequality implies $a_{11}a_{22} - a_{12}a_{21} < 0$. Thus, if $\det \begin{pmatrix} a_{11} & a_{12} \\ a_{21} & a_{22} \end{pmatrix} > 0$, then founder control is not possible, no matter what the growth rates are.

Theorem 1.2.7 *(in [19], page 207) System (1.2.6) is permanent iff it satisfies conditions (1-3) above; in addition, in the case when it admits a heteroclinic cycle, the coefficients must satisfy*

$$\left(\frac{a_{31}r_1}{a_{11}r_3} - 1\right)\left(\frac{a_{12}r_2}{a_{22}r_1} - 1\right)\left(\frac{a_{23}r_3}{a_{33}r_2} - 1\right) < \left(1 - \frac{a_{21}r_1}{a_{11}r_2}\right)\left(1 - \frac{a_{32}r_2}{a_{22}r_3}\right)\left(1 - \frac{a_{13}r_3}{a_{33}r_1}\right), \tag{1.2.9}$$

or, equivalently,

$$(a_{31}r_1 - a_{11}r_3)(a_{12}r_2 - a_{22}r_1)(a_{23}r_3 - a_{33}r_2) <$$

$$(a_{11}r_2 - a_{21}r_1)(a_{22}r_3 - a_{32}r_2)(a_{33}r_1 - a_{13}r_3).$$

If system is permanent, any solution will either approach the interior fixed point (in case it is stable), or a limit cycle (in case the interior fixed point is unstable).

1.3 Individual movement models

Almost all living organisms move in space. Thus, we introduce the space variable, x, in order to derive a model for the dynamics of the spatial distribution of the population. In addition to the usual growth dynamics of a population, we consider diffusive (random) movement of individuals, and a possible advective motion (such as the drift motion in a stream). We describe two ways of deriving the diffusion-reaction or diffusion-reaction-advection equation: via a stochastic process approach (random walk), and via a conservation law. We also discuss possible boundary conditions for such an equation, including Dirichlet (hostile) and Danckwerts' (outflow). Our main reference is [26].

1.3.1 Random walk

This approach originates from stochastic processes and ignores birth and death dynamics. We think about the location of an individual as a random variable, and associate with it a probability density function (PDF). This function changes with time as the individual performs random movements. We deduce the equation for the PDF known as the Fokker-Planck equation.

Let us consider the probability density function for the location of an individual, who takes steps from x to the right, to the left or stays at the same place with probabilities $R(x)$, $L(x)$, $N(x)$ respectively. The length of the step (δ) and the time between steps (τ) are fixed. Then the probability density satisfies the following master equation

$$u(t+\tau, x) = R(x-\delta)u(t, x-\delta) + L(x+\delta)u(t, x+\delta) + N(x)u(t, x). \tag{1.3.1}$$

We are interested in a continuous time, continuous space process, i.e. in the limit as $\tau, \delta \to 0$. One of the ways for calculating the probability density function $u(t, x)$ is showing that it satisfies the Fokker-Planck equation, which can be deduced from

(1.3.1). It turns out that, in the case of the simple movement model, the solution of the Fokker-Planck equation can be easily found.

We expand the right and the left sides of (1.3.1) using Taylor series expansion, assuming

$$R + L = \mu(x), \quad L - R = \beta(x)\delta, \tag{1.3.2}$$

where the function μ is called the motility and the function β is called bias (see [1]). Thus,

$$u(t,x) + \tau\frac{\partial u}{\partial t}(t,x) + \frac{\tau^2}{2}\frac{\partial^2 u}{\partial t^2}(t,x) + \text{h.o.t.} = N(x)u(t,x)$$
$$+ \left(R(x) - \delta\frac{\partial R}{\partial x}(x) + \frac{\delta^2}{2}\frac{\partial^2 R}{\partial x^2}(x) + \text{h.o.t}\right)\left(u(t,x) - \delta\frac{\partial u}{\partial x}(t,x) + \frac{\delta^2}{2}\frac{\partial^2 u}{\partial x^2}(t,x) + \text{h.o.t.}\right)$$
$$+ \left(L(x) + \delta\frac{\partial L}{\partial x}(x) + \frac{\delta^2}{2}\frac{\partial^2 L}{\partial x^2}(t,x) + \text{h.o.t.}\right)\left(u(t,x) + \delta\frac{\partial u}{\partial x}(t,x) + \frac{\delta^2}{2}\frac{\partial^2 u}{\partial x^2} + \text{h.o.t}\right),$$

where h.o.t. stands for higher order terms in the Taylor expansion. Using (1.3.2) and taking the limit as $\tau, \delta \to 0$, in such a way that $\frac{\delta^2}{2\tau} \to D$, the above equation can be reduced to the Fokker-Planck equation

$$u_t = D(\mu u)_{xx} - (\beta u)_x. \tag{1.3.3}$$

Particularly, taking $R = 0.5 + \gamma\delta$ and $L = 0.5 - \gamma\delta$ yields an advection-diffusion equation

$$u_t + vu_x = Du_{xx}, \tag{1.3.4}$$

where $\frac{\gamma\delta^2}{2\tau} \to v$, as $\delta, \tau \to 0$. For $\gamma = 0$, (1.3.3) can be simplified to a diffusion equation

$$u_t = Du_{xx}, \tag{1.3.5}$$

where $\frac{\delta^2}{2\tau} \to D$, as $\delta, \tau \to 0$. The fundamental solution of (1.3.5) is the solution of the Fokker-Planck equation for an individual which starts moving at $x = 0$, $t = 0$. This fundamental solution is in fact the solution of the initial value problem $u(x,0) = \delta_0(x)$ (where δ_0 is the δ-distribution). It is given by the Gaussian distribution

$$G(t,x) = \frac{1}{\sqrt{4\pi Dt}}e^{-\frac{x^2}{4Dt}}.$$

For the diffusion equation with a general initial condition $u(x,0) = f(x)$, the solution has the following form (see [8]):

$$u(t,x) = (f * G(\cdot,t))(x) = \int_{-\infty}^{\infty} f(y)G(x-y,t)dy = \frac{1}{\sqrt{4\pi Dt}} \int_{-\infty}^{\infty} f(y)e^{-\frac{(x-y)^2}{4Dt}}dy.$$

In case of the advection-diffusion equation (1.3.4), we use the change of variables

$$U(t,x) = u(t, x+vt).$$

Then we have

$$U_t = u_t + vu_x, \quad U_x = u_x, \quad U_{xx} = u_{xx},$$

and (1.3.4) reduces to (1.3.5). Therefore the fundamental solution to (1.3.4) (or the solution of the Fokker-Planck equation with advection v) has the following form:

$$u(t,x) = \frac{1}{\sqrt{4\pi Dt}} e^{-\frac{(x-vt)^2}{4Dt}}. \tag{1.3.6}$$

Note that equation (1.3.3) only takes into account the diffusive and advective movement of the organisms. To make our model biologically interesting, we add growth of individuals in the form of the reaction term. For example, in the case of logistic growth, we get the following reaction-diffusion-advection equation:

$$u_t = Du_{xx} - vu_x + ru\left(1 - \frac{u}{K}\right). \tag{1.3.7}$$

1.3.2 Fickian flux

This approach originates from mathematical physics. We use a conservation law to obtain the model equation. The flux of individuals ($\vec{J}(t,x)$) corresponds to drift and random movement (we will drop the vector notation in the 1-dimensional case and just write $J(t,x)$).

Let us consider the total number of individuals in the interval $(x, x+\Delta x)$ at time t. Consider the rate of change of the number of individuals in the given interval, which is

$\frac{\partial}{\partial t}(u(t,x)\Delta x)$ = growth in $(x, x+\Delta x)$+ rate of entry at x − rate of departure at $x+\Delta x$,

or

$$\frac{\partial u}{\partial t}\Delta x = f(t,x,u)\Delta x + J(t,x) - J(t,x+\Delta x),$$

where $f(t,x,u)$ is the function describing the growth rate of the population per unit length. Note that the rate of entry may be negative if more individuals leave through the left endpoint of $(x, x+\Delta x)$ than enter. Similarly, the rate of departure through $x+\Delta x$ may also be negative. Dividing by Δx we get

$$\frac{\partial u}{\partial t} = f(t,x,u) - \frac{J(t,x+\Delta x) - J(t,x)}{\Delta x}.$$

Taking the limit as Δx approaches zero gives the conservation law in one dimension

$$\frac{\partial u}{\partial t} = f(t,x,u) - \frac{\partial J}{\partial x}.$$

The equation above can be generalized to higher spatial dimensions. Let $u(t,x)$ be the density of individuals, $x \in \mathbb{R}^n$ and $\Omega \subset \mathbb{R}^n$ be the domain with smooth boundary Γ. If the individuals move inside the given domain and do not cross its boundary, then their total amount does not change.

The size of the population in Ω changes if we have growth of the population and/or a non-zero flux $\vec{J}$ of individuals through the boundary. The population flux $\vec{J}(t,x) \in \mathbb{R}^n$ is a vector that points in the direction of the movement of the individuals and whose norm $|\vec{J}(t,x)|$ is proportional to the amount of the particles that move in that direction per time unit:

$$\frac{d}{dt}\int_\Omega u(t,x)dx = -\int_\Gamma \vec{J}(t,x)d\vec{S} + \int_\Omega f(t,x,u)dx, \tag{1.3.8}$$

where $d\vec{S}$ is the vector element of the boundary Γ. When the angle between the normal vector to the boundary and $\vec{J}$ is obtuse - and thus the scalar product of the flux $\vec{J}$ and $d\vec{S}$ is negative - then the change of the density $u(t,x)$ is positive, and

thus individuals move into the domain Ω. When the angle is acute, individuals move out of the domain Ω, since the scalar product of $\vec{J}$ and $d\vec{S}$ is positive. Using the divergence theorem, we get

$$\int_{\Gamma} \vec{J}(t,x)d\vec{S} = \int_{\Omega} \mathrm{div}\vec{J}(t,x)dx. \tag{1.3.9}$$

Putting (1.3.8) and (1.3.9) together gives us

$$\int_{\Omega} [u_t(t,x) + \mathrm{div}\vec{J}(t,x) - f(t,x,u)]dx = 0. \tag{1.3.10}$$

Since equation (1.3.10) holds for every domain Ω, it follows that

$$u_t + \mathrm{div}\vec{J}(t,x) - f = 0. \tag{1.3.11}$$

Next, we use Fick's law to express the flux in terms of the population density. According to the law, the flux is proportional to the negative gradient of the density of the individuals, i.e.

$$\vec{J} = -D\nabla u. \tag{1.3.12}$$

We can interpret this as follows. The gradient of the density points in the direction that turns out to be the "most populated" place in the neighborhood. Therefore the individuals spread out (we observe the population flux) from that location.

If we only have transportation of individuals with advection $\vec{v}$ then the flux is given by

$$\vec{J} = \vec{v}u. \tag{1.3.13}$$

If we combine (1.3.12) and (1.3.13), then we get:

$$\frac{\partial u}{\partial t} + \mathrm{div}(-D\nabla u) + \mathrm{div}(\vec{v}u) - f = 0,$$

or

$$u_t + \nabla(\vec{v}u) = D\Delta u + f. \tag{1.3.14}$$

The equation above is a reaction-diffusion-advection equation. If $f = 0$ and $v = 0$, we simply obtain the diffusion equation.

To summarize, we have used two different approaches in deriving our model. One approach used stochastic arguments based on the Brownian motion model for the probability density function. Another approach was based on a conservation law: we used the notion of flux and the divergence theorem to obtain the reaction-diffusion equation. The master equation for the probability density function lead to Fokker-Planck equation, which reduced to the same reaction-diffusion equation.

Boundary conditions

Ideally, we want any reaction-diffusion-advection problem to be well-posed, i.e.
(a) a solution should exist,
(b) the solution should be unique,
(c) the solution should be stable (should depend continuously on initial and boundary data).

Prescribing the following conditions (see [25]) will lead to well-posed problems for the 1-dimensional diffusion and diffusion-advection equations (1.3.4) or (1.3.5)

(1) Cauchy Problem (Initial Value Problem): $u(0,x) = u_0(x)$, $x \in \mathbb{R}$, i.e. we only need an initial population density; some additional boundedness conditions at infinity may also be imposed;

(2) Initial Boundary Value Problem: unlike the previous case, the spatial domain is now bounded. We specify an initial condition only on a patch (an interval in the 1-dimensional case): $u(0,x) = u_0(x), x \in [0,L]$. We then specify the behavior of individuals on the boundary. The typical boundary conditions that can be prescribed for the diffusion equation are as follows.

Dirichlet conditions are given by:

$$u(t,0) = b_1(t),$$

$$u(t,L) = b_2(t).$$

If $b_1 = b_2 = 0$, then the individuals who reach the left border ($x = 0$) and the right border ($x = L$) never come back (the area outside the patch $[0, L]$ is uninhabitable). These boundary conditions are often called hostile;

Neumann conditions (or flux conditions in case of (1.3.5)) are given by:

$$u_x(t,0) = b_1(t),$$

$$u_x(t,L) = b_2(t).$$

Earlier we noticed that the flux was proportional to the negative gradient of density (1.3.12). In particular, if $b_1 = b_2 = 0$, we have no flux of individuals through the boundaries: either individuals move only inside their bounded habitat or they can cross the boundaries and come back. However, in the latter case, fluxes into domain and out of domain cancel each other. These are also called reflecting boundary conditions (for non-advective environment);

Robin conditions are given by:

$$-Du_x(t,0) + \alpha u(t,0) = \alpha b_1(t),$$

$$-Du_x(t,L) - \alpha u(t,L) = -\alpha b_2(t).$$

The flux at the boundary is proportional to the difference between the density at the boundary and a fixed function. For example, in the presence of advection (of the given velocity v), the no-flux (outflow) condition for (1.3.4) at 0 would take form $Du_x(t,0) - vu(t,0) = 0$ (this condition is also known as Danckwerts' condition, see

Chapter 2).

Periodic conditions are given by:

$$u(t,0) = u(t,L),$$

$$u_x(t,0) = u_x(t,L).$$

These conditions are adequate for models describing populations in periodically varying habitats.

1.4 Mathematical concepts and tools

In this section, we review several diffusion and reaction-diffusion linear and nonlinear models to study the question of persistence on bounded domains with certain boundary conditions. Since a population can persist if it grows at low density, we use the linearization of the nonlinear model at the zero steady state to study persistence. We analyze the associated eigenvalue problem to derive the persistence condition that also depends on boundary conditions. The persistence condition gives rise to one of the fundamental notions of spatial ecology: the critical domain size L_c, i.e. the minimal size of habitat which ensures survival of the population. On the other hand, a population always survives in diffusion or reaction-diffusion models with no-flux boundary conditions, regardless of the habitat length. We finish section 1.4 with a review of another important concept of spatial ecology: population spread. We study population spread in the form of a travelling wave solution, which moves as a fixed profile with constant speed. In the case of logistic growth, the travelling wave connects the two steady state solutions (the zero state and the carrying capacity state). We derive the minimal travelling wave speed $c_{\min}$. In the case of logistic

growth, we deduce that the precise value of $c_{\min}$ is $2\sqrt{Dr}$, where D is the diffusion coefficient and r is the intrinsic growth rate.

Note that existence and uniqueness of solutions for the type of problems considered in this thesis is well established (see [33], [46]) and will not be our main focus.

1.4.1 Critical domain size: eigenvalue problems on bounded domains

Let us consider the diffusion equation with initial condition (we will refer to it as Model 1) on a bounded domain (we follow [25]).

$$\begin{cases} \frac{\partial y}{\partial t} = D\frac{\partial^2 y}{\partial x^2}, & 0 \le x \le L \\ y(0,x) = y_0(x). \end{cases} \tag{1.4.1}$$

This model may describe behavior of a population that inhabits a one-dimensional domain of the fixed length L. The individuals simply spread (diffuse) inside the habitat, but do not grow. In addition to (1.4.1), we have homogeneous Dirichlet boundary conditions: $y(t,0) = y(t,L) = 0$ for all $t \ge 0$.

Thus, we assume that the region outside the domain is hostile: as soon as individuals reach the borders, they are lost from the domain. Intuitively, it is clear that, in the long term, all individuals will reach the boundary and the whole population will go extinct.

In order to solve the problem mathematically, we will use the method of separation of variables. We convert the PDE into an ODE by representing the solution as a product of spatial and temporal terms

$$y(x,t) = S(x)T(t). \tag{1.4.2}$$

Substituting (1.4.2) back into (1.4.1) gives us

$$\frac{dT}{dt}S = DT\frac{d^2S}{dx^2},$$

or

$$\frac{1}{DT}\frac{dT}{dt} = \frac{1}{S}\frac{d^2S}{dx^2}. \tag{1.4.3}$$

Since the right hand side of (1.4.3) depends only on x and the left hand side only on t, both sides are equal to some constant value $-\lambda$. Now we are able to solve the two equations separately:

$$\frac{dT}{dt} = -\lambda DT, \tag{1.4.4}$$

$$\frac{d^2S}{dx^2} + \lambda S(x) = 0. \tag{1.4.5}$$

If $\lambda < 0$, then $S(x) = ae^{\sqrt{-\lambda}x} + be^{-\sqrt{-\lambda}x}$. We also have $S(0) = S(L) = 0$. The only solution that satisfies the above boundary problem is the trivial one. The same is true if $\lambda = 0$. Therefore $\lambda > 0$, and a potential solution takes the form

$$y(x,t) = e^{-\lambda Dt}(a\sin\sqrt{\lambda}x + b\cos\sqrt{\lambda}x). \tag{1.4.6}$$

It is easy to show that (1.4.6) will satisfy both boundary conditions if $b = 0$ and $a\sin\sqrt{\lambda}L = 0$. Since we are seeking a nontrivial solution, we require $a \neq 0$ and $\sin\sqrt{\lambda}L = 0$, or $\lambda_k = (\frac{k\pi}{L})^2$, $k \in \mathbb{Z}$. Thus, we have solutions of the form

$$y_k(x,t) = e^{-D(\frac{k\pi}{L})^2 t}\sin\left(\frac{k\pi x}{L}\right). \tag{1.4.7}$$

The linear combination of solutions (1.4.7) gives us the general solution

$$y(x,t) = \sum_{k=1}^{\infty} a_k e^{-D(\frac{k\pi}{L})^2 t}\sin\left(\frac{k\pi x}{L}\right). \tag{1.4.8}$$

In order to find the coefficients a_k, we use the initial condition. Namely,

$$y(x,0) = y_0(x) = \sum_{k=1}^{\infty} a_k \sin\left(\frac{\pi k x}{L}\right),$$

i.e. our initial function is written as a Fourier sine series. Using orthogonality of the basis of the sine functions above, we get the coefficient a_k:

$$a_k = \frac{2}{L}\int_0^L y_0(x)\sin\left(\frac{k\pi x}{L}\right)dx.$$

Note that $\lim_{t\to\infty} y(x,t) = 0$, which confirms our hypothesis regarding extinction of the population.

Note that if we change the boundary condition in the above model to no-flux boundary conditions, namely

$$y_x(0,t) = y_x(L,t) = 0,$$

then there will be a spatially constant steady state solution, and the population will persist on any domain.

Now consider a slightly different model: we let our population grow exponentially (call this Model 2).

$$\begin{cases} \frac{\partial y}{\partial t} = ry + D\frac{\partial^2 y}{\partial x^2}, \quad 0 \le x \le L, \\ y(0,t) = 0, \\ y(L,t) = 0, \\ y(0,x) = y_0(x). \end{cases} \tag{1.4.9}$$

The transformation $w(x,t) = e^{-rt}y(x,t)$, gives us Model 1 ($w_t = Dw_{xx}$), for which we already know the solution:

$$w(x,t) = \sum_{k=1}^{\infty} a_k e^{-D(\frac{k\pi}{L})^2 t}\sin\left(\frac{k\pi x}{L}\right).$$

Thus,

$$y(x,t) = \sum_{k=1}^{\infty} a_k e^{\left(r-D(\frac{k\pi}{L})^2\right)t}\sin\left(\frac{k\pi x}{L}\right). \tag{1.4.10}$$

Let $\lambda_k = r - D(\frac{k\pi}{L})^2$, $k \in \mathbb{Z}$. The eigenvalues λ_k form an infinite decreasing sequence: $\lambda_1 > \lambda_2 > \ldots$ The population will grow if $\lambda_k > 0$ for some k. Therefore,

if we let the dominant eigenvalue λ_1 be greater than zero, then the population will survive. Thus, $\lambda_1 = r - \frac{D\pi^2}{L^2} > 0$ or

$$L > \pi\sqrt{\frac{D}{r}} = L_c \tag{1.4.11}$$

ensures that the population will not go extinct. We call L_c the critical domain size. If the population inhabits a smaller patch, it will collapse, otherwise it will grow.

Note that if we again change the boundary condition in the above model to no-flux conditions, then the population will persist and grow unboundedly on any domain.

Let us consider the model, in which the population grows logistically (Model 3):

$$\begin{cases} \frac{\partial y}{\partial t} = D\frac{\partial^2 y}{\partial x^2} + ry(1 - \frac{y}{K}), \quad 0 \leq x \leq L \\ y(0,t) = 0 \\ y(L,t) = 0 \\ y(x,0) = y_0(x). \end{cases} \tag{1.4.12}$$

System (1.4.12) has two steady states (in time) $y_1 = 0$ and $y_2 = K$. The second equilibrium does not satisfy the boundary conditions. The linearization around the first steady state gives us Model 2 with the critical domain size $L_c = \pi\sqrt{\frac{D}{r}}$.

Suppose the critical domain size is exceeded and the population grows. How far will it grow? After we rescale the density $u(x,t) = \frac{y(x,t)}{K}$, (1.4.12) takes the form

$$\begin{cases} \frac{\partial u}{\partial t} = ru(1-u) + D\frac{\partial^2 u}{\partial x^2}, \quad 0 \leq x \leq L \\ u(0,t) = 0 \\ u(L,t) = 0 \\ u(x,0) = u_0(x). \end{cases} \tag{1.4.13}$$

The equilibria can be found from

$$ru(1-u) + Du'' = 0, \tag{1.4.14}$$

$$u(0) = u(L) = 0. \tag{1.4.15}$$

We use phase-plane methods and a first integral (or invariant of motion) to find a solution (or to analyze this equation). The trivial solution satisfies both (1.4.14) and the homogeneous boundary condition (1.4.15). We seek a positive solution of (1.4.14) that satisfies (1.4.15). Multiplying equation (1.4.14) by u' and integrating with respect to x gives

$$\frac{Du'^2}{2} + r\left(\frac{1}{2}u^2 - \frac{1}{3}u^3\right) = C.$$

Setting $u' = v$, we rewrite the above equation as

$$\frac{v^2}{2} + \frac{r}{D}F(u) = C, \tag{1.4.16}$$

where $F(u) = \frac{u^2}{2} - \frac{u^3}{3}$.

The level curves of (1.4.16) satisfy (1.4.14). We want to find non-trivial orbits that also satisfy the boundary conditions (1.4.15). Assume that such a solution exists. Rewriting (1.4.16) gives us

$$\frac{1}{2}v^2 + \frac{r}{D}F(u) = \frac{r}{D}F(\mu),$$

where μ is the maximum value of u (when $v = \frac{du}{dx} = 0$). Due to symmetry, the maximum is attained at $x = \frac{L}{2}$. Therefore

$$v = \frac{du}{dx} = \begin{cases} \sqrt{\frac{2r}{D}(F(\mu) - F(u))}, & 0 < x < \frac{L}{2}, \\ -\sqrt{\frac{2r}{D}(F(\mu) - F(u))}, & \frac{L}{2} < x < L. \end{cases}$$

Integrating over the first half of the orbit we get

$$\sqrt{\frac{D}{2r}}\int_0^\mu \frac{du}{\sqrt{F(\mu) - F(u)}} = \int_0^{\frac{L}{2}} dx = \frac{L}{2},$$

and

$$L = \sqrt{\frac{2D}{r}}\int_0^\mu \frac{du}{\sqrt{F(\mu) - F(u)}}. \tag{1.4.17}$$

Note that integration over the second half of the orbit gives us the same result as (1.4.17).

After substituting $z = \frac{u}{\mu}$, we have

$$L = \sqrt{\frac{2D}{r}} \int_0^1 \frac{\mu dz}{\sqrt{(F(\mu) - F(\mu z))}}. \tag{1.4.18}$$

The following is observed in [25] regarding formula (1.4.18):

- L is an increasing function of μ, $0 \leq \mu < 1$.
- L is concave up for $0 < \mu < 1$.
- $\lim L(\mu) = \infty$ as $\mu \to 1$.
- $\lim L(\mu) = L_c = \pi\sqrt{\frac{D}{r}}$ as $\mu \to 0$. Indeed,

$$\begin{aligned} L_c &= \lim_{\mu \to 0} \sqrt{\frac{2D}{r}} \int_0^1 \frac{\mu dz}{\sqrt{(F(\mu) - F(\mu z)}} \\ &= \lim_{\mu \to 0} \sqrt{\frac{2D}{r}} \int_0^1 \frac{\mu dz}{\sqrt{\frac{1}{2}\mu^2(1-z)(1+z+\frac{2}{3}\mu(1+z+z^2))}}, \\ L_c &= 2\sqrt{\frac{D}{r}} \int_0^1 \frac{dz}{\sqrt{1-z^2}} = 2\sqrt{\frac{D}{r}} \arcsin z|_0^1 = \pi\sqrt{\frac{D}{r}}. \end{aligned}$$

Thus, we have found a unique steady state solution for equation (1.4.13) with homogeneous Dirichlet boundary conditions, where the domain size exceeds the critical domain size. The obtained solution coincides with the zero solution when the domain is smaller than the critical one.

For $L < L_c$, the trivial solution of (1.4.13) is stable, since we have shown that the trivial solution of the linearization of (1.4.13) (Model 2) is stable for $L < L_c$.

Note that with no-flux boundary conditions, (1.4.13) has a constant steady state solution given by the carrying capacity, and thus the population will persist regardless of the domain size.

Our next goal is to analyze stability of the nontrivial solution $u(x)$ for the PDE (1.4.13). Let $u(t,x) = u(x) + \phi(t,x)$, where $|\phi(t,x)| << 1$. Consider the linearization of (1.4.13) about $u(x)$:

$$\frac{\partial}{\partial t}[u(x) + \phi(t,x)] = r(u(x) + \phi(t,x))(1 - u(x) - \phi(t,x)) + D\left(\frac{\partial^2 u(x)}{\partial x^2} + \frac{\partial^2 \phi(t,x)}{\partial x^2}\right),$$

$$\frac{\partial \phi}{\partial t}(x,t) = r\left[u(x) - (u(x))^2 - 2u(x)\phi(t,x) + \phi(t,x) - (\phi(t,x))^2\right] + D\frac{\partial^2 u(x)}{\partial x^2} + D\frac{\partial^2 \phi(t,x)}{\partial x^2}$$

$$= r(1 - 2u(x))\phi(t,x) + \frac{\partial^2 \phi(t,x)}{\partial x^2}.$$

Thus, we have the linearization as:

$$\begin{cases} \frac{\partial \phi}{\partial t} = r(1 - 2u(x))\phi + \frac{\partial^2 \phi}{\partial x^2}, \\ \phi(t,0) = \phi(t,L) = 0. \end{cases} \tag{1.4.19}$$

We use the separation of variables technique again ($\phi(t,x) = S(x)T(t)$) to obtain the temporal equation

$$\frac{dT}{dt} = -\lambda D T,$$

and the spatial equation

$$\frac{d^2 S}{dx^2} + \left(\lambda + \frac{r}{D}(1 - 2u(x))\right) S = 0, \tag{1.4.20}$$

with boundary conditions

$$S(0) = S(L) = 0. \tag{1.4.21}$$

The steady state $u(x)$ is unknown; nevertheless, we are able to determine its stability applying by Sturm-Liouville theory [25], since (1.4.20) and the boundary conditions (1.4.21) form a regular Sturm-Liouville problem. Therefore, the spectrum of equations (1.4.20) and (1.4.21) consists of an infinite ordered sequence of eigenvalues $\lambda_1 < \lambda_2 < \ldots$ Moreover, the eigenfunction $S_1(x)$ corresponding to λ_1 does not change sign on $(0, L)$. Let us rewrite equation (1.4.20) for $\lambda = \lambda_1$ and $S(x) = S_1(x)$:

$$\frac{d^2S_1}{dx^2} + \left(\lambda_1 + \frac{r}{D}(1-2u(x))\right) S_1 = 0 \tag{1.4.22}$$

Next, we multiply the above equation by $u(x)$ and integrate by parts between 0 and L:

$$\frac{d^2S_1}{dx^2}u(x) + u(x)\left(\lambda_1 + \frac{r}{D}(1-2u(x))\right) S_1 = 0,$$

$$\frac{dS_1}{dx}u|_0^L - \int_0^L \frac{dS_1}{dx}\frac{du}{dx}dx + \left(\lambda_1 + \frac{r}{D}\right)\int_0^L uS_1 dx - 2\frac{r}{D}\int_0^L u^2 S_1 dx = 0. \tag{1.4.23}$$

We take equation (1.4.14), multiply it by $S_1(x)$ and integrate it by parts between 0 and L:

$$\frac{r}{D}uS_1(1-u) + u''S_1 = 0,$$

$$\frac{r}{D}\int_0^L uS_1 dx - \frac{r}{D}\int_0^L u^2 S_1 dx + uS_1|_0^L - \int_0^L uS_1' dx = 0. \tag{1.4.24}$$

Taking the difference between (1.4.23) and (1.4.24) and applying the boundary conditions (1.4.15) and (1.4.21), we obtain:

$$\lambda_1 = \frac{\frac{r}{D}\int_0^L u^2(x)S_1(x)dx}{\int_0^L u(x)S_1(x)dx}.$$

Since $u(x)$ is positive away from the boundary and S_1 does not change sign on the interval $(0, L)$, it follows that λ_1 is positive.

Therefore, the dominant term of $\phi(t, x)$ is of the form $S(x)e^{-\lambda_1 Dt}$ and $u(x,t) = u(x) + \phi(x,t) \to u(x)$ as $t \to \infty$. We have shown that the nontrivial steady state is stable for the domains larger then the critical size domain.

1.4.2 Variational formula for the principal eigenvalue

In many cases, we need to study models with coefficients varying in space. It is usually quite a formidable task to compute eigenvalues and eigenfunctions for such problems

analytically. Nevertheless, we can use variational techniques that allow us to estimate eigenvalues and obtain enough information to investigate stability of the solutions. We are mainly concerned with principal eigenvalues and their eigenfunctions, so we focus on those.

In [10], Cantrell and Cosner consider the eigenvalue problem

$$\begin{cases} \bigtriangledown \cdot d(x) \bigtriangledown \psi + m(x)\psi = \sigma\psi \ \text{ in } \ \Omega \\ d(x)\frac{\partial \psi}{\partial \vec{n}} + \rho(x)\psi = 0, \ \text{ on } \ \partial\Omega \end{cases} \tag{1.4.25}$$

associated with the following model on the bounded domain $\Omega \subset \mathbb{R}^n$ with smooth boundary:

$$\begin{cases} u_t = \bigtriangledown \cdot d(x) \bigtriangledown u + m(x)u \ \text{ in } \ \Omega \times (0,\infty) \\ d(x)\frac{\partial u}{\partial \vec{n}} + \rho(x)u = 0, \ \text{ on } \ \partial\Omega \times (0,\infty), \end{cases} \tag{1.4.26}$$

where $\vec{n}$ denotes the outward pointing unit normal to $\partial\Omega$.

The authors provide the following variational formula for the principal eigenvalue σ^* of (1.4.25), assuming that $d(x)$ is smooth on $\bar{\Omega}$ and $d(x) \geq d_0$ for some $d_0 > 0$, $m(x) \in L^\infty(\Omega)$, and $\rho(x) \in L^\infty(\partial\Omega)$:

$$\sigma^* = \max_{\psi \in W^{1,2}(\Omega),\ \int_\Omega (\psi(x))^2 dx = 1} \left\{ -\int_\Omega d(x) | \bigtriangledown \psi|^2 dx + \int_\Omega m(x)(\psi(x))^2 dx - \int_{\partial\Omega} \rho(x)(\psi(x))^2 dS \right\}. \tag{1.4.27}$$

We give a derivation of this formula in the following, slightly less general case, studied in [46]. We will consider the following operator and boundary conditions, which will appear in the next chapters when we reduce a reaction-advection-diffusion model to a reaction-diffusion model by eliminating the advection term. Here, q is the advection speed, d is the diffusivity coefficient, and $a(x)$ is assumed to be a continuous function

on $[0, L]$. Namely, let

$$\mathcal{L}(U) = dU_{xx} + a(x)U$$

on $W_2^1([0, L])$, subject to boundary conditions

$$U_x(0) = \frac{q}{2d}U(0),$$
$$U_x(L) = -\frac{q}{2d}U(L).$$

Define a functional $Q : W_2^1([0, L]) \to \mathbb{R}$ by

$$Q(\phi) = \frac{\int_0^L (-(\phi_x)^2 + a(x)\phi^2)dx - \frac{q}{2d}((\phi(0))^2 + (\phi(L))^2)}{\int_0^L \phi^2 dx}. \tag{1.4.28}$$

and the bilinear form

$$F(\phi, \psi) = \int_0^L (-\phi_x\psi_x + a(x)\phi\psi)dx - \frac{q}{2d}\phi(0)\psi(0) - \frac{q}{2d}\phi(L)\psi(L). \tag{1.4.29}$$

Let

$$\lambda_1 = \sup_{\phi \in W_2^1([0,L])} Q(\phi). \tag{1.4.30}$$

Note that λ_1 is a finite number since

$$Q(\phi) \leq \frac{\int_0^L a(x)\phi^2 dx}{\int_0^L \phi^2 dx} \leq \frac{\int_0^L K\phi^2 dx}{\int_0^L \phi^2 dx} = K,$$

where $K = \max_{x\in[0,L]} |a(x)|$.

Note that $Q(\mu\phi) = Q(\phi)$ for any nonzero $\mu \in \mathbb{R}$ and $\phi \in W_2^1([0, L])$, so we may assume that $\|\phi\|_{L_2} = 1$.

The following was shown in [46] for $\phi_1 \in W_2^1([0, L])$, such that $\|\phi_1\|_{L_2} = 1$ and $\lambda_1 = Q(\phi_1)$ (i.e. ϕ_1 is the maximizer).

Proposition 1.4.1 *The maximizer ϕ_1 satisfies $\mathcal{L}\phi_1 = \lambda_1\phi_1$ and boundary conditions*

$$\phi_{1_x}(0) = \frac{q}{2d}\phi_1(0),$$

$$\phi_{1_x}(L) = -\frac{q}{2d}\phi_1(L).$$

Proof: Let $\phi \in W_2^1([0,L])$ be an arbitrary function. For any $c \in \mathbb{R}$ we have $Q(\phi_1 + c\phi) \leq \lambda_1$. Now,

$$\begin{aligned}
Q(\phi_1 + c\phi) = \frac{F(\phi_1 + c\phi, \phi_1 + c\phi)}{\int_0^L (\phi_1 + c\phi)^2 dx} &= \\
\frac{F(\phi_1,\phi_1) + 2cF(\phi_1,\phi) + c^2F(\phi,\phi)}{\int_0^L (\phi_1 + c\phi)^2 dx} &= \\
\frac{\int_0^L \phi_1^2 dx Q(\phi_1) + 2cF(\phi_1,\phi) + c^2Q(\phi)\int_0^L \phi^2 dx}{\int_0^L (\phi_1^2 + 2c\phi_1\phi + c^2\phi^2)dx} &= \\
\frac{\lambda_1 + 2cF(\phi_1,\phi) + c^2Q(\phi)\int_0^L \phi^2 dx}{\int_0^L \phi_1^2 dx + 2c\int_0^L \phi_1\phi dx + c^2\int_0^L \phi^2 dx} &\leq \lambda_1,
\end{aligned}$$

and thus,

$$\begin{aligned}
\lambda_1 + 2cF(\phi_1,\phi) + c^2Q(\phi)\int_0^L \phi^2 dx &\leq \\
\lambda_1\left(1 + 2c\int_0^L \phi_1\phi dx + c^2\int_0^L \phi^2 dx\right) &= \\
\lambda_1 + 2\lambda_1 c\int_0^L \phi_1\phi dx + \lambda_1 c^2\int_0^L \phi^2 dx,
\end{aligned}$$

or

$$2c\left(F(\phi_1,\phi) - \lambda_1\int_0^L \phi_1\phi dx + \frac{c}{2}(Q(\phi) - \lambda_1)\int_0^L \phi^2 dx\right) \leq 0.$$

Here c is arbitrary. Taking $c > 0$, we get

$$F(\phi_1,\phi) - \lambda_1\int_0^L \phi_1\phi dx \leq -\frac{c}{2}(Q(\phi) - \lambda_1)\int_0^L \phi^2 dx.$$

Let $c \to 0$. Then

$$F(\phi_1,\phi) - \lambda_1\int_0^L \phi_1\phi dx \leq 0.$$

For $c < 0$, we get

$$F(\phi_1, \phi) - \lambda_1 \int_0^L \phi_1 \phi dx \geq -\frac{c}{2}(Q(\phi) - \lambda_1) \int_0^L \phi^2 dx.$$

Let $c \to 0$. Then $F(\phi_1, \phi) - \lambda_1 \int_0^L \phi_1 \phi dx \geq 0$.

Thus,

$$F(\phi_1, \phi) = \lambda_1 \int_0^L \phi_1 \phi dx,$$

or

$$\int_0^L (-\phi_{1x}\phi_x + a(x)\phi_1\phi)dx - \frac{q}{2d}\phi_1(0)\phi(0) - \frac{q}{2d}\phi_1(L)\phi(L) = \lambda_1 \int_0^L \phi_1 \phi dx.$$

Integration by parts gives

$$-\int_0^L \phi_{1x}\phi_x dx = -\phi_{1x}\phi|_0^L + \int_0^L \phi\phi_{1xx} = -\phi_{1x}(L)\phi(L) + \phi_{1x}\phi(0) + \int_0^L \phi(\mathcal{L}(\phi_1) - a(x)\phi_1)dx.$$

Thus, we get

$$\int_0^L \phi(\mathcal{L}(\phi_1) - \lambda_1\phi_1)dx = \phi(L)\left[\frac{q}{2d}\phi_1(L) + \phi_{1x}(L)\right] + \phi(0)\left[\frac{q}{2d}\phi_1(0) - \phi_{1x}(0)\right].$$

Since ϕ is an arbitrary function in $W_2^1([0, L])$, we claim that

$$\begin{aligned} \mathcal{L}(\phi_1) &= \lambda_1\phi_1, \\ \phi_{1x}(0) &= \frac{q}{2d}\phi_1(0), \\ \phi_{1x}(L) &= -\frac{q}{2d}\phi_1(L). \end{aligned}$$

First, consider a sequence $\phi_n \in W_2^1([0, L])$ such that $\phi_n \to 0$ uniformly on $[0, L]$, $\phi_n(0) = 1$ and $\phi_n(L) = 0$. Then

$$\frac{q}{2d}\phi_1(0) - \phi_{1x}(0) = \int_0^L \phi_n(\mathcal{L}(\phi_1) - \lambda_1\phi_1)dx \to 0,$$

and thus,

$$\phi_{1_x}(0) = \frac{q}{2d}\phi_1(0).$$

Similarly, by choosing $\phi_n(0) = 0$ and $\phi_n(L) = 1$, we get

$$\phi_{1_x}(L) = -\frac{q}{2d}\phi_1(L).$$

Now, we have

$$\int_0^L \phi(\mathcal{L}(\phi_1) - \lambda_1\phi_1)dx = 0,$$

for any $\phi \in W_2^1([0, L])$. It follows that $\mathcal{L}(\phi_1) = \lambda_1\phi_1$. Therefore, λ_1 is an eigenvalue of $\mathcal{L}$ subject to the boundary conditions

$$\begin{aligned} \phi_x(0) &= \frac{q}{2d}\phi(0), \\ \phi_x(L) &= -\frac{q}{2d}\phi(L). \end{aligned}$$

∎

We now show that λ_1 is the maximal such eigenvalue, i.e. for any $\lambda \in \mathbb{R}$ such that there exists a non-zero $\phi_\lambda \in W_2^1([0, L])$ with

$$\begin{aligned} \mathcal{L}(\phi_\lambda) &= \lambda\phi_\lambda, \\ \phi_{\lambda_x}(0) &= \frac{q}{2d}\phi_\lambda(0), \\ \phi_{\lambda_x}(L) &= -\frac{q}{2d}\phi_\lambda(L), \end{aligned}$$

we have $\lambda \leq \lambda_1$.

We may assume that $\|\phi_\lambda\| = 1$. Recall that

$$\lambda_1 = \sup_{\phi \in W_2^1([0,L])} Q(\phi).$$

It suffices to show that $Q(\phi_\lambda) = \lambda$ (then $\lambda = Q(\phi_\lambda) \leq \lambda_1$).

Now,

$$\begin{aligned} Q(\phi_\lambda) &= \frac{\int_0^L (-{\phi_\lambda}_x^2 + a(x){\phi_\lambda}^2)dx - \frac{q}{2d}((\phi_\lambda(0))^2) + (\phi_\lambda(L))^2)}{\int_0^L \phi_\lambda^2 dx} \\ &= -\int_0^L \phi_{\lambda x}\phi_{\lambda x}dx + \int_0^L a(x)\phi_\lambda^2 dx - \frac{q}{2d}((\phi_\lambda(0))^2) + (\phi_\lambda(L))^2). \end{aligned}$$

Integrating by parts,

$$\begin{aligned} \int_0^L \phi_{\lambda x}\phi_{\lambda x}dx &= \\ \phi_\lambda\phi_{\lambda x}|_0^L - \int_0^L \phi_\lambda\phi_{\lambda xx}dx &= \\ \phi_\lambda\phi_{\lambda x}|_0^L - \int_0^L \phi_\lambda(\mathcal{L}(\phi_\lambda) - a(x)\phi_\lambda)dx &= \\ \phi_\lambda\phi_{\lambda x}|_0^L - \int_0^L \phi_\lambda(\lambda\phi_\lambda - a(x)\phi_\lambda)dx &= \\ \phi_\lambda\phi_{\lambda x}|_0^L - \int_0^L \lambda(\phi_\lambda)^2 dx + \int_0^L a(x)(\phi_\lambda)^2 dx & \end{aligned}$$

and plugging it in the above expression, gives us

$$\begin{aligned} -\phi_\lambda\phi_{\lambda x}|_0^L + \int_0^L \lambda\phi_\lambda^2 dx - \int_0^L a(x)\phi_\lambda^2 dx + \int_0^L a(x)\phi_\lambda^2 dx - \frac{q}{2d}(\phi_\lambda^2(0) + \phi_\lambda^2(L))) &= \\ \phi_\lambda(0)\phi_{\lambda x}(0) - \phi_\lambda(L)\phi_{\lambda x}(L) - \frac{q}{2d}(\phi_\lambda(0))^2 - \frac{q}{2d}(\phi_\lambda(L))^2 + \lambda &= \\ \phi_\lambda(0)[\phi_{\lambda x}(0) - \frac{q}{2d}\phi_\lambda(0)] - \phi_\lambda(L)[\phi_{\lambda x}(L) + \frac{q}{2d}\phi_\lambda(L)] + \lambda &= \lambda, \end{aligned}$$

as needed.

Thus, we have proved the following.

Proposition 1.4.2 *(compare [46]) Let λ_1 be the principal eigenvalue of the operator*

$$\mathcal{L}(U) = U_{xx} + a(x)U$$

on $W_2^1([0, L])$, with boundary conditions

$$U_x(0) = \frac{q}{2d}U(0),$$

$$U_x(L) \;=\; -\frac{q}{2d}U(L).$$

Then

$$\lambda_1 = \sup_{\phi\in W_2^1([0,L])}\left(\frac{\int_0^L(-(\phi_x)^2+a(x)\phi^2)dx-\frac{q}{2d}((\phi(0))^2+(\phi(L))^2)}{\int_0^L\phi^2dx}\right)$$

$$= \sup_{\phi\in W_2^1([0,L]),\ \int_0^L\phi^2dx=1}\left(\int_0^L(-(\phi_x)^2+a(x)\phi^2)dx-\frac{q}{2d}((\phi(0))^2+(\phi(L))^2)\right). \tag{1.4.31}$$

1.4.3 Spreading speeds, travelling wave speed

In this subsection, we review some notions and facts related to the spread of population in reaction-diffusion models, in particular the notion of travelling wave speed. We follow [25], see also [36] and [37].

The reaction-diffusion model for growth and spread in one spatial dimension has the following form:

$$\frac{\partial y}{\partial t} = D\frac{\partial^2 y}{\partial x^2} + f(y), \tag{1.4.32}$$

where $f(y) = ry(1-\frac{y}{K})$ is a typical growth function.

We rescale the population density by the carrying capacity, time and space by characteristic time and length:

$$u = \frac{y}{K}, \quad \tilde{t} = rt, \quad \tilde{x} = \sqrt{\frac{r}{D}}x, \tag{1.4.33}$$

$$\frac{\partial y}{\partial t} = \frac{\partial y}{\partial \tilde{t}}\frac{d\tilde{t}}{dt} = \frac{\partial(uK)}{\partial\tilde{t}}\frac{d\tilde{t}}{dt} = K\frac{\partial u}{\partial\tilde{t}}r = Kr\frac{\partial u}{\partial\tilde{t}},$$

$$\frac{\partial y}{\partial x} = \frac{\partial y}{\partial \tilde{x}}\frac{d\tilde{x}}{dx} = \frac{\partial(uK)}{\partial\tilde{x}}\sqrt{\frac{r}{D}} = K\sqrt{\frac{r}{D}}\frac{\partial u}{\partial\tilde{x}},$$

$$\frac{\partial^2 y}{\partial x^2} = \frac{\partial}{\partial x}\left(K\sqrt{\frac{r}{D}}\frac{\partial u}{\partial \tilde{x}}\right) = K\frac{r}{D}\frac{\partial^2 u}{\partial \tilde{x^2}}.$$

Therefore our new equation is

$$Kr\frac{\partial u}{\partial \tilde{t}} = Kr\frac{\partial^2 u}{\partial \tilde{x}^2} + ruK\left(1 - \frac{uK}{K}\right),$$

or

$$\frac{\partial u}{\partial \tilde{t}} = \frac{\partial^2 u}{\partial \tilde{x}^2} + u(1-u).$$

For notational simplicity, we now drop the tildes on t and x and obtain

$$\frac{\partial u}{\partial t} = \frac{\partial^2 u}{\partial x^2} + u(1-u). \tag{1.4.34}$$

This equation can describe the spread of a population with logistic growth and Fickian diffusion. Model (1.4.34) was introduced by Fisher in 1937, who used it to describe the spread of advantageous gene into a new environment [15].

We consider solutions of (1.4.34) in the form of travelling waves. These solutions are characterized by fixed profile and constant speed c. The travelling wave solution connects the zero steady state $u = 0$ and the carrying capacity steady state $u = 1$. Note that the travelling wave can move to the left or to the right. In view of later applications in advective environments, we call these waves upstream and downstream, respectively. Thus, the downstream (right moving) travelling wave ansatz with the boundary conditions is given by

$$u(t,x) = \phi(x - ct), \tag{1.4.35}$$

$$\phi(-\infty) = 1, \quad \phi(+\infty) = 0, \quad c > 0. \tag{1.4.36}$$

The parameter c is called the wave speed, $z = x - ct$ is the wave variable, and the function $\phi(z)$ is called the profile.

Substituting (1.4.35) in (1.4.34) gives

$$-c\phi' = \phi'' + \phi(1-\phi). \tag{1.4.37}$$

We rewrite the second order differential equation (1.4.37) as a system of first order differential equations

$$\begin{cases} \phi' = \psi, \\ \psi' = -c\psi - \phi(1-\phi), \end{cases} \tag{1.4.38}$$

and use phase-plane methods to analyze this equation. The system above has two steady states: $P_1 = (\phi_1, \psi_1) = (0,0)$ and $P_2 = (\phi_2, \psi_2) = (1,0)$. The travelling wave profile that we are looking for is a heteroclinic connection between these steady states. Linearization at these states gives

$$\begin{pmatrix} \phi' \\ \psi' \end{pmatrix} = \begin{pmatrix} 0 & 1 \\ -1+2\phi & -c \end{pmatrix} \begin{pmatrix} \phi \\ \psi \end{pmatrix} = J \begin{pmatrix} \phi \\ \psi \end{pmatrix},$$

$J(0,0) = \begin{pmatrix} 0 & 1 \\ -1 & -c \end{pmatrix}$. At P_1 we get $\det J(0,0) = 1$, $\mathrm{tr}J(0,0) = -c$. We have

$$\lambda_1 = \frac{-c + \sqrt{c^2-4}}{2}, \quad \lambda_2 = \frac{-c - \sqrt{c^2-4}}{2}.$$

If $c > 0$ then P_1 is a stable equilibrium. For $c > 2$, P_1 is a stable node, and for $0 < c < 2$, P_1 is a stable spiral.

$J(1,0) = \begin{pmatrix} 0 & 1 \\ 1 & -c \end{pmatrix}$, $\det J(1,0) = -1$, $\mathrm{tr}J(1,0) = -c$.

Therefore P_2 is an unstable steady state (saddle point), since

$$\lambda_1 = \frac{-c + \sqrt{c^2+4}}{2} > 0, \quad \lambda_2 = \frac{-c - \sqrt{c^2+4}}{2} < 0.$$

Since the function ϕ is the profile of the population density, the case $0 < c < 2$ (when u becomes negative) is biologically irrelevant. We conclude that the necessary condition for existence of travelling waves is the existence of a heteroclinic connection,

which is possible if $c \geq 2$. Furthermore, the above condition gives us a notion of a minimum wave speed for travelling waves. In terms of nondimensional model (1.4.34), $c_{\min} = 2$, and for original model (1.4.32), $c_{\min} = 2\sqrt{Dr}$.

Note: the left moving wave solution has the form $u(t, x) = \phi(x + ct)$. For upstream waves we want $\phi(-\infty) = 0$ and $\phi(+\infty) = 1$. In the case of upstream spreading, equation (1.4.34) takes form $c\phi' = \phi'' + \phi(1-\phi)$. It has two equilibria points: $P_1(0, 0)$ and $P_2(1, 0)$. The point P_1 is an unstable node if $c > 2$ and an unstable spiral if $0 < c < 2$. Like in the previous case (downstream waves), the second steady state is a saddle point. In order for the upstream travelling wave solution to exist, we need to have the heteroclinic connection between the unstable node P_1 and the saddle point P_2 (thus we again require $c \geq 2$).

Going back to the downstream travelling wave solution, let us find a sufficient condition for the existence of a heteroclinic orbit. When does the orbit starting at P_2 come to P_1?

We create a triangular "trapping region" with three sides I, II and III (from [26]):

I: $\phi = 1$, $\psi < 0$;

II: $0 < \phi < 1$, $\psi = 0$;

III: $0 < \phi < 1$, $\psi = -\alpha\phi$.

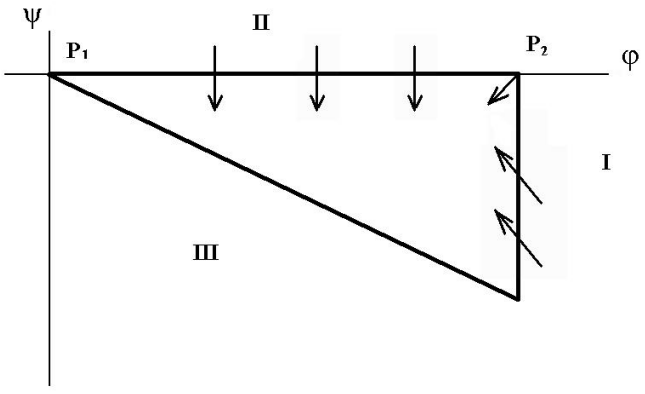

On side I: $\phi' = \psi < 0$ and $\psi' = -c\psi > 0$, and vector field (1.4.38) points into the

region. On side II: $\phi' = \psi = 0$ and thus ϕ is constant, while $\psi' = -\phi(1-\phi) < 0$, $0 < \phi < 1$ and ψ is decreasing. For the hypotenuse III, consider the dot product of the normal vector to the hypotenuse and the vector field:

$$(\alpha, 1)\cdot(\phi', \psi') = (\alpha, 1)\cdot(\psi, -c\psi - \phi(1-\phi)) = \alpha\psi - c\psi - \phi(1-\phi) = \alpha(-\alpha\phi) - c(-\alpha\phi) - \phi(1-\phi)$$

$$= -\alpha^2\phi + c\alpha\phi - \phi + \phi^2 = -\phi(\alpha^2 - c\alpha + (1-\phi)).$$

We want to choose α such that the angle between the inward normal $(\alpha, 1)$ and the vector field (ϕ', ψ') is acute (therefore the vector field gets inside the trapping region by crossing the hypotenuse). Thus, we need the dot product of these two vectors to be positive, or $\alpha^2 - c\alpha + 1 - \phi < 0$. Since

$$\alpha^2 - c\alpha + 1 - \phi < \alpha^2 - c\alpha + 1$$

for $0 < \phi < 1$, we want to find a positive α such that $\alpha^2 - c\alpha + 1 \leq 0$. The equation $\alpha^2 - c\alpha + 1 = 0$ has two positive real roots if $c \geq 2$:

$$\alpha_{1,2} = \frac{c \pm \sqrt{c^2 - 4}}{2}.$$

If we choose α from the interval $(\frac{c-\sqrt{c^2-4}}{2}, \frac{c+\sqrt{c^2-4}}{2})$, then the expression $\alpha^2 - c\alpha + 1$ is negative, which is exactly what we want. Hence for all $c > 2$, we can choose α such that the trapping region exists. Therefore for all $c > 2$ there is a travelling wave.

Thus, the unstable manifold that is leaving P_2 cannot cross any of the sides of the triangle. There are no more equilibrium points in the interior of the "trapping region" either. The only way that the orbit will not end at P_1 is when there exists a closed orbit inside the region. In order to prove that there are no such orbits, we use the Bendixson's negative criterion again, this time with $B = 1$.
In our case, $\frac{\partial}{\partial\phi}(\psi) + \frac{\partial}{\partial\psi}(-c\psi - \phi(1-\phi)) = -c \neq 0$. Therefore, the unstable manifold will come to P_1. Consequently, we have shown that $c \geq 2$ is the necessary and sufficient condition for the Fisher equation to have a travelling wave solution.

1.5 Literature review for systems with advection

In this section, we review several reaction-diffusion models describing dynamics of a population in an advective environment. We begin with the Speirs-Gurney model [47] for a single species, that generalizes the classical Fisher's equation. Then we describe a two-compartment model [38]. In both models, there is an appropriate notion of critical domain size, which increases with advection. Then we review the model in [20], which describes a slightly different biological situation involving the vertical movements of plankton, where the role of advection is played by the downward motion due to gravity (sinking). We finish the chapter with an overview of results in [30], where the authors describe how advection affects the competition of two species.

1.5.1 Single species models

A wide variety of organisms inhabit streams, rivers and other environments where they are continually subjected to downstream drift. The first problem in this context is to find the conditions under which survival of the population is possible, even though the individuals drift downstream ("drift paradox", see [34], [35]). This has been discussed by several authors recently (see [29], [38]). We review their approaches here. More generally, the question is how unidirectional movement affects population persistence in a bounded patch. The drift phenomenon is not limited to streams and rivers; it has been observed and studied in the context of ocean currents [16], sinking phytoplankton [20], and the ecological impact of moving temperature isoclines [40].

Speirs and Gurney's model

The model proposed by Speirs and Gurney [47] is described by the reaction-diffusion-advection equation:

$$\frac{\partial n}{\partial t} = p(n)n - v\frac{\partial n}{\partial x} + D\frac{\partial^2 n}{\partial x^2}, \tag{1.5.1}$$

where $n(x,t)$ is the population density, and $p(n)$ is the per capita growth rate of the population in the absence of dispersal. The second term on the right in (1.5.1) is responsible for the movement of the individuals caused by the drift. The last term represents diffusive movement of the individuals (due to self propelling and/or water turbulence).

In addition to the equation, the authors consider the following boundary conditions:

$$vn(t,0) - D\left(\frac{\partial n}{\partial x}\right)\Big|_{x=0} = 0 \quad (v > 0), \tag{1.5.2}$$

$$n(t,L) = 0, \tag{1.5.3}$$

It is assumed that individuals from the interior of the domain (in our case, it is a part of a stream or a river), who reach the upstream border are being reflected from it. At the same time, no individuals enter at the top of the stream. At the right border of the habitat ($x = L$), the organisms leave their domain and never come back, which leads to (1.5.3), the hostile boundary condition.

Proposition 1.5.1 *(In [47]) Let $p(n) = r$ be constant. Then we have:*
(a) In the absence of advection and diffusion (ideal situation), the solution of (1.5.1) has the form

$$n(t,x) = e^{rt}n(0,x),$$

where r is per capita growth rate and $n(0,x)$ is the initial spatial distribution.
(b) In the presence of water movement and random movements of individuals, the general solution of (1.5.1) with the boundary conditions (1.5.2) and (1.5.3) is given by

$$n(t,x) = \sum_{k=1}^{\infty} e^{\lambda_k t}(A_k e^{\xi x}\cos\theta_k x + B_k e^{\xi x}\sin\theta_k x), \tag{1.5.4}$$

where

$$\theta_k = \frac{\sqrt{4D(r-\lambda_k) - v^2}}{2D}, \quad \xi = \frac{v}{2D},$$

and λ_k *are the eigenvalues of the operator* $D\frac{d^2f}{dx^2} - v\frac{df}{dx} + rf$, *with boundary conditions*

$$vf(0) - D\left(\frac{df}{dx}\right)|_{x=0} = 0,$$

$$f(L) = 0.$$

Matching the right-hand boundary conditions gives us $-\frac{A_k}{B_k} = \tan\theta_k L$. To match the left-hand boundary condition we require $\frac{A_k}{B_k} = \frac{2D\theta_k}{v}$. Thus, the solution that matches both boundary conditions requires

$$\tan\theta_k L = -\frac{2D\theta_k}{v}. \tag{1.5.5}$$

Remark: We have $0 \leq \theta_1 < \theta_2 < \ldots$ and $r \geq \lambda_1 > \lambda_2 > \ldots$ The solution of (1.5.5) was obtained numerically in [47].

We nondimensionalize by setting

$$L_d = \sqrt{\frac{D}{r}},$$

$$v_d = 2\sqrt{Dr},$$

$$\theta_k' = \sqrt{1 - \frac{\lambda_k}{r} - \left(\frac{v}{v_d}\right)^2}.$$

Then (1.5.5) becomes

$$\tan(\theta_k'\frac{L}{L_d}) = -\frac{v_d\theta_k'}{v}. \tag{1.5.6}$$

The authors calculate the critical domain size L_c, i.e. the value of L such that in any domain of smaller size persistence of the population is impossible. This means that L_c corresponds to $\lambda_1 = 0$. Letting $\lambda_1 = 0$ gives $\theta_1' = \sqrt{1 - \frac{v^2}{v_d^2}}$. Substituting it into (1.5.6) gives us

$$\frac{L_c}{L_d} = \left(\pi - \arctan\sqrt{\frac{v_d^2 - v^2}{v^2}}\right)\sqrt{\frac{v_d^2}{v_d^2 - v^2}}. \tag{1.5.7}$$

In [47], it was found numerically that if the advection velocity is low and the habitat is large enough, the long-term growth rate λ_1 approaches the per capita

(ideal) growth rate r. Increasing advection velocity leads to a decrease in λ_1. Once the advection velocity exceeds the critical value v_c, λ_1 becomes negative and we observe a washout of the population. The value of v_c approaches v_d (from below) as L increases. It is possible to think of v_d as the critical advection for an infinite domain size. In fact, v_d is the Fisher speed in the absence of drift.

Huisman's plankton model

In the paper [20], Huisman et al. study the problem of sinking phytoplankton. The phenomenon is directly related to the "drift paradox". However, instead of the typical horizontal habitat, the domain lies in the vertical direction. This change takes place since the phytoplankton is mostly moving vertically between the surface and the bottom of the lake i.e. individuals do not get pushed out of the domain by directed movement, but they get pushed towards a region where the growth rate is negative. Diffusion allows individuals to move against the direction of gravity. Hence, the similar balance is observed between directed and undirected motions as in the previous subsection. The bottom and the top of the lake are reflecting boundaries.

Huisman et al. consider the following model, describing the above situation:

$$\frac{\partial u}{\partial t} = g(I)u - v\frac{\partial u}{\partial z} + D\frac{\partial^2 u}{\partial z^2},$$

where $u(z,t)$ is the density of the phytoplankton at depth z and time t, $g(I)$ is the intrinsic growth rate as a function of local light intensity I, and v is the sinking speed. The growth rate is defined by $g(I) = p(I) - l$, where $p(I)$ is the birth rate such that $p(0) = 0$ and l is the loss rate. The authors assume that $p(I)$ has the form

$$p(I) = \frac{p_{\max} I}{H + I},$$

where $p_{\max}$ is the maximal rate, and H is the half-saturation constant. In particular, the growth rate is not constant. Note that since light is absorbed by the plankton (as

well as other substances), its intensity also depends on the density of the plankton in the water column above the given depth. Specifically, the authors assumed

$$I(z,t) = I_{in} e^{-\int_0^z ku(\sigma,t)d\sigma - Kz},$$

where k and K are certain constants.

In addition, zero-flux boundary conditions are imposed at both boundaries:

$$vu(t,z) - D\frac{\partial u}{\partial z}(t,z) = 0$$

at $z = 0$ and $z = L$ (maximum depth). This is intuitively understandable, since density of the organisms is higher than water density, so without any diffusive movements the organisms sink down to the lake floor. As a result, the population goes extinct because there is not enough light for the population to grow. On the other hand, if the diffusivity is very high, the phytoplankton could end up in the deep water again. Therefore, in order to survive, organisms have to perform some medium-diffusive movements, so they could stay in well-lit area of the habitat and still not reach the lake floor.

The authors study the problem numerically, and find two steady states (one of which is trivial). They notice dependence of the profile of the nontrivial steady state on the diffusivity. Namely, as diffusivity decreases, the profile changes from uniform to the one with high density in the surface layers and low density at the bottom layers. Interestingly, if D decreases even more (beyond the certain threshold value $D_{\min}$), then the population starts sinking to the bottom, where it eventually vanishes. Using the light intensity notion, the authors gave the formulae for the critical depth (beyond it the loss rate exceeds the birth rate). They analyze the threshold values of the diffusion: $D_{\min}$ and $D_{\max}$. The authors show numerically that in the relatively deep waters, if the diffusivity stays between those two values, then the population exhibits "bloom development" toward the positive steady state.

Recently, Kolokolnikov et al. [24] have studied the same model, and found an analytical proof of existence of nonconstant steady states for any depth (generalizing

results in [44] where the authors assume an infinite depth). Kolokolnikov et al. have also established local stability of such solutions, and analyzed their spatial profiles.

Single species: two compartment model

Many organisms have two different stages in their life cycle: mobile (when the organisms move through their habitat) and stationary. In rivers, many benthic invertebrates, i.e. invertebrates living at the lowest level of a body of the water, fall in this category. Typically, reproduction occurs during the stationary stage. To distinguish between the two stages, the population is split into two compartments, according to the individual's life stage. This approach originates in [27] where the authors extended the previously studied Fisher's model [15]. The authors calculated the travelling wave speed in this context. The same model has also been studied in [17]. It was generalized to the advective case in [38]. The whole population is divided into two compartments: benthic and drift. The individuals from the first group live and reproduce on the benthos. The second group is composed of the organisms who enter and move with the drift. These assumptions lead to the following model:

$$\begin{cases} \dfrac{\partial n_d}{\partial t} = \mu n_b - \sigma n_d - v\dfrac{\partial n_d}{\partial x} + D\dfrac{\partial^2 n_d}{\partial x^2}, \\ \\ \dfrac{\partial n_b}{\partial t} = p(n_b)n_b - \mu n_b + \sigma n_d, \end{cases} \tag{1.5.8}$$

where n_b is the population density on the benthos, n_d is the population density in the drift, $p(n_b)$ is the per capita rate of increase of the benthic population (it is assumed that the maximum per capita growth rate is at low densities, μ is the per capita rate at which individuals in the benthos enter the drift, σ is the per capita rate at which the organisms return to the benthos. The meanings of D and v stay unchanged.

Critical domain size. The first goal in [38] was to study persistence criteria for a

population described by (1.5.8). In addition to the equations, there are the following boundary conditions

$$\begin{aligned} vn_d(t,0) - D\left(\frac{\partial n_d}{\partial x}\right)_{x=0} &= 0, \\ n_d(t,L) &= 0. \end{aligned}$$

The ordinary differential equation for the stationary population does not require any boundary conditions.

It was assumed that the maximum per capita growth rate is at low densities. If population is able to grow at small densities then persistence of the organisms is guaranteed. Therefore, we linearize system (1.5.8) around the zero steady state and seek conditions under which the population will not go extinct.

We nondimensionalize model (1.5.8) by defining the new variables

$$\tilde{t} = rt,\ \tilde{\mu} = \frac{\mu}{r},\ \tilde{\sigma} = \frac{\sigma}{r},\ \tilde{x} = \frac{x}{\sqrt{\frac{D}{r}}},\ \tilde{v} = \frac{v}{\sqrt{Dr}}.$$

Dropping the tildes for notational simplicity, we get

$$\begin{cases} \dfrac{\partial n_d}{\partial t} = \mu n_b - \sigma n_d - v\dfrac{\partial n_d}{\partial x} + \dfrac{\partial^2 n_d}{\partial x^2}, \\ \dfrac{\partial n_b}{\partial t} = (1-\mu)n_b + \sigma n_d. \end{cases} \tag{1.5.9}$$

It is reasonable to consider two cases.

If $\mu < 1$, then the benthic population grows at least exponentially and persistence of the whole population is guaranteed (irrespective of the size of the domain and the advection velocity). Namely,

$$\frac{\partial n_b}{\partial t} = (1-\mu)n_b + \sigma n_d \geq (1-\mu)n_b. \tag{1.5.10}$$

If $\mu > 1$, then persistence is possible, provided that some conditions are satisfied. Let us look at them more closely.

Theorem 1.5.2 *(In [38]) The general solution of system (1.5.9) has the following form:*

$$n_b(t,x) = e^{-(\mu-1)t}n_b(0,x) + \sigma e^{-(\mu-1)t}\int_0^t e^{(\mu-1)\tau}n_d(\tau,x)d\tau, \tag{1.5.11}$$

$$\begin{aligned} n_d(t,x) &= \textstyle\sum_{n=1}^{\infty}[c_1 m_{1n}e^{(m_{1n}-(\mu-1))t} + c_2 m_{2n}e^{(m_{2n}-(\mu-1))t}] \\ &\times[e^{\frac{vx}{2}}(a_1\cos(\tfrac{\sqrt{4\lambda_n - v^2}}{2}x) + a_2\sin(\tfrac{\sqrt{4\lambda_n-v^2}}{2}x))], \end{aligned} \tag{1.5.12}$$

where a_1, a_2 are constants,

$$\begin{aligned} m_{1n} = m_1(\lambda_n) &= \tfrac{-(a+\lambda_n)+\sqrt{(a+\lambda_n)^2+4\mu\sigma}}{2}, \\ m_{2n} = m_2(\lambda_n) &= \tfrac{-(a+\lambda_n)-\sqrt{(a+\lambda_n)^2+4\mu\sigma}}{2}, \end{aligned} \tag{1.5.13}$$

$a = \sigma - \mu + 1$ and λ_n are solutions $\lambda_n(v,L)$ of

$$\frac{\sqrt{4\lambda - v^2}}{v} + \tan(\frac{\sqrt{4\lambda - v^2}}{2}L) = 0, \tag{1.5.14}$$

with $\lambda_1 < \lambda_2 < \ldots$

Without loss of generality, we may assume that initially there are no individuals in the stationary pool, i.e. $n_b(0,x) = 0$. Formula (1.5.11) can be obtained by applying the variation of constant technique to the second equation of system (1.5.9). Substituting (1.5.11) into the first equation of (1.5.9) gives us an equation that can be solved by separation of variables method. Then we have (1.5.12).

As we see from (1.5.12), $n_d \to 0$ as $t \to \infty$ if

$$c_1 m_{1n}e^{(m_{1n}-(\mu-1))t} + c_2 m_{2n}e^{(m_{2n}-(\mu-1))t} \to 0$$

or $m_{1n} - (\mu-1)$ and $m_{2n} - (\mu-1)$ are negative. Since $m_{1n} > m_{2n}$, it suffices that

$$m_{11} - (\mu-1) = \frac{-(a+\lambda_1(v,L))^2 + \sqrt{a+\lambda_1(v,L)^2 + 4\mu\sigma}}{2} - (\mu-1) < 0. \tag{1.5.15}$$

Consequently, the whole population goes extinct. Therefore, for persistence we require (1.5.15) to be positive. After some algebra, we get the necessary condition for a population to survive:

Corollary 1.5.3 *If the population persists, then*

$$\lambda_1 < \frac{\sigma}{\mu - 1}. \tag{1.5.16}$$

Note that m_{1n} is a decreasing function of λ_n, i.e. $m_{11} > m_{12} > \ldots$, and λ_1 is the smallest real eigenvalue that satisfies

$$\frac{\sqrt{4\lambda_1 - v^2}}{v} + \tan\left(\frac{\sqrt{4\lambda_1 - v^2}}{2} L\right) = 0. \tag{1.5.17}$$

Using (1.5.16) and (1.5.17), we find the critical domain size:

$$L_c = \frac{2}{\sqrt{\frac{4\sigma}{\mu-1} - v^2}} \left(\pi - \arctan\left(\frac{1}{v}\sqrt{\frac{4\sigma}{\mu - 1} - v^2}\right)\right). \tag{1.5.18}$$

Consequently, in the case when the leaving rate of the benthic population into drift is higher than the local growth rate (i.e. $\mu > 1$), we can still observe persistence. In order for the population not to die out, we need (1.5.16) to be satisfied, or the domain of the habitat to be large enough with respect to the advection speed. For any domain of size $L < L_c$, the population will be extinct. Critical domain size L_c increases with increasing advection velocity and goes to infinity when v approaches the threshold value

$$v_L^* = 2\sqrt{\frac{\sigma}{\mu - 1}}. \tag{1.5.19}$$

Corollary 1.5.4 *If $\mu \to 1$, then v_L^* goes to infinity, and the persistence condition is automatically satisfied (species will never go extinct).*

Propagation speed. For Fisher's equation without advection (see equation (1.4.34) Section 3.3.3) the population spreads in the form of travelling waves with minimum speed $c^* = 2\sqrt{Dr}$ ($c^* = 2$ in nondimensional case). If we take advection into consideration, then we have to distinguish between upstream and downstream propagation. Obviously, with increasing advection v, the downstream propagation speed for the Fisher equation increases and the upstream propagation speed decreases.

In the paper [38], the authors determine the up- and downstream propagation speed for the system (1.5.9) by using analytical and numerical methods.

In the case $\mu \leq 1$, as was shown before, the population persists and spreads in both directions. It spreads faster downstream and it moves slower upstream.

When the intrinsic growth rate is less than the rate at which individuals get into the drift ($\mu > 1$), and if advection is large enough, the population will be washed out. To determine the propagation speeds in both directions, we consider the system (1.5.9) with the logistic growth:

$$\begin{cases} \dfrac{\partial n_d}{\partial t} = \mu n_b - \sigma n_d - v\dfrac{\partial n_d}{\partial x} + D\dfrac{\partial^2 n_d}{\partial x^2}, \\ \dfrac{\partial n_b}{\partial t} = n_b(1 - n_b) - \mu n_b + \sigma n_d. \end{cases} \tag{1.5.20}$$

There are two spatially homogeneous steady state solutions to the system (1.5.20): $(n_b, n_d) = (0, 0)$ and $(n_b^*, n_d^*) = (1, \frac{\mu}{\sigma})$. We assume that there is a travelling wave connecting the nonzero and zero steady states.

We transform (1.5.20) into a system in travelling wave coordinates:

$$(n_b, n_d)(x, t) = (N_b, N_d)(x - ct) :$$

$$\begin{cases} N_d' = M, \\ M' = -\mu N_b + \sigma N_d - (c - v)M, \\ N_b' = \frac{N_b^2}{c} - \frac{(1-\mu)N_b}{c} - \frac{\sigma}{c}N_d. \end{cases} \tag{1.5.21}$$

The boundary conditions for downstream propagating waves are:

$$N_b(-\infty) = 1,\ N_d(-\infty) = \frac{\mu}{\sigma},\ M(-\infty) = 0,$$

$$N_b(\infty) = 0,\ N_d(\infty) = 0,\ M(\infty) = 0.$$

The boundary conditions for upstream propagating waves are

$$N_b(-\infty) = 0,\ N_d(-\infty) = 0,\ M(-\infty) = 0,$$

$$N_b(\infty) = 1,\ N_d(\infty) = \frac{\mu}{\sigma},\ M(\infty) = 0.$$

Note that if $c > 0$, the population moves with the flow in the same direction; otherwise the population is spreading upstream.

The linearization of (1.5.21) around the two equilibria gives us two characteristic polynomials $P_0(\lambda)$ and $P_1(\lambda)$. If at least one of the roots of the first polynomial is negative, then the zero steady state has at least a one-dimensional stable manifold. Similarly, if the second polynomial has at least one positive root we have at least a one-dimensional unstable manifold around the nontrivial equilibrium $(1, \frac{\mu}{\sigma})$. By using numerical and analytical computations, Pachepsky et al. [38] show that if both assumptions above are satisfied, then the heteroclinic orbit connecting the steady states above exists. Using methods similar to those of Lewis and Schmitz [27], the authors numerically calculated the minimal wave speed for the given parameters v, μ and σ.

Moreover, in case when $\mu \leq 1$, the upstream propagation speed of the population as a function of the advection velocity v never becomes negative. Consequently, the population will always spread upstream. On the other hand, when $\mu > 1$, at the critical value $v_c^* = 2\sqrt{\frac{\sigma}{\mu-1}}$, the upstream propagation speed becomes negative, which means a washout. In the paper [38], the authors conclude that if the rate of transfer into the drift does not exceed the intrinsic growth rate, the population will spread up- and downstream.

To summarize, in the presence of advection, persistence is very much dependent on the ability to propagate upstream, since without it, in the long term, the population will not stay in its original domain.

1.5.2 Competing species in advective environment.

In [30], Lutscher et al. investigate numerically how two competitors can coexist in homogeneous and heterogeneous environments with unidirectional flow.

The authors study the following model of two competing species:

$$\begin{cases} \frac{\partial u_1}{\partial t} = D_1 \frac{\partial^2 u_1}{\partial x^2} - v_1 \frac{\partial u_1}{\partial x} + u_1(R_1(x) - A_{11}u_1 - A_{21}u_2), \\ \frac{\partial u_2}{\partial t} = D_2 \frac{\partial^2 u_2}{\partial x^2} - v_2 \frac{\partial u_1}{\partial x} + u_2(R_2(x) - A_{12}u_1 - A_{22}u_2), \end{cases} \tag{1.5.22}$$

where $R_1(x)$ and $R_2(x)$ are growth rates for the first and second species, respectively, A_{ij} are inter- and intraspecific competition coefficients (note: carrying capacities are given by $K_j = \frac{R_j}{A_{ij}}$), and D_i, v_i are diffusion coefficients and advective velocities for the two species. Let $x = 0$ be the top of the river where individuals neither leave nor enter (zero flux). Unlike the previously studied hostile conditions at $x = L$, we have Danckwerts' downstream boundary conditions. Namely, $\frac{\partial u_i}{\partial x} = 0$, $x = L$, $i = 1, 2$, i.e. the left boundary (downstream) is located farther away and does not have much influence on individuals inside the domain.

The reaction dynamics of (1.5.22) (i.e. $D_i = v_i = 0$) are Lotka-Volterra dynamics, and we know that there are four cases possible; see Subsection 1.2.3. One asks the question whether space, and, in particular, advection can change the result. When $v_i = 0$, we have no-flux boundary conditions, and the system has the same long-term behavior as the nonspatial system. Let us fix parameters so that Species 1 is competitively superior, but Species 2 has the higher growth rate at low density, and study whether advection can change this outcome.

To keep the number of parameters to a minimum, the authors assume that

$$\frac{R_2}{R_1} = \rho > 1, \quad A_{21}\rho < A_{22}, \quad A_{11}\rho < A_{12}, \quad D_1 = D_2 = D, \quad v_1 = v_2 = v.$$

Based on biological observation of downstream increasing nutrients, let R_1, R_2 be linear nondecreasing functions.

Two competitors in a homogeneous advective environment

The homogeneous spatial model is characterized by constant growth rate. The result of competition in (1.5.22) strongly depends on the advection speed:

(a) The flow speed is low. In this case, Species 1 out-competes Species 2 and will move all the way to the upstream boundary.

(b) The flow speed is intermediate. In this case coexistence is possible. It occurs in a boundary layer close to the upstream boundary. In particular, the intermediate advection speed causes a decline in the density of the first species. Therefore, at a low density of Species 1, Species 2 starts growing and occupies the territory close to the upstream boundary (to the left of Species 1). The coexistence region near the boundary becomes larger with the increase of v.

(c) Case of relatively high advection. When v is less than the critical advection for Species 1 and Species 2 is not present, Species 1 is able to persist in the domain. However, due to the competition, Species 2 occupies the habitat and the existence of Species 1 is not necessarily given. Additional increase in the advection (v is less than the critical advection for Species 2 only), leads to persistence of Species 2 alone. Under such condition, the existence of Species 1 in the domain is absolutely impossible. When v is very high, neither one of the species persists.

Figure 1.2 shows how in the case of low and high flow speeds both species propagate upstream.

Two competitors in the heterogeneous habitat

We observe various forms of heterogeneity in rivers, typically downstream gradients. For example, temperature and nutrient load increase with increasing distance from the source. In [30] Lutscher et al. consider a model for such a resource gradient.

The model equation for a single species is given by

$$\frac{\partial u}{\partial t} = D\frac{\partial^2 u}{\partial x^2} - v\frac{\partial u}{\partial x} + u(R(x) - Au),$$

where A is a positive constant.

Assume that the habitat exceeds the critical domain size. Since the nutrient concentration increases downstream, it makes sense to assume that so does the growth

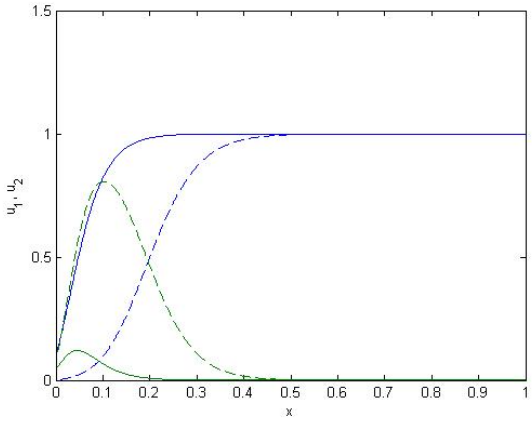

Figure 1.2: Spatial profiles of two competing species for low (solid) and high (dashed) values of advection. Species 1 (u_1) dominates most of the habitat, while Species 2 (u_2) emerges in the upstream region, "pushing" Species 1 downstream for higher values of advection.

rate. Numerical simulations show that there exists a unique point x^* in the domain such that an upstream spreading wave comes to a complete stop at this point, i.e. $v = 2\sqrt{DR(x^*)}$. Such x^* is called the invasion limit point. The authors compute it explicitly using the model parameters.

The behavior of single species population with non-constant growth rate can be summarized as follows:

(1) The species occupies the downstream end with density near carrying capacity, and with almost zero density at the top of the stream.

(2) Species spreads in a form of upstream waves that stall at the invasion limit point.

In the case of heterogeneous environment, the growth rates of both populations change monotonically in space. In the absence of its competitor, each species has its own invasion limit x_1^* and x_2^*, where $v = \sqrt{DR_1(x_1^*)} = \sqrt{DR_2(x_2^*)}$.

Observation 1: We have $x_2^* < x_1^*$, because of the assumption of the higher growth rate of Species 2. In addition to the notion of the invasion limit considered above,

the authors introduced the second one, which is obtained by fixing the density of the competitor at its single-species carrying capacity. As a result, a reduced growth rate $R_i - A_{ij}\frac{R_j}{A_{jj}}$, $i, j = 1, 2$ is used in place of the original growth rate. The second invasion limit is given by x_i^{**} such that

$$v = 2\sqrt{D\left(R_i(x_i^{**}) - A_{ij}\frac{R_j(x_i^{**})}{A_{jj}}\right)}. \tag{1.5.23}$$

Clearly, in the absence of the competitor ($A_{ij}\frac{R_j}{A_{jj}} = 0$), expression (1.5.23) is reduced to $v = 2\sqrt{DR_i(x_i^*)}$.

Observation 2: Due to the additional decrease in the growth rate, $x_i^* < x_i^{**}$. First, Species 2 propagates as a fast travelling wave and stops at the invasion limit x_2^*. Downstream, Species 1 outcompetes Species 2 and moves upstream. As a result of the interaction between two species, the first species stops at the "modified" invasion limit x_1^{**} and occupies the downstream part of the habitat.

In conclusion, it is necessary to mention that there are some distinguishing features of the two environments. In the homogeneous case, one can observe the appearance of the boundary layer (coexistence region near the boundary), which increases and decreases with the advection speed. When v is small, Species 1 outcompetes Species 2, and vice versa when v is large. Practical implications of this observation are that changes in the flow speed of rivers due to human activity (building dams, canals, etc) affect the balance between various aquatic organisms.

The second case (heterogeneous environment) corresponds to a more realistic situation. Usually the amount of nutrients in rivers and other habitats increases downstream. As a result, the growth rate of aquatic populations increases downstream as well. The weaker competitor (with higher growth rate) establishes upstream and propagates downstream with the flow. In the long term, depending on v, it has the ability to occupy the whole region. Therefore, despite the fact that the other species is a better competitor, it is being pushed away by the weaker one. Note that there

is a coexistence zone in the heterogeneous environment as well. But this zone occurs near the reduced invasion limit of the first species, rather than close to the upstream boundary like in the homogeneous case.

1.5.3 Two competitors in a moving habitat

The model and the results from the previous subsection are closely related to the following model describing the ecological phenomenon caused by the global warming, which at first does not seem to have much in common with the advective environments.

One of the possible consequences of global warming is the shift of the habitat boundaries for certain species. In [40], Potapov and Lewis study the effect of moving range boundaries on the population dynamics of two competing species.

In the following model, $u_1(t,x)$ and $u_2(t,x)$ and $x_1(t) < x_2(t)$ are densities of two competing species and the moving habitat boundaries, respectively. For simplicity, it is assumed that the length of the moving domain is fixed ($x_2(t) - x_1(t) = L$) and the velocity $\frac{dx_1(t)}{dt} = \frac{dx_2(t)}{dt} = c$ is constant. The model describes the dispersal, growth and competition inside the moving habitat, while, outside the habitat, the species are assumed to die without competing or reproducing:

$$\frac{\partial u_1}{\partial t} = D_1 \frac{\partial^2 u_1}{\partial x^2} + (r_1 - \alpha_{11}u_1 - \alpha_{12}u_2)u_1, \tag{1.5.24}$$

$$\frac{\partial u_2}{\partial t} = D_2 \frac{\partial^2 u_2}{\partial x^2} + (r_2 - \alpha_{21}u_1 - \alpha_{22}u_2)u_2, \tag{1.5.25}$$

for $x_1(t) \leq x \leq x_2(t)$ and

$$\frac{\partial u_1}{\partial t} = D_1 \frac{\partial^2 u_1}{\partial x^2} - \kappa_1 u_1, \tag{1.5.26}$$

$$\frac{\partial u_2}{\partial t} = D_2 \frac{\partial^2 u_2}{\partial x^2} - \kappa_2 u_2, \tag{1.5.27}$$

for $x \notin [x_1(t), x_2(t)]$.

By introducing a change of variables $x \to x - ct$, one can reduce the situation to a fixed domain with advection (c being the advection speed), which has the following nondimensionalized form ($D = \frac{D_2}{D_1}$, $r = \frac{r_2}{r_1}$):

$$\frac{\partial u_1}{\partial t} = \frac{\partial^2 u_1}{\partial x^2} + c\frac{\partial u_1}{\partial x} + (1 - u_1 - \alpha_{12}u_2)u_1, \tag{1.5.28}$$

$$\frac{\partial u_2}{\partial t} = D\frac{\partial^2 u_2}{\partial x^2} + c\frac{\partial u_2}{\partial x} + (r - u_2 - \alpha_{21}u_1)u_2, \tag{1.5.29}$$

for $0 \leq x \leq L$, and

$$\frac{\partial u_1}{\partial t} = \frac{\partial^2 u_1}{\partial x^2} + c\frac{\partial u_1}{\partial x} - \kappa_1 u_1, \tag{1.5.30}$$

$$\frac{\partial u_2}{\partial t} = D\frac{\partial^2 u_2}{\partial x^2} + c\frac{\partial u_2}{\partial x} - \kappa_2 u_2, \tag{1.5.31}$$

for $x < 0$ or $x > L$, with the continuity condition for u_i and u_{ix}. The authors also assume $\kappa_1 = \kappa_2$.

In the absence of competitor, the situation is analogous to the Speirs-Gurney model, and thus, each species has its critical advection speed: $c_1^* = 2$, $c_2^* = 2\sqrt{Dr}$. When the speed $|c|$ exceeds c_i^*, the ith species cannot survive.

For a steady state solution ($\frac{\partial u_i}{\partial t} = 0$) the authors make an exponential ansatz $u_i(x) \sim e^{k_i x}$ outside of the domain $[0, L]$, which allows them to reduce the stationary problem to the interval $[0, L]$ with Robin's boundary conditions:

$$\frac{\partial^2 u_1}{\partial x^2} + c\frac{\partial u_1}{\partial x} + (1 - u_1 - \alpha_{12}u_2)u_1 = 0, \quad 0 < x < L, \tag{1.5.32}$$

$$D\frac{\partial^2 u_2}{\partial x^2} + c\frac{\partial u_1}{\partial x} + (r - u_2 - \alpha_{21}u_1)u_2 = 0 \quad 0 < x < L, \tag{1.5.33}$$

$$\frac{\partial u_i}{\partial x} - k_i^+ u_i = 0, \quad x = 0, \quad i = 1, 2, \tag{1.5.34}$$

$$\frac{\partial u_i}{\partial x} - k_i^- u_i = 0, \quad x = 0, \quad i = 1, 2, \tag{1.5.35}$$

where $k_i^+ > 0$, $k_i^- < 0$ are the roots of the characteristic equations for the exponential ansatz in the cases $x < 0$, $x > L$ respectively. The solution of (1.5.32-1.5.35) is also a stationary solution of the following boundary value problem:

$$\frac{\partial u_1}{\partial t} = \frac{\partial^2 u_1}{\partial x^2} + c\frac{\partial u_1}{\partial x} + (1 - u_1 - \alpha_{12} u_2)u_1, \quad 0 < x < L, \tag{1.5.36}$$

$$\frac{\partial u_2}{\partial t} = D\frac{\partial^2 u_2}{\partial x^2} + c\frac{\partial u_2}{\partial x} + (r - u_2 - \alpha_{21} u_1)u_2, \quad 0 < x < L, \tag{1.5.37}$$

$$\frac{\partial u_i}{\partial x} - k_i^+ u_i = 0, \quad x = 0, \quad i = 1, 2, \tag{1.5.38}$$

$$\frac{\partial u_i}{\partial x} - k_i^- u_i = 0, \quad x = 0, \quad i = 1, 2, \tag{1.5.39}$$

Although (1.5.28-1.5.31) and (1.5.36-1.5.39) have different nonstationary solutions, it turns out that the stationary solutions of (1.5.28-1.5.31) and (1.5.36-1.5.39) are either both stable or both unstable, provided κ or c are nonzero. The system (1.5.36-1.5.39) has been used by the authors to perform numerical analysis of the stationary solutions and invasibility of the original model.

The authors find that habitat motion slows down the growth, leads to the increase of the critical domain size for each species, facilitates coexistence, and may reverse the invasion: the weaker competitor may become more successful. This is similar to the findings in the previous section, where the outcome of the competition was being affected by the advection speed.

The reaction-advection-diffusion models described above did not consider explicitely the dynamics of the nutrient. However, in some ecological settings, it makes sense to make density of the nutrient a part of the model. In a series of papers [3], [4], [5], Ballyk et al. study a model of the so called "flow reactor", where one or several microbial species grow and compete for an explicit nutrient in the domain of fixed length L. Inside the tubular reactor, liquid medium moves at constant velocity. The nutrient enters the flow at a constant concentration, and the unused portion of the nutrient exits at the outflow (as do the organisms). Unlike the chemostat, in this model, the medium inside the reactor is not well-mixed and the authors take into consideration the spatial component. The authors use a system of reaction-advection-diffusion equations to describe dynamics of a nutrient and a single species, or two competing species and a nutrient. In the case of a single species, the authors find an eigenvalue condition equivalent to the instability of the "washout state", and establish the existence of a non-trivial steady state solution in this case. They also use numerics investigate its stability. In the case of competing species, they found that the outcome of the competition strongly depends on the motility (diffusivity) of the two species. We will not go into more details, since throughout this thesis we will not consider an explicit nutrient.

1.6 Outline of the thesis

We will now give a brief outline of the next three chapters. The chapters can be read independently. In Chapter 2, we study a reaction-diffusion-advection model for a single logistically growing species in advective environment. In this context, we give a possible explanation of the drift paradox. Namely, we show that there is a nontrivial stable steady state for the model, and the population approaches this steady state in the long term. In addition, we perform qualitative analysis of the steady state. A steady state of our PDE model can be viewed as a solution of a second order ordinary

differential equation (or a system of two first order ODE). We use this ODE approach based on phase-plane analysis.

In Chapter 3, we study the spatial Lotka-Volterra competition model in an advective environment. We use linearization at single-species steady states to analyze mutual invasion conditions. Here, we use variational formulas for principal eigenvalues, "nonspatial approximation" technique (reducing to the nonspatial Lotka-Volterra model, with an extra "death term", as introduced in the end of Chapter 2), and perform numerical simulations to obtain various bifurcation diagrams.

In Chapter 4, we study a spatial Lotka-Volterra competition model for three species in an advective environment. We use nonspatial approximation (introduced in Chapter 2 and used in Chapter 3) to analyze the behavior of our model as we change advection. We analyze the effect of advection on persistence and permanence, focusing on two special cases, and using techniques from linear algebra. We compare numerical simulations of the spatial model with our results.

Chapter 2

Single species

2.1 Introduction

Streams, rivers and coastlines with longshore currents are aquatic ecosystems characterized by unidirectional water movement. As a result, many organisms that inhabit these systems are carried downstream by the bias in movement. Examples include plankton, algae, stream insects, or larvae of benthic organisms such as sea urchins. Despite this bias, populations resist washout and manage to persist over many generations in such advective environments. This biological phenomenon has been recognized and studied for more than half of a century, and is known as the "drift paradox" (see [34, 35]). The most commonly cited resolution for the paradox is that many stream insects have winged adult stages, during which individuals can travel upstream [50].

A different mechanism for persistence that does not require a winged adult stage was given by Speirs and Gurney [47]. Using a linear model, these authors showed that a sufficient amount of (unbiased) random movement can balance the biased movement and lead to population persistence. A similar (nonlinear) model with biased and unbiased movement arises in models for microbes in the gut [4] and in the study

of phytoplankton blooms [20, 44]. Gravity causes phytoplankton to sink (biased) whereas diffusion in the water column gives rise to unbiased movement. Huisman et al. obtained a variety of numerical results for such a model [20], several analytical results were recently given for a similar model by Kolokolnikov et al. [24]. The model by Speirs and Gurney was recently extended to study more realistic situations by including a benthic compartment [32, 38], spatial heterogeneity [29] or a competing species [30].

Most of the results pertaining to streams and rivers cited above are based either on linear analysis [38, 47] or on numerical simulation [30]. The topic of this chapter is to analytically study the underlying nonlinear equation, its non-trivial steady state and its dependence on parameters. More specifically, we study the (non-dimensional) reaction-advection-diffusion equation

$$\frac{\partial u}{\partial t} = \frac{\partial^2 u}{\partial x^2} - q\frac{\partial u}{\partial x} + u(1-u), \tag{2.1.1}$$

where $u(t,x)$ is the population density at location x at time t, and q is the advection speed. We consider this equation together with reflecting boundary conditions upstream, i.e., $\frac{\partial u}{\partial x} = qu$ at $x = 0$, and "outflow" boundary conditions downstream, i.e. $\frac{\partial u}{\partial x} = 0$. A derivation of these boundary conditions from random walks together with a biological interpretation was given in [29].

Equation (2.1.1) is a generalization of the well-known and well-studied Fisher equation

$$\frac{\partial u}{\partial t} = \frac{\partial^2 u}{\partial x^2} + u(1-u), \tag{2.1.2}$$

that describes unbiased random movement [15]. One typically considers this equation on a bounded domain $[0, L]$ with "hostile" boundary conditions $u = 0$ at $x = 0$ and $x = L$. The steady-state solutions of (2.1.2) satisfy a two-dimensional system of ODEs that happens to be Hamiltonian (see e.g. [25]). Using the explicitly available Hamiltonian function, one can show under what conditions non-trivial steady states

exist, give explicit formulas for the domain length L and establish the bifurcation structure [25]; see Subsection 1.4.1 in the Introduction.

Unfortunately, the system with advection (2.1.1) is not Hamiltonian, and none of the analysis mentioned above carries over to the general case. The goal of this chapter is to establish existence, uniqueness, stability and qualitative dependence on parameters of the non-trivial steady state of (2.1.1), using phase-plane methods for the steady-state equations. Some of this analysis is similar in spirit to the recent work by Kolokolnikov et al. [24], who studied a similar equation, but with zero-flux second boundary condition and a different nonlinear reaction term.

This chapter is organized as follows. In Section 2.2, we briefly discuss the linear model and deduce the formula for the "critical domain size" L^c (the minimal length of the interval for which the trivial steady state is unstable) in our context, i.e. with boundary conditions different from the ones used by Speirs and Gurney [47]. In Section 2.3, we introduce the nonlinear model and make some preliminary observations regarding existence and non-existence of steady-state solutions. In Section 2.4, we analyze the behavior of the domain size $L = L_\mu$ or $L = L^\nu$ as a function of downstream density $\mu = u(L)$ or upstream density $\nu = u(0)$, respectively. We show that L^ν (L_μ) is a strictly increasing function of ν (of μ). Furthermore, L_μ approaches the critical domain size L^c from the linear model as $\mu \to 0$ and goes to infinity as μ approaches the carrying capacity (scaled to one). In Section 2.5, we show existence and uniqueness of a nontrivial steady-state solution for $L > L^c$ for the case of finite and infinite ($L = \infty$) domains. We also show that the positive steady state solution is stable in case of finite domains. The remaining sections are devoted to the qualitative behavior of the positive steady state solution. In Sections 2.6 and 2.7, we show that the density at the steady-state decreases pointwise for increasing advection q for infinite and finite domains, respectively. For finite domains, we also show that the density at the steady state increases pointwise if we increase the growth rate. In Section 2.8, we investigate the conditions under which the steady-state profile has an inflection point

and derive an approximate expression for the distance of the inflection point to the upstream boundary. In Section 2.9, we summarize our results, give their biological interpretation and present some reallife examples.

The last two sections are somewhat independent of the rest of the chapter. Section 2.9 deals with a minor generalization of the two-compartment model studied in [38]. Section 2.10 introduces a "nonspatial" approximation of the reaction-diffusion-advection operator, which will be used in Chapters 3 and 4.

One final comment is on order before we embark on the analysis. The challenge that we set ourselves here was to remain within the theory of ODEs and phase-plane analysis and see how many of the results for the Hamiltonian system ($q = 0$) can still be obtained without the Hamiltonian structure available. However, for some of the results presented in Sections 2.5 and 2.7, we provide alternative proofs obtained by PDE methods.

2.2 The model and its linearization

Let $u(t, x)$ be the population density at a distance x from the upstream boundary at time t. We consider the single population model in an advective environment, described by the reaction-diffusion-advection equation

$$\frac{\partial u}{\partial t} = D\frac{\partial^2 u}{\partial x^2} - Q\frac{\partial u}{\partial x} + ru\left(1 - \frac{u}{K}\right). \tag{2.2.1}$$

The first term on the right in (2.2.1) corresponds to diffusive movement of individuals (due to self-propelling and/or water turbulence) with diffusion coefficient D. The second term represents movement of the organisms that is caused by drift (Q is the effective speed of the current). The third term reflects the assumption that the population grows logistically, with intrinsic growth rate r and environmental carrying capacity K. We assume that all parameters are positive. We consider some biological examples in Chapter 5 of the thesis.

In addition, we consider so-called "Danckwerts' boundary conditions" [4]

$$\begin{cases} Qu(t,0) - D\dfrac{\partial u}{\partial x}(t,0) = 0, \\ \dfrac{\partial u}{\partial x}(t,L) = 0. \end{cases} \tag{2.2.2}$$

These boundary conditions are well-established in the context of so-called Plug Flow Tubular Reactors; see p. 569 in [2] and models for nutrient transport in the gut [4]. They have also been derived from an individual random walk in [29].

The reflecting upstream boundary condition tells us that individuals cannot cross the upstream boundary ($x = 0$) and move beyond the top of the stream. The downstream condition indicates that net outflux from the domain is due to advection only and not to diffusion. This can be seen in a variety of ways. For example, if one considers the flux J of individuals, as a combination of advective and diffusive fluxes,

$$J = J_{\text{diff}} + J_{\text{adv}} = -D\frac{\partial u}{\partial x} + Qu,$$

then this flux reduces to the advective flux at the boundary. The random-walk interpretation in [29] gives the same. Alternatively, if one considers the movement equation only - i.e., (2.2.1) with $r = 0$ - and integrates over the domain, then one obtains

$$\frac{d}{dt}\int_0^L u(t,x)dx = -Qu(L).$$

Hence, the change is due to individuals leaving the domain by advection. Biologically, this situation may most closely describe a river flowing into non-advective freshwater habitat, such as a lake. The flow takes individuals into the lake, but since conditions in the lake are not hostile, individuals can also diffuse back and forth so that the net diffusive flux is zero.

Speirs and Gurney [47] studied the reaction-diffusion-advection equation with a linear growth term:

$$\frac{\partial u}{\partial t} = D\frac{\partial^2 u}{\partial x^2} - Q\frac{\partial u}{\partial x} + ru.$$

Instead of the "outflow" boundary condition $\frac{\partial u}{\partial x}(t, L) = 0$, the authors considered "hostile" downstream boundary condition $u(t, L) = 0$, i.e. organisms are being removed from the system as soon as they reach the left border of domain, see Section 1.5. The following is analogous to Proposition 1.5.1 in Section 1.5, Chapter 1.

In our case, we get the Speirs-Gurney equation (with outflow downstream boundary condition) if we linearize (2.2.1) at zero:

$$\begin{cases} \frac{\partial u}{\partial t} = D\frac{\partial^2 u}{\partial x^2} - Q\frac{\partial u}{\partial x} + ru, \\ Qu(t,0) - D\dfrac{\partial u}{\partial x}(t,0) = 0, \\ \dfrac{\partial u}{\partial x}(t,L) = 0. \end{cases} \tag{2.2.3}$$

Proposition 2.2.1 *The general solution of (2.2.3) is given by* $u(t,x) = \sum_{k=1}^{\infty} e^{\lambda_k t}\left(A_k e^{\frac{Q}{2D}x}\cos\frac{\sqrt{4D(r-\lambda_k)-Q^2}}{2D}x + B_k e^{\frac{Q}{2D}x}\sin\frac{\sqrt{4D(r-\lambda_k)-Q^2}}{2D}x\right)$, *where λ_k are eigenvalues of the operator*

$$D\frac{\partial^2 f}{\partial x^2} - Q\frac{\partial f}{\partial x} + rf$$

with boundary conditions

$$Qf(0) - Df'(0) = 0, \qquad f'(L) = 0.$$

Proof: Standard separation of variables technique. ∎

Classical Sturm-Liouville theory states that the eigenvalues λ_k above form an infinite decreasing sequence $\lambda_1 > \lambda_2 > \ldots$ [7]. If λ_k are all negative, then the population goes extinct in the long term. On the other hand, if for some k we have $\lambda_k > 0$, the population exhibits unbounded growth. Setting $\lambda_1 = 0$ and applying boundary conditions to the general solution of (2.2.3) gives us the critical domain

size L^c:

$$L^c(Q) = \begin{cases} \frac{\arctan\left(\frac{Q\sqrt{4rD-Q^2}}{2rD-Q^2}\right)}{\theta}, & 0 < Q \leq \sqrt{2rD}, \\ \\ \frac{\pi+\arctan\left(\frac{Q\sqrt{4rD-Q^2}}{2rD-Q^2}\right)}{\theta}, & \sqrt{2rD} < Q < 2\sqrt{rD}, \end{cases} \tag{2.2.4}$$

where

$$\theta = \frac{\sqrt{4rD - Q^2}}{2D}.$$

Note that for $Q = \sqrt{2rD}$, both formulas give us $L^c(\sqrt{2rD}) = \frac{\pi}{2\theta}$, and thus L^c depends continuously on Q.

Remark 2.2.2 When advection reaches its critical value $Q_c = 2\sqrt{Dr}$, the critical domain size becomes infinite and the entire population is washed downstream, i.e. persistence is not possible. For $Q < Q_c$ and $L < L^c$, the population goes extinct as well. For $Q < Q_c$ and $L > L^c$, the population in the linearized model experiences unlimited growth.

2.3 The nonlinear system, steady state solutions, and connection with the Fisher equation

We now consider the nonlinear model. We will make our first observations regarding the existence and nonexistence of a nontrivial steady state solution as we vary the advection speed. We start by nondimensionalizing (2.2.1) and (2.2.2). We rescale the population density by the carrying capacity, time and space by characteristic time and length:

$$\tilde{u} = \frac{u}{K}, \quad \tilde{t} = rt, \quad \tilde{x} = \sqrt{\frac{r}{D}}x, \quad q = \frac{Q}{\sqrt{Dr}}.$$

We omit the tildes for convenience, so that (2.2.1, 2.2.2) become

$$\begin{cases} \frac{\partial u}{\partial t} = \frac{\partial^2 u}{\partial x^2} - q\frac{\partial u}{\partial x} + u\,(1-u)\,, \\ \\ qu(t,0) - \frac{\partial u(t,0)}{\partial x} = 0, \qquad \frac{\partial u(t,L)}{\partial x} = 0. \end{cases} \tag{2.3.1}$$

We investigate the properties of non-zero steady state solutions of (2.3.1); i.e. solutions that do not depend on time. Such a steady state solution satisfies

$$u'' - qu' + u(1-u) = 0 \tag{2.3.2}$$

with boundary conditions

$$\begin{cases} u' = qu, & x = 0, \\ u' = 0, & x = L. \end{cases} \tag{2.3.3}$$

Equation (2.3.2) is equivalent to the following system of two differential equations:

$$\begin{cases} u' = v, \\ v' = qv - u(1-u), \end{cases} \tag{2.3.4}$$

with boundary conditions

$$\begin{cases} v = qu, & x = 0, \\ v = 0, & x = L. \end{cases} \tag{2.3.5}$$

Hence, we are looking for orbits of (2.3.4) connecting the straight lines $v = qu$ and $v = 0$. Let us refer to such solutions as "connecting orbits".

Next, we use the classical result of Fisher [15] and point out the similarity of equation (2.3.1) with the Fisher equation written in travelling wave coordinates.

Remark 2.3.1 (a) For Fisher's equation (2.1.2) on the real line, there exists a special solution in form of a monotone, positive travelling wave $u(t,x) = \phi(x+ct)$ (moving from the right to the left) iff $c \geq 2$ ($c \geq 2\sqrt{Dr}$ in the dimensional case) [15, 25]; see Subsection 1.4.3 in the Introduction. In travelling wave coordinates, Fisher's equation takes the form

$$c\phi' = \phi'' + \phi(1-\phi) \tag{2.3.6}$$

with boundary conditions $\phi(\infty) = 1$ and $\phi(-\infty) = 0$. More specifically, a travelling wave solution of Fisher's equation corresponds to a (unique) heteroclinic connection, located in the first quadrant of the uv-plane and connecting two fixed points: $(0, 0)$ and $(1, 0)$ of (2.3.4) obtained from (2.3.2). Since equation (2.3.2) is the same as (2.3.6), with $c = q$, we can use Fisher's results in our setting. Note that one can consider a solution of the form $u(t, x) = \phi(x - ct)$ with the boundary conditions $\phi(-\infty) = 1$ and $\phi(\infty) = 0$ (travelling wave moving from the left to the right). However the corresponding heteroclinic orbit is located in the fourth quadrant, and this is not applicable in our discussions.

(b) Note that if $q \geq 2$ then the fixed point $(0, 0)$ of the system (2.3.4) is an unstable node and we have "node-saddle" heteroclinic connection (travelling wave). For $q < 2$, point $(0, 0)$ is an unstable spiral and we observe "focus-saddle" heteroclinic connection from $(0, 0)$ to $(1, 0)$, approaching the fixed point $(1, 0)$ from the first quadrant. There is no nonnegative travelling wave in this case.

First we show that when the advection speed is greater than the threshold value $q^* = 2$ ($Q^* = 2\sqrt{Dr}$ in the dimensional case), then the population will not be able to persist.

Lemma 2.3.2 *There are no nontrivial solutions of (2.3.4, 2.3.5) for $q \geq q^*$.*

Proof: By Remark 2.3.1(a), we have a heteroclinic connection

$$u = u_1(x), v = v_1(x),$$

between the origin and the fixed point $(1, 0)$, located entirely in the first quadrant, approaching $(0, 0)$ and $(1, 0)$ as $x \to -\infty$ and $x \to \infty$, respectively.

Note that the slope of the vector field defined by (2.3.4) at any point in the uv-plane is given by

$$\frac{v'}{u'} = \frac{qv - u(1-u)}{v} = q - \frac{u(1-u)}{v} < q.$$

Thus, for any $0 < u < 1$ and $v > 0$, the slope of any solution of (2.3.4) (including the heteroclinic orbit) is less than q. Therefore, for $u > 0$, the line $v = qu$ will always stay above the curve $u = u_1(x)$, $v = v_1(x)$.

Suppose there exists a solution of (2.3.4) that starts at $v = qu$ for $x = 0$ and reaches $v = 0$ when $x = L$ for some $L > 0$. In this case the solution (connecting orbit) must intersect $v = 0$ when $u \in [0, 1]$. Indeed, if $u > 1$, then the slope of the vector field on $\{v = 0\}$ is positive, and we will not be able to reach $v = 0$. Thus, since the connecting orbit reaches the segment $[0, 1]$ of $\{v = 0\}$, it must intersect the heteroclinic orbit or pass through the fixed point. Neither one can happen, because two solution curves cannot intersect (by uniqueness), and the fixed point $(1, 0)$ cannot be reached for a finite L. ∎

From here on, we assume that $0 \leq q < q^* = 2$. We show that when advection is less than critical, there are nontrivial steady states for some domain size L.

Lemma 2.3.3 *For any $0 \leq q < q^*$, there exists $L > 0$ for which (2.3.4, 2.3.5) has a nontrivial solution.*

Proof: The linearization of system (2.3.4) at $(0, 0)$ is given by

$$\begin{cases} u' = v, \\ v' = qv - u. \end{cases} \tag{2.3.7}$$

The Jacobian of this system has the two complex roots $\lambda_{1,2} = \frac{q \pm \sqrt{q^2-4}}{2}$. Therefore, the origin of the linear system is an unstable focus. By Grobman-Hartman Theorem (see [39]), the origin for the nonlinear system is an unstable focus as well. Thus, there exist solutions for appropriately chosen L. Namely, in a small neighborhood of the origin, the trajectories of system (2.3.4) spiral away from the origin and cross both lines corresponding to the boundary conditions. Consequently, there exist

solutions of the non-linear system (2.3.4) that start on the line $\{v = qu\}$ and end on the line $\{v = 0\}$ (second boundary condition). ∎

2.4 More on the steady state: domain size as the function of upstream/downstream density

In this section, we analyze the relationship between the domain size L and the upstream/downstream density in the case of a positive steady state of our model. Essentially, we show that higher density corresponds to larger domains.

Let $(u_1(x), v_1(x))$ be a solution of

$$\begin{cases} u' = v, \\ v' = qv - u(1-u), \end{cases} \tag{2.4.1}$$

satisfying $(u_1(-\infty), v_1(-\infty)) = (0, 0)$ and $(u_1(\infty), v_1(\infty)) = (1, 0)$. Such a solution exists (and its orbit is unique) by Remark 2.3.1(b). Since such a curve (the heteroclinic connection) will necessarily intersect the line $v = qu$, we may assume that $v_1(0) = qu_1(0)$, and $u_1(x), v_1(x) > 0$ for $x > 0$ (i.e. the "last" intersection of heteroclinic connection with $\{v = qu\}$ happens when $x = 0$). Then such a solution is unique.

Let $\nu_{\max} = u_1(0)$. For any $0 < \nu < \nu_{\max}$ let $(u_\nu(x), v_\nu(x))$ be the (unique) solution of (2.4.1) satisfying $(u_\nu(0), v_\nu(0)) = (\nu, q\nu)$ (see Figure 2.1 for illustration).

Considering the region bounded by the line $v = qu$, the positive u-axis, and the heteroclinic connection, we see that the curve $(u_\nu(x), v_\nu(x))$ will eventually cross the u-axis between $u = 0$ and $u = 1$. For any $0 < \nu < \nu_{\max}$, let $L^\nu > 0$ be such that $v_\nu(L^\nu) = 0$. Let $\mu_\nu = u_\nu(L^\nu)$. Then $0 < \mu_\nu < 1$ (again, see Figure 2.1). Note that $(u_\nu(x), v_\nu(x))$ is a continuous function of x and ν (e.g. see [39], p.78), and hence both L^ν (as the solution of $v_\nu(x) = 0$) and $\mu_\nu = u_\nu(L^\nu)$ are continuous functions of $\nu \in (0, \nu_{\max})$.

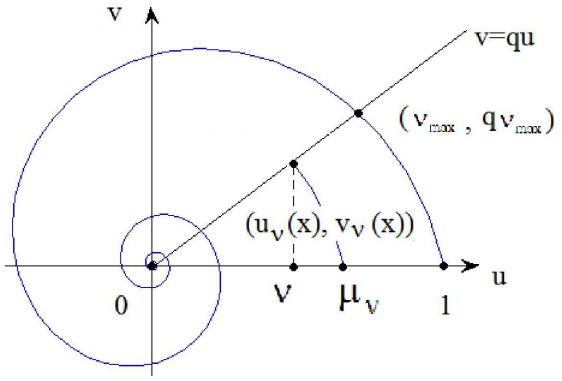

Figure 2.1: Connecting orbit for a finite domain and heteroclinic orbit in the uv-plane.

In this and later sections of the paper, some proofs are more conveniently formulated using upstream density ν whereas others become easier using downstream density μ. The following Lemma connects the two parameters.

Lemma 2.4.1 *The mapping $\nu \mapsto \mu_\nu$ is a continuous, strictly increasing function from $(0, \nu_{\max})$ onto $(0, 1)$. In particular, $\lim_{\nu\to 0} \mu_\nu = 0$ and $\lim_{\nu\to\nu_{\max}} \mu_\nu = 1$.*

Proof: Continuity is observed above, and the fact that μ_ν is strictly increasing with respect to ν follows from the observation that solution curves of (2.4.1) do not intersect. Note for any $0 < \mu < 1$ there exists a solution curve of (2.4.1) passing through $(\mu, 0)$. It will necessarily pass through a point $(\nu, q\nu)$ for some $0 < \nu < \nu_{\max}$. Hence $\mu = \mu_\nu$, and the mapping $\nu \mapsto \mu_\nu$ is onto. ∎

For $0 < \mu < 1$ let $L_\mu = L^\nu$ where $\mu = \mu_\nu$. So, L_μ is a continuous function of $\mu \in (0, 1)$. Now, we look at the behavior of L_μ as $\mu \to 0$. Our goal is to prove that $\lim_{\mu\to 0} L_\mu = L^c$, where L^c is the critical domain size for the linear system, given by (2.2.4).

It is slightly more convenient to consider the change of variables $x \mapsto -L + x$; i.e., we consider the boundary conditions $v(0) = 0, v(-L_\mu) = qu(-L_\mu)$. The solution of the nonlinear system (2.3.4) is given by the variation of constants formula as

$$\begin{bmatrix} u(x) \\ v(x) \end{bmatrix} = e^{Ax} \begin{bmatrix} \mu \\ 0 \end{bmatrix} + \int_0^x e^{A(x-s)} \begin{bmatrix} 0 \\ u^2(s) \end{bmatrix} ds, \qquad A = \begin{bmatrix} 0 & 1 \\ -1 & q \end{bmatrix}.$$

We denote by $[\hat{u}, \hat{v}]^T$ the solution of the linearized system (2.3.7) with $\hat{u} = 1, \hat{v} = 0$. Then $\hat{v}(-L^c) = q\hat{u}(-L^c)$. The solution with $\hat{u} = \mu, \hat{v} = 0$ is given by $\mu[\hat{u}, \hat{v}]^T$

If $u(0) = \mu$, then $u(x) < \mu$ for all $x < 0$. Hence, we can bound the distance between the solution of the nonlinear problem and the linear problem, starting at $(\mu, 0)$ for $x = -L_\mu$ from above by

$$\|[u(x) - \mu\hat{u}(x), v(x) - \mu\hat{v}(x)]^T\| \leq \mu^2 \left\| \int_0^x e^{A(x-s)} ds \right\|.$$

Therefore, there is a constant $C > 0$, for which

$$|\mu\hat{v}(-L_\mu) - q\mu\hat{u}(-L_\mu)| \leq \mu^2 C.$$

Since the solution of the linear problem satisfies the condition $\hat{v}(-L^c) = q\hat{u}(-L^c)$, we have proved the following theorem.

Theorem 2.4.2 *$L_\mu \to L^c$ as $\mu \to 0$ (equivalently, $L^\nu \to L^c$ as $\nu \to 0$).*

Remark 2.4.3 Figure 2.2 shows the graph of L^ν vs. ν for $q = 1$, obtained numerically. Note that by (2.2.4) for $q = 1$, $L^c(1) = \frac{2\pi}{3\sqrt{3}} \approx 1.2$, which agrees with the graph. Note also that L^ν appears to increase with ν, and goes to infinity as ν approaches a threshold value $\nu_{\max} \approx 0.212$.

Next, we give an analytical proof that L^ν is an increasing function of ν (as suggested by the numerics), following the idea of the proof of Lemma 2.1 in [6].

Proposition 2.4.4 *If $\nu_1 < \nu_2 < \nu_{\max}$, then $L^{\nu_1} < L^{\nu_2}$.*

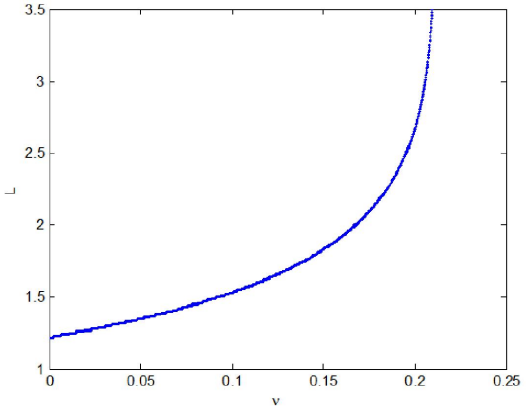

Figure 2.2: The graph of domain size $L = L^\nu$ as a function of upstream density ν, for $q = 1$ (obtained numerically).

Proof: Let $u(x)$ be the steady state solution of (2.1.1). Then

$$-(e^{-qx}u_x)_x = -e^{-qx}(-qu_x + u_{xx}) = e^{-qx}u(1-u).$$

Thus, the following equalities take place:

$$-(e^{-qx}u_x^{\nu_1})_x u^{\nu_2} = e^{-qx}u^{\nu_1}(1-u^{\nu_1})u^{\nu 2},$$

$$-(e^{-qx}u_x^{\nu_2})_x u^{\nu_1} = e^{-qx}u^{\nu_2}(1-u^{\nu_2})u^{\nu 1}.$$

Taking the difference between the above expressions and then integrating it between 0 and any $\alpha \in (0, \min(L^{\nu_1}, L^{\nu_2})]$ we obtain

$$e^{-qx}\left[u_x^{\nu_2}(x)u^{\nu 1}(x) - u_x^{\nu_1}(x)u^{\nu_2}(x)\right]|_0^\alpha = \int_0^\alpha e^{-qx}u^{\nu_1}(x)u^{\nu_2}(x)(u^{\nu_2}(x) - u^{\nu_1}(x))dx.$$

Using the boundary conditions at $x = 0$ we get

$$e^{-q\alpha}\left[u_x^{\nu_2}(\alpha)u^{\nu_1}(\alpha) - u_x^{\nu_1}(\alpha)u^{\nu_2}(\alpha)\right] = \int_0^\alpha e^{-qx}u^{\nu_1}(x)u^{\nu_2}(x)(u^{\nu_2}(x) - u^{\nu_1}(x))dx. \tag{2.4.2}$$

Next, we want to show that for all $x \in [0, \min(L^{\nu_1}, L^{\nu_2})]$ we have $u^{\nu_1}(x) < u^{\nu_2}(x)$. Note that since $u^{\nu_1}(0) = \nu_1 < \nu_2 = u^{\nu_2}(0)$ this is true for $x = 0$.

Suppose the statement is not true, then there exists $0 < \beta \leq \min(L^{\nu_1}, L^{\nu_2})$ such that $u^{\nu_1}(x) < u^{\nu_2}(x)$ for $x \in [0, \beta)$, but $u^{\nu_1}(\beta) = u^{\nu_2}(\beta)$. Then taking $\alpha = \beta$ in (2.4.2) and using

$$u^{\nu_1}(\beta) = u^{\nu_2}(\beta),$$

we get

$$e^{-q\beta} u^{\nu_1}(\beta) \left[u_x^{\nu_2}(\beta) - u_x^{\nu_1}(\beta)\right] = \int_0^\beta e^{-qx} u^{\nu_1}(x) u^{\nu_2}(x)(u^{\nu_2}(x) - u^{\nu_1}(x))dx. \qquad (2.4.3)$$

Note that the right hand side of (2.4.3) is positive, and therefore $u_x^{\nu_2}(\beta) > u_x^{\nu_1}(\beta)$. On the other hand, for $z(x) = u^{\nu_2}(x) - u^{\nu_1}(x)$ we have $z(x) > 0$ for $x \in [0, \beta)$ and $z(\beta) = 0$, which implies $z'(\beta) = u_x^{\nu_2}(\beta) - u_x^{\nu_1}(\beta) \leq 0$, a contradiction. Thus, we have proved that for any $x \in [0, \min(L^{\nu_1}, L^{\nu_2})]$ $u^{\nu_1}(x) < u^{\nu_2}(x)$.

Now, suppose $L^{\nu_2} \leq L^{\nu_1}$, so $\min(L^{\nu_1}, L^{\nu_2}) = L^{\nu_2}$. Then taking (2.4.2) with $\alpha = L^{\nu_2}$ and using the boundary condition $u_x^{\nu_2}(L^{\nu_2}) = 0$, we get

$$e^{-qL^{\nu_2}} \left[-u_x^{\nu_1}(L^{\nu_2}) u^{\nu_2}(L^{\nu_2})\right] = \int_0^{L^{\nu_2}} e^{-qx} u^{\nu_1}(x) u^{\nu_2}(x)(u^{\nu_2}(x) - u^{\nu_1}(x))dx > 0.$$

In the above equality, the right hand side is positive since $u^{\nu_2}(x) > u^{\nu_1}(x)$ on $[0, L^{\nu_2}]$, while the left hand side is negative, a contradiction. Thus, $L^{\nu_1} < L^{\nu_2}$.

∎

Finally, we look at the behavior of L^ν as $\nu \to \nu_{\max}$, or, equivalently, the behavior of L_μ as $\mu \to 1$. In the following theorem, we confirm the numerical observations made in Remark 2.4.3.

Theorem 2.4.5 *$L_\mu \to \infty$ as $\mu \to 1$ (equivalently, $L^\nu \to \infty$ as $\nu \to \nu_{\max}$).*

Proof: We use the standard result on continuous dependence on initial data to prove this theorem, see e.g. Theorem 1, Section 2.3 in [39]. Pick any $0 < X < \infty$ and $\epsilon > 0$. Since $(1, 0)$ is a steady state, we can pick $\delta > 0$ small enough so that the solution with initial data $(\mu, 0)$ and $|\mu - 1| < \delta$ remains within ϵ of $(1, 0)$ up to "time" X. Hence, as $\mu \to 1$, it will take the solution arbitrarily long to leave an ϵ-neighborhood of $(1, 0)$. In particular, $L_\mu \to \infty$. ∎

2.5 Existence, uniqueness and stability of the steady state

We use the results about L^ν to show existence and uniqueness of the solution of (2.3.4)-(2.3.5) for any $L > L^c$.

Theorem 2.5.1 *For any $L > L^c$ (2.3.4)-(2.3.5) has a unique positive solution. Equivalently, for any $L > L^c$ (2.3.1) has a unique positive steady state.*

Proof: We know that L^ν (as a function of ν) is continuous and increasing on $(0, \nu_{\max})$. It has finite limit L^c at 0 and goes to infinity as $\nu \to \nu_{\max}$. Clearly, for any $L > L^c$, there is exactly one $\nu \in (0, \nu_{\max})$ such that $L^\nu = L$. By the definition of L^ν, this means that there exists $(u(x), v(x))$ satisfying (2.3.4)-(2.3.5), such that $(u(0), v(0)) = (\nu, q\nu)$. Since $\nu \neq 0$, this solution is positive. Moreover, such a solution is unique (as a solution of an initial value problem). ∎

We now turn to the case of infinite domain.

Theorem 2.5.2 *For any $0 \leq q < 2$ there exists a unique solution $(u(x), v(x))$ of (2.4.1) satisfying $v(0) = qu(0)$ and $v(\infty) = 0$.*

Proof: Suppose $0 \leq q < 2$. We know that the solution $(u_1(x), v_1(x))$ of (2.4.1) with $u_1(0) = \nu_{\max}$ satisfies $\lim_{x\to\infty}(u_1(x), v_1(x)) = (1, 0)$. This implies existence of a steady state solution. Uniqueness follows from the fact that there is a unique solution of (2.4.1) satisfying $(u(0), v(0)) = (\nu_{\max}, q\nu_{\max})$, and if the solution does not pass through this point, it either reaches u-axis in finite "time" L, or does not approach to it at all. ∎

Our next goal is to prove stability of the positive steady state solution of (2.3.1) (when it exists). We linearize around the steady state, and make the ansatz $u(t, x) = u(x) + \phi(x)e^{-\lambda t}$. Substituting into (2.3.1) and keeping the leading order terms, gives the following eigenvalue problem:

$$\begin{cases} -\lambda\phi(x) = \phi''(x) - q\phi'(x) + \phi(x)(1 - 2u(x)), \\ \phi'(0) = q\phi(0), \\ \phi'(L) = 0. \end{cases} \tag{2.5.1}$$

To eliminate the advection term, we consider $\psi(x) = e^{-\frac{qx}{2}}\phi(x)$. Then (2.5.1) becomes

$$\begin{cases} \psi''(x) + (1 - \frac{q^2}{4} - 2u(x) + \lambda)\psi(x) = 0, \\ \psi'(0) - \frac{q}{2}\psi(0) = 0, \\ \psi'(L) + \frac{q}{2}\psi(L) = 0. \end{cases} \tag{2.5.2}$$

This problem has the same eigenvalues as (2.5.1). They form an increasing sequence $\lambda_1 < \lambda_2 < \ldots$ [7]. To prove stability, we need to show $\lambda_1 > 0$. Suppose $\psi_1(x)$ is the eigenfunction corresponding to the dominant eigenvalue λ_1. From classical Sturm-Liouville theory it follows that $\psi_1(x)$ is of one sign in $[0, L]$, so we may assume that $\psi_1(x) > 0$ for any $x \in (0, L)$.

Let $w(x) = e^{-\frac{qx}{2}}u(x)$. Substituting into (2.3.2) we get

$$\begin{cases} w''(x) + (1 - \frac{q^2}{4})w(x) - e^{\frac{q}{2}x}(w(x))^2 = 0, \\ w'(0) - \frac{q}{2}w(0) = 0, \\ w'(L) + \frac{q}{2}w(L) = 0. \end{cases} \tag{2.5.3}$$

Multiplying the equations in (2.5.3) by $\psi_1(x)$, and in (2.5.2) by $w(x)$, integrating between 0 and L, and taking the difference of the two expressions, we get

$$\int_0^L \psi_1''(x)w(x)dx - \int_0^L w''(x)\psi_1(x)dx + \lambda_1 \int_0^L \psi_1(x)w(x)dx -$$

$$-2\int_0^L u(x)\psi_1(x)w(x)dx + \int_0^L e^{\frac{q}{2}x}(w(x))^2\psi_1(x)dx = 0.$$

Note that

$$\int_0^L \psi_1''(x)w(x)dx - \int_0^L \psi_1(x)w''(x)dx =$$

$$\left(\psi_1'(x)w(x)|_0^L - \int_0^L \psi_1'(x)w'(x)dx\right) - \left(\psi_1(x)w'(x)|_0^L - \int_0^L \psi_1'(x)w'(x)dx\right) =$$

$$-\frac{q}{2}\psi_1(L)w(L) - \frac{q}{2}\psi_1(0)w(0) - \left(-\frac{q}{2}w(L)\psi_1(L) - \frac{q}{2}w(0)\psi_1(0)\right) = 0.$$

Also note that $e^{\frac{q}{2}x}(w(x))^2 = u(x)w(x)$. Thus we have

$$\lambda_1 \int_0^L \psi_1(x)w(x)dx - \int_0^L u(x)w(x)\psi_1(x)dx = 0,$$

or

$$\lambda_1 = \frac{\int_0^L u(x)w(x)\psi_1(x)dx}{\int_0^L \psi_1(x)w(x)dx} > 0.$$

With this result on eigenvalues, we are ready to prove stability of the steady state in case of a finite domain.

Theorem 2.5.3 *The positive steady state solution $u = u^*(x)$ of (2.3.1) with $0 < L < \infty$ is stable.*

Proof: The preceding calculation about eigenvalues shows that all solutions of the linearized problem decay exponentially, i.e. the linearized system is stable. We show that this implies that the steady state for the nonlinear system is stable as well. We use the Lumer-Philips theorem (Theorem 11.22 in [41]) to demonstrate that the linear differential operator in (2.3.1) generates a contraction semigroup. Theorem 11.22 in [46] together with compactness of the second-order differential operator imply that $u^*(x)$ is stable.

Consider the operator $A = \partial^2/\partial x^2 + q\partial/\partial x$, defined on the space

$$\mathcal{D} = \{U \in \mathcal{H}^2(0,L) | U_x(0) - qU(0) = 0,\ U_x(L) = 0\} \subset \mathcal{L}^2(0,L). \tag{2.5.4}$$

Considering the inner product on this space, we calculate

$$\begin{aligned} \int_0^L UAUdx &= \int_0^L UU_{xx}dx - q\int_0^L UU_x dx \\ &= UU_x|_0^L - \int_0^L U_x^2 dx - \frac{q}{2}(U^2)_x dx \\ &= -\int_0^L U_x^2 dx - \frac{q}{2}(U^2(L) + U^2(0)) < 0. \end{aligned}$$

Since the operator is compact, it has point spectrum, and it is easy to see that all eigenvalues are negative for $q > 0$. Hence, the operator $A - \xi I$ is invertible for all positive ξ. Therefore, A generates a contraction semigroup. ∎

2.6 Dependence of the steady state on advection speed for infinite domains

In this section, we investigate how changes in advection affect the steady state profile in the case of an infinite domain.

Consider the diffusion-advection-reaction equation with logistic growth term, reflecting boundary condition upstream and "outflow" condition at ∞.

$$\begin{cases} \frac{\partial u}{\partial t} = \frac{\partial^2 u}{\partial x^2} - q\frac{\partial u}{\partial x} + u\,(1-u)\,, \\ \\ qu(t,0) - \frac{\partial u(t,0)}{\partial x} = 0, \qquad \lim_{x\to\infty} \frac{\partial u(t,x)}{\partial x} = 0. \end{cases} \tag{2.6.1}$$

We are interested in the steady state solution, so we set $u_t = 0$ and $u = u(x)$. Thus, we consider the equation $u'' - qu' + u(1-u) = 0$, or, written as a first order system:

$$\begin{cases} u' = v, \\ v' = qv - u(1-u). \end{cases} \tag{2.6.2}$$

The above system has two fixed points: $(0,0)$ and $(1,0)$. It is known (see Remark 2.3.1b) that, for $q < q^*(= 2)$ the origin is an unstable spiral and $(1,0)$ is a saddle point. The heteroclinic orbit that connects these two fixed points also intersects the line corresponding to the boundary condition $v = qu$ in the first quadrant of uv-space. More specifically, there exists an orbit (u_q, v_q) such that

$$v_q(0) = qu_q(0) \tag{2.6.3}$$

and

$$\lim_{x\to\infty} (u_q(x), v_q(x)) = (1,0). \tag{2.6.4}$$

We have changed notations to stress the fact that we study the dependence of steady states on advection speeds, assuming that $\mu = 1$. Thus, we are interested in the behavior of $(u_q(x), v_q(x))$ with respect to the advection speed q. We may view this orbit as the graph of $v = v_q(u)$ (since $u'(x) = v(x) > 0$ in the first quadrant). Note that the curve $v = v_q(u)$ is the stable manifold of the fixed point $(1,0)$. Therefore, at this point, the curve is tangent to an eigenvector of the Jacobian of (2.6.2) at $(1,0)$ corresponding to the negative eigenvalue. Thus, we can find the slope of $v = v_q(u)$ at

$u = 1$ by analyzing that Jacobian. Namely, we have

$$J(u,v) = \begin{pmatrix} 0 & 1 \\ -1+2u & q \end{pmatrix}$$

and

$$J(1,0) = \begin{pmatrix} 0 & 1 \\ 1 & q \end{pmatrix}.$$

The eigenvalues of $J(1,0)$ are

$$\lambda_1 = \frac{q - \sqrt{q^2+4}}{2} < 0 \qquad \text{and} \qquad \lambda_2 = \frac{q + \sqrt{q^2+4}}{2} > 0.$$

An eigenvector corresponding to λ_1 is given by $\bar{v}_1 = (1, \frac{q-\sqrt{q^2+4}}{2})$. Thus, the slope of $v = v_q(u)$ at $(1,0)$ is $m(q) = \frac{q-\sqrt{q^2+4}}{2}$.

In the following, let $2 > q_1 > q_2$.

Lemma 2.6.1 $m(q_1) > m(q_2)$.

Proof: Note that $m'(q) = \frac{1}{2}\left(1 - \frac{q}{\sqrt{q^2+4}}\right) > 0$. Therefore, $m(q)$ is an increasing function of q and $m(q_1) > m(q_2)$.

∎

Lemma 2.6.2 *There exists* $0 < u^* < 1$ *such that* $v_{q_1}(u) < v_{q_2}(u)$ *for all* $u \in (u^*, 1)$.

Proof:

Let $w(u) = v_{q_1}(u) - v_{q_2}(u)$. The statement now follows from $w(1) = 0$ and $w'(1) = v'_{q_1}(1) - v'_{q2}(1) = m(q_1) - m(q_2) > 0$.

∎

Lemma 2.6.3 $v_{q_1}(u) < v_{q_2}(u)$ *for all* $\max(u_{q_1}(0), u_{q_2}(0)) \le u < 1$ *(common domain of* $v_{q_1}(u)$ *and* $v_{q_2}(u)$*).*

Proof: We know that $v_{q_1}(u) < v_{q_2}(u)$ for all $u^* < u < 1$. If this is not true for all

$$\max(u_{q_1}(0), u_{q_2}(0)) \leq u < 1,$$

there exists $0 < \bar{u} < 1$ such that $v_{q_1}(\bar{u}) = v_{q_2}(\bar{u}) = \bar{v}$. Then

$$(v_{q_2})_u(\bar{u}) = \lim_{u \to \bar{u}^+} \frac{v_{q_2}(u) - v_{q_2}(\bar{u})}{u - \bar{u}} = \lim_{u \to \bar{u}^+} \frac{v_{q_2}(u) - v_{q_1}(\bar{u})}{u - \bar{u}} \geq$$

$$\lim_{u \to \bar{u}^+} \frac{v_{q_1}(u) - v_{q_1}(\bar{u})}{u - \bar{u}} = (v_{q_1})_u(\bar{u}). \tag{2.6.5}$$

On the other hand,

$$(v_{q_2})_u(\bar{u}) = q_2 - \frac{\bar{u}(1-\bar{u})}{\bar{v}} < q_1 - \frac{\bar{u}(1-\bar{u})}{\bar{v}} = (v_{q_1})_u(\bar{u}), \tag{2.6.6}$$

a contradiction. ∎

Lemma 2.6.4 $u_{q_1}(0) < u_{q_2}(0)$.

Proof: Note that the slope of the line $v = q_2 u$ is q_2. The slope of the solution $v = v_{q_2}(u)$ is less than q_2:

$$\frac{dv}{du} = q_2 - \frac{u(1-u)}{v} < q_2.$$

Therefore $v_{q_2}(u) \leq q_2 u$ for any $u \in [\max(u_{q_1}(0), u_{q_2}(0)), 1)$. Thus, by Lemma 2.6.3, we have

$$v_{q_1}(u) < v_{q_2}(u) \leq q_2 u < q_1 u, \tag{2.6.7}$$

so $v_{q_1}(u) < q_1 u$ for all $u \in [\max(u_{q_1}(0), u_{q_2}(0)), 1)$. Thus, since $v_{q_1}(u_{q_1}(0)) = q_1 u_{q_1}(0)$, we conclude that $u_{q_1}(0) < \max(u_{q_1}(0), u_{q_2}(0)) = u_{q_2}(0)$. ∎

We are now ready to prove the main result of this section: the steady-state density decreases pointwise with increasing advection.

Theorem 2.6.5 *$u_{q_1}(x) < u_{q_2}(x)$ for any $x \geq 0$.*

Proof: By the above lemma, this statement is true for $x = 0$. If this is not true for some $x > 0$, then there exists $\bar{x} > 0$ such that $u_{q_1}(\bar{x}) = u_{q_2}(\bar{x})$. We may assume that $\bar{x}$ is the smallest such. Let $\bar{u} = u_{q_1}(\bar{x}) = u_{q_2}(\bar{x})$. First, note that by Lemma 2.6.3,

$$(u_{q_1})_x(\bar{x}) = v_{q_1}(u_{q_1}(\bar{x})) = v_{q_1}(\bar{u}) < v_{q_2}(\bar{u}) = v_{q_2}(u_{q_2}(\bar{x})) = (u_{q_2})_x(\bar{x}). \tag{2.6.8}$$

On the other hand, by the choice of $\bar{x}$, for any $0 < x < \bar{x}$ we have $u_{q_1}(x) < u_{q_2}(x)$, so

$$u_{q_1}(x) - u_{q_1}(\bar{x}) = u_{q_1}(x) - \bar{u} < u_{q_2}(x) - \bar{u} = u_{q_2}(x) - u_{q_2}(\bar{x}). \tag{2.6.9}$$

Since $x - \bar{x} < 0$, we get

$$\frac{u_{q_1}(x) - u_{q_1}(\bar{x})}{x - \bar{x}} > \frac{u_{q_2}(x) - u_{q_2}(\bar{x})}{x - \bar{x}}. \tag{2.6.10}$$

Taking a limit as $x \to \bar{x}^-$, we get

$$(u_{q_1})_x(\bar{x}) \geq (u_{q_2})_x(\bar{x}). \tag{2.6.11}$$

This is a contradiction. ∎

2.7 Dependence of the steady state on advection speed for finite domains

Now we consider the case of a domain of finite length and investigate the dependence of the steady state solution of (2.3.1) on the advection speed. The situation here is somewhat more complicated than in the previous section for an infinite domain, where the "endpoint" ($u(\infty) = 1$) was the same for all possible solutions.

Setting $u_t = 0$, we get the first order system:

$$\begin{cases} u' = v, \\ v' = qv - u(1-u), \\ v(0) = qu(0), \\ v(L) = 0. \end{cases} \tag{2.7.1}$$

We want to show that given $0 < q_2 < q_1 < q^* = 2$, a population inside a habitat of length L with advection speed q_1 will have lower density than a population in the same habitat with advection speed q_2, at any point of the domain $[0, L]$.

Our goal is to prove the following.

Theorem 2.7.1 *If $0 < q_2 < q_1 < 2$, $u_{q_1}(x)$ and $u_{q_2}(x)$ are the steady state solutions of (2.3.1) with $q = q_1$ and $q = q_2$ respectively, then*

$$u_{q_1}(x) < u_{q_2}(x), \quad x \in [0, L]. \tag{2.7.2}$$

Note that in the first quadrant ($u, v > 0$) any trajectory of system (2.7.1) can be viewed as a graph of a function $v = \bar{v}(u)$ (since $u' = v \neq 0$). Moreover, such curves are solution curves of the ODE $\dfrac{dv}{du} = q - \dfrac{u(1-u)}{v}$. In particular, no two such curves intersect.

First, we notice the effect of increasing the advection on the phase portrait of the ODE $\dfrac{dv}{du} = q - \dfrac{u(1-u)}{v}$.

Lemma 2.7.2 *Given $q_1 > q_2$, at any point (u^*, v^*) (in the first quadrant), the slope of the direction field of $\dfrac{dv}{du}|_{u=u^*} = q_1 - \dfrac{u^*(1-u^*)}{v^*}$ is greater than that of the equation $\dfrac{dv}{du}|_{u=u^*} = q_2 - \dfrac{u^*(1-u^*)}{v^*}$.*

Proof: Follows easily from the assumption $q_1 > q_2$. ∎

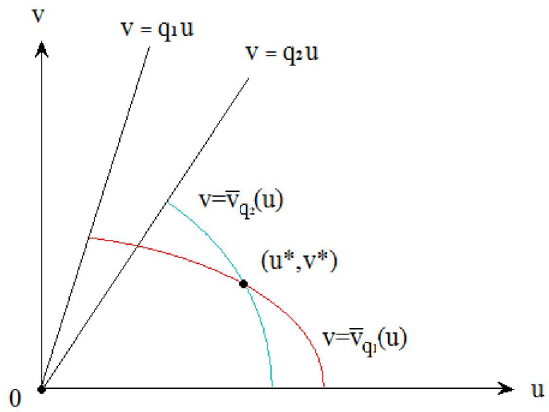

Figure 2.3: Intersection of orbits corresponding to different advection speeds.

Lemma 2.7.3 *Suppose $q_1 > q_2$. Let $v = \bar{v}_{q_1}(u)$ and $v = \bar{v}_{q_2}(u)$ be the solutions of*

$$\frac{dv}{du} = q_1 - \frac{u(1-u)}{v} \tag{2.7.3}$$

and

$$\frac{dv}{du} = q_2 - \frac{u(1-u)}{v} \tag{2.7.4}$$

respectively, both passing through a point (u^*, v^*) with $u^*, v^* > 0$. Then $\bar{v}_{q_1}(u) < \bar{v}_{q_2}(u)$ for $u < u^*$ and $\bar{v}_{q_2}(u) < \bar{v}_{q_1}(u)$ for $u^* < u$ (on the common domain of $\bar{v}_{q_1}$ and $\bar{v}_{q_2}$, see Figure 2.3).

Proof: Let $w(u) = \bar{v}_{q_1}(u) - \bar{v}_{q_2}(u)$. Thus, $w(u^*) = \bar{v}_{q_1}(u^*) - \bar{v}_{q_2}(u^*) = 0$ and $\frac{dw}{du}|_{u=u^*} = \frac{d}{du}(\bar{v}_{q_1}(u) - \bar{v}_{q_2}(u))|_{u=u^*} = \frac{d\bar{v}_{q_1}}{du}|_{u^*} - \frac{d\bar{v}_{q_2}}{du}|_{u^*} = q_1 - q_2 > 0$. This means that $w(u)$ has at most one zero and we have $w(u) < 0$ for $u < u^*$ and $w(u) > 0$ for $u > u^*$, as needed. ∎

Let $(u_{q_1}(x), v_{q_1}(x))$ be a solution of (2.7.1) with $q = q_1$. Let $v = \bar{v}_{q_1}(u)$ be the corresponding solution of $\frac{dv}{du} = q_1 - \frac{u(1-u)}{v}$, defined on the interval $(u_{q_1}(0), u_{q_1}(L))$.

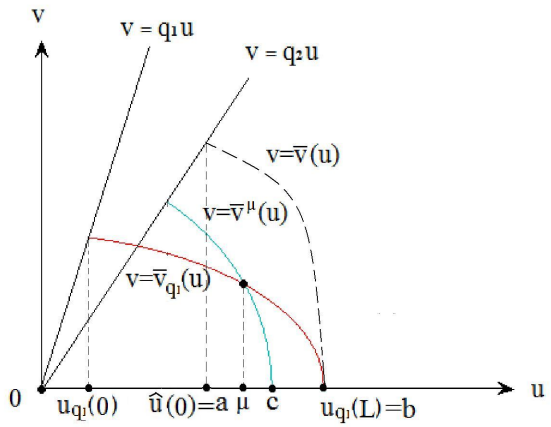

Figure 2.4: For given downstream density b, orbit corresponding to the higher advection (solid curve), lies below the orbit corresponding to the lower advection (dashed curve).

Let $(\hat{u}(x), \hat{v}(x))$ be the solution of (2.6.2) with $q = q_2$ passing through the point $(u_{q_1}(L), 0)$ such that $\hat{v}(0) = q_2\hat{u}(0)$, and let $v = \bar{v}(u)$ be the equation of this curve as a solution of $\dfrac{dv}{du} = q_2 - \dfrac{u(1-u)}{v}$, defined on the interval $(\hat{u}(0), u_{q_1}(L)) = (a, b)$.

Lemma 2.7.4 *For any $u \in (a, b)$, $\bar{v}(u) > \bar{v}_{q_1}(u)$.*

Proof: Take any $\mu \in (a, b)$. Let $v = \bar{v}^{\mu}(u)$ be the solution of $\dfrac{dv}{du} = q_2 - \dfrac{u(1-u)}{v}$ passing through the point $(\mu, \bar{v}_{q_1}(\mu))$. By Lemma 2.7.3, with $(u^*, v^*) = (\mu, \bar{v}_{q_1}(\mu))$, $\bar{v}^{\mu}(u) < \bar{v}_{q_1}(u)$ for any $u \in (\mu, c)$, where $c < b$ is the point where the curve $v = v^{\mu}(u)$ crosses the u-axis (see Figure 2.4). Since $v = \bar{v}(u)$ and $v = \bar{v}^{\mu}(u)$ cannot intersect, we have $\bar{v}(\mu) > \bar{v}^{\mu}(\mu) = \bar{v}_{q_1}(\mu)$, as needed. ∎

Let $L' > 0$ be such that $\hat{v}(L') = 0$. Let us prove that, in order to reach a certain downstream density (in our case, b), a population that is subject to a higher advection needs a larger habitat.

Lemma 2.7.5 $L > L'$.

Proof:

$$L = \int_{u_{q_1}(0)}^{b} \frac{du}{\bar{v}_{q_1}(u)} > \int_{a}^{b} \frac{du}{\bar{v}_{q_1}(u)} > \int_{a}^{b} \frac{du}{\bar{v}(u)} = L'.$$

∎

For any $0 < \mu < 1$, let $L_\mu > 0$ be such that, for the solution of

$$\begin{cases} u' = v, \\ v' = q_2 v - u(1-u), \\ v(0) = q_2 u(0), \\ v(L_\mu) = 0, \end{cases} \tag{2.7.5}$$

we have $u(L_\mu) = \mu$. In other words, L_μ is the size of the habitat corresponding to the downstream density μ in the case of the smaller advection q_2.

As proved earlier, $L_\mu \to \infty$ as $\mu \to 1$, and, as we know, L_μ is increasing with respect to μ. Thus, if $(u_{q_2}(x), v_{q_2}(x))$ is the solution of (2.6.2) with advection $q = q_2$, then $L > L'$ implies $u_{q_2}(L) > \hat{u}(L') = u_{q_1}(L)$.

We are now ready to prove our theorem.

Proof of Theorem 2.7.1:

Proof: We consider two cases.

Case 1: $u_{q_1}(L) < u_{q_2}(0)$ (the ranges of u_{q_1} and u_{q_2} do not overlap).

In this case, for any $x \in [0, L]$, we have

$$u_{q_1}(x) \le u_{q_1}(L) < u_{q_2}(0) \le u_{q_2}(x),$$

as needed.

Case 2: $u_{q_1}(L) \ge u_{q_2}(0)$ (there is an overlap, see Figure 2.5).

Note first that, since $u_{q_2}(L) > \hat{u}(L')$, the curve $v = \bar{v}_{q_2}(u)$ is located above the curve $v = \bar{v}(u)$ on the common domain $[u_{q_2}(0), u_{q_1}(L)]$. Thus, by Lemma 2.7.4, for any $u \in [u_{q_2}(0), u_{q_1}(L)]$,

$$\bar{v}_{q_1}(u) < \bar{v}_{q_2}(u).$$

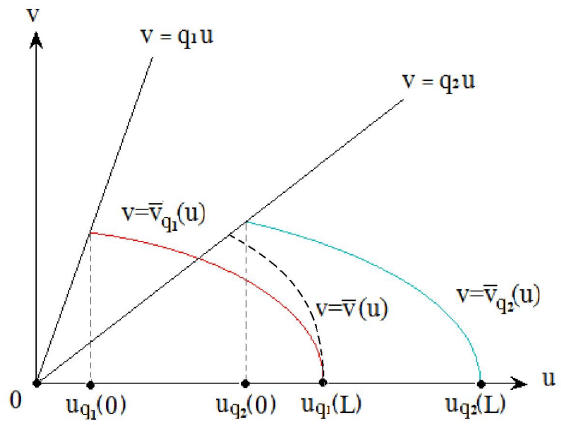

Figure 2.5: The case of overlapping domains.

Note that $v_{q_2}(u_{q_2}(0)) = q_2(u_{q_2}(0))$ and

$$\frac{d\bar{v}_{q_2}}{du}|_{u=u_{q_2}(0)} = q_2 - \frac{u_{q_2}(0)(1-u_{q_2}(0))}{\bar{v}_{q_2}(u_{q_2}(0))} < q_2, \tag{2.7.6}$$

and therefore, since $v = \bar{v}_{q_2}(u)$ is concave down, we have $\bar{v}_{q_2}(u) < q_2 u$ for $u > u_{q_2}(0)$. Now, for $u \in [u_{q_2}(0), u_{q_1}(L)]$, we have $\bar{v}_{q_1}(u) < \bar{v}_{q_2}(u) \le q_2 u < q_1 u$.

So, $\bar{v}_{q_1}(u) < q_1 u$ for all $u \in [u_{q_2}(0), u_{q_1}(L)]$.

Since $\bar{v}_{q_1}(u_{q_1}(0)) = q_1 u_{q_1}(0)$, we conclude that $u_{q_1}(0) \notin [u_{q_2}(0), u_{q_1}(L)]$, i.e. $u_{q_1}(0) < u_{q_2}(0)$.

We want to show that for any $x \in [0, L]$ $u_{q_1}(x) < u_{q_2}(x)$. Suppose this is not the case, and consider the smallest $\bar{x} > 0$ such that $u_{q_1}(\bar{x}) = u_{q_2}(\bar{x})$. Let $\bar{u} = u_{q_1}(\bar{x}) = u_{q_2}(\bar{x})$. Note that $\bar{u} \in [u_{q_2}(0), u_{q_1}(L)]$.

Now, we have

$$\frac{du_{q_1}}{dx}|_{x=\bar{x}} = \bar{v}_{q_1}(u_{q_1}(\bar{x})) = \bar{v}_{q_1}(\bar{u}) < \bar{v}_{q_2}(\bar{u}) = \bar{v}_{q_2}(u_{q_2}(\bar{x})) = \frac{du_{q_2}}{dx}|_{x=\bar{x}}. \tag{2.7.7}$$

On the other hand, by the choice of $\bar{x}$, for any $0 < x < \bar{x}$, we have $u_{q_1}(x) < u_{q_2}(x)$, so

$$u_{q_1}(x) - u_{q_1}(\bar{x}) = u_{q_1}(x) - \bar{u} < u_{q_2}(x) - \bar{u} = u_{q_2}(x) - u_{q_2}(\bar{x}). \tag{2.7.8}$$

Since $x - \bar{x} < 0$, we get

$$\frac{u_{q_1}(x) - u_{q_1}(\bar{x})}{x - \bar{x}} > \frac{u_{q_2}(x) - u_{q_2}(\bar{x})}{x - \bar{x}}. \tag{2.7.9}$$

Taking the limit as $x \to \bar{x}^-$, we get

$$\frac{du_{q_1}}{dx}|_{x=\bar{x}} \geq \frac{du_{q_2}}{dx}|_{x=\bar{x}}, \tag{2.7.10}$$

a contradiction.

∎

Note that, in this chapter, we have been consistently using ODE methods (except for the stability result) to analyze the steady states of our partial differential equation. However, some of our proofs can be shortened by using some powerful PDE techniques. For example, an alternative and short way to prove Theorem 2.7.1 without involving the phase-plane analysis is presented below.

Consider the steady state $u(t, x) = u_{q_2}(x)$ of the single-species model (2.7.1). We know that $u_x > 0$, and we assume $q_2 < q_1$. We get

$$0 = u_{xx} - q_2 u_x + (r - u)u = u_{xx} - q_1 u_x + (q_1 - q_2)u_x + (r - u)u \tag{2.7.11}$$

The term $(q_1 - q_2)u_x$ is positive; hence

$$u_{xx} - q_1 u_x + (r - u)u < 0 = \frac{\partial}{\partial t}u. \tag{2.7.12}$$

Thus, the steady state of the equation with q_2 is a supersolution for the equation with $q_1 > q_2$.

Therefore, by Theorem 3 [12], we conclude that $u_{q_1}(x)$ is bounded above by $u_{q_2}(x)$. In particular, the steady state is a pointwise decreasing function of advection

speed.

In a similar way, we can deal with differences in growth rates. Suppose $r_1 > r_2$. Then

$$u_{xx} - qu_x + (r_2 - u)u = u_{xx} - qu_x + u[(r_1 - u) + r_2 - r_1] = u(r_2 - r_1) < 0. \quad (2.7.13)$$

Hence, the steady state with r_1 is a supersolution for the equation with $r_2 < r_1$, and therefore the steady state of the equation with r_2 is bounded above by the steady state with r_1. In other words, the steady state is pointwise increasing in r.

Thus, we have the following.

Theorem 2.7.6 *If $0 < r_2 < r_1 < 2$, $u_{r_1}(x)$ and $u_{r_2}(x)$ are the steady state solutions of (2.3.1) with $r = r_1$ and $r = r_2$ respectively, then*

$$u_{r_1}(x) > u_{r_2}(x), \quad x \in [0, L]. \quad (2.7.14)$$

2.8 Qualitative aspects of the steady state solution

Although we do not have an explicit formula for the positive steady state solution $u = u(x)$ of (2.3.1), we know (e.g. from the phase plane analysis) that $u(x)$ is an increasing function on $[0, L]$, and for x close to L, it is concave down (since $u'(L) = 0$). A natural question is whether $u(x)$ is concave down throughout the habitat $[0, L]$, or whether $u(x)$ has an inflection point $x^* \in [0, L]$.

We start by analyzing the cases of low, intermediate and high advection.

Lemma 2.8.1 *The solution $u = u(x)$ of (2.3.2, 2.3.3) has an inflection point if and only if $u(0) > 1 - q^2$.*

Proof: Let $(u(x), v(x)) = (u(x), u'(x))$. Then $u(x)$ has an inflection point if and only if its orbit in the uv-plane intersects the v-nullcline $v = \frac{1}{q}u(1-u)$, which happens exactly when the point $(u(0), v(0)) = (u(0), qu(0))$ lies above the v-nullcline. This is

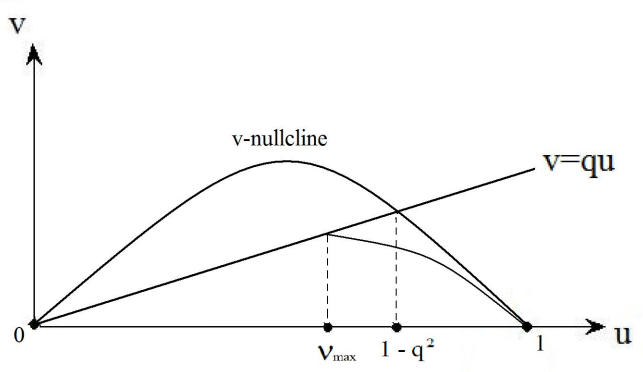

Figure 2.6: No inflection points for $q < \frac{1}{\sqrt{2}}$.

equivalent to

$$qu(0) > \frac{1}{q}u(0)(1-u(0)),$$

or

$$u(0) > 1 - q^2,$$

as needed. ∎

Proposition 2.8.2 *(i) For $q > 1$, every solution of (2.3.2)-(2.3.3) has an inflection point.*

(ii) For $q < \frac{1}{\sqrt{2}}$, no solution of (2.3.2)-(2.3.3) has an inflection point (see Figure 2.6).

Proof: (i) Follows by Lemma 2.8.1 and the fact that $u(0) > 0$ (upstream density is positive).

(ii) If $u(x)$ has an inflection point, by Lemma 2.8.1, we have $u(0) > 1 - q^2 > \frac{1}{2}$. But if an orbit of (2.3.4) starts at a point located above the v-nullcline and to the right from $u = \frac{1}{2}$, from phase plane analysis we can conclude that it will never cross the u-axis, hence will not satisfy the second boundary condition. Thus, $u(x)$ has no inflection

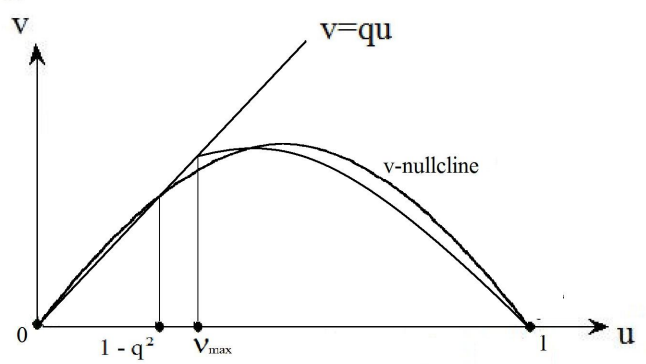

Figure 2.7: The case of intermediate advection ($\frac{1}{\sqrt{2}} < q < 1$).

point. ∎

Remark 2.8.3 If $\frac{1}{\sqrt{2}} < q < 1$, then

- if $\nu_{\max} \leq 1 - q^2$, then no solution has an inflection point;
- if $\nu_{\max} > 1 - q^2$, then, by Lemma 2.8.1, solutions with $1 - q^2 < u(0) \leq \nu_{max}$ have inflection points, and solutions with $u(0) < 1 - q^2$ do not have inflection points; in other words, inflection points only occur for large domains; see Figure 2.7.

In the case when upstream density is low, we can use linearization around the zero steady state to obtain the distance from the upstream boundary to the inflection point (length of boundary layer). Note that the solution of the linear system will only have an inflection point if $q > 1$ (otherwise the v-nullcline $v = \frac{1}{q}u$ will be above the first boundary condition $v = qu$). The system linearized at the origin takes the form

$$\begin{cases} u' = v, \\ v' = qv - u. \end{cases} \tag{2.8.1}$$

The general solution of the above system is given by:

$$u(x) = e^{\frac{qx}{2}}(\alpha \cos \theta x + \beta \sin \theta x),$$

where

$$\theta = \frac{\sqrt{4-q^2}}{2}.$$

Using the first equation of the linearized system, we obtain

$$v(x) = u'(x) = \alpha e^{\frac{qx}{2}} \left(q \cos \theta x + \left(\frac{q^2}{4\theta} - \theta \right) \sin \theta x \right).$$

Differentiating the above expression gives

$$u''(x) = \frac{\alpha q}{2} e^{\frac{qx}{2}} \left(q \cos \theta x + \left(\frac{q^2}{4} - \theta \right) \sin \theta x \right) + \alpha e^{\frac{qx}{2}} \left(-q\theta \sin \theta x + \left(\frac{q^2}{4} + \theta \right) \theta \cos \theta x \right). \tag{2.8.2}$$

If $u(x)$ has an inflection point at $x = x^*$, then $u''(x^*) = 0$. Setting the right-hand side of (2.8.2) equal to zero, we find the expression for x^*:

$$x^* = \begin{cases} \frac{1}{\theta} \arctan \left(\frac{\frac{3q^2}{4} - \theta^2}{\frac{3q\theta}{2} - \frac{q^3}{8\theta}} \right), 1 < q \leq \sqrt{3}, \\ \frac{1}{\theta} \left(\pi + \arctan \left(\frac{\frac{3q^2}{4} - \theta^2}{\frac{3q\theta}{2} - \frac{q^3}{8\theta}} \right) \right), \sqrt{3} < q < 2. \end{cases} \tag{2.8.3}$$

As we can see from Figure 2.8, for small upstream densities, formula (2.8.3) gives a good approximation of the inflection point of the solution in nonlinear case (found numerically, by following the orbit in the u-v-plane).

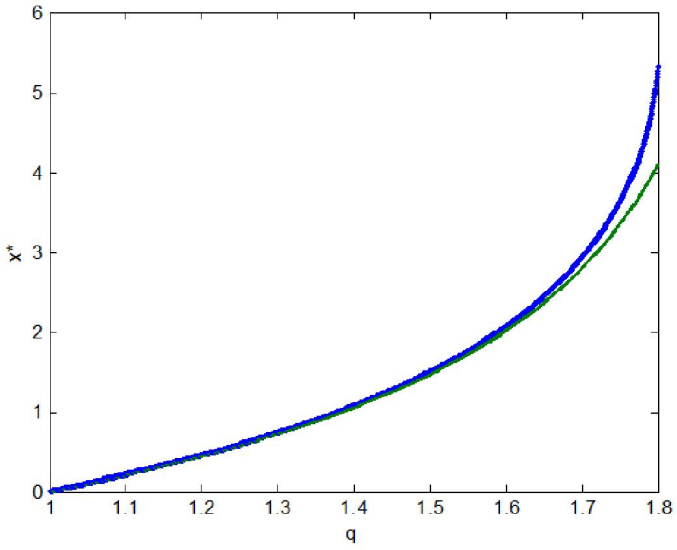

Figure 2.8: Distance from upstream boundary to the inflection point vs. advection as given by numerical simulation (thick) and analytically (2.8.3) (thin), for upstream density $u(0) = 0.001$.

2.9 A more general mobile-stationary model

We consider the following generalization of the two-compartment model (1.5.8), in which the population grows in the stationary and the mobile stage:

$$\frac{\partial n_d}{\partial t} = D\frac{\partial^2 n_d}{\partial x^2} - v\frac{\partial n_d}{\partial x} + f(n_d)n_d - \sigma n_d + \mu n_b, \tag{2.9.1}$$

$$\frac{\partial n_b}{\partial t} = g(n_b)n_b + \sigma n_d - \mu n_b \tag{2.9.2}$$

with boundary conditions

$$D\frac{\partial n_d}{\partial x} - v n_d = 0, \quad x = 0, \quad n_d = 0, \quad x = L. \tag{2.9.3}$$

Linearizing (2.9.1, 2.9.2) at the steady state $(0, 0)$ we get

$$\frac{\partial n_d}{\partial t} = D\frac{\partial^2 n_d}{\partial x^2} - v\frac{\partial n_d}{\partial x} + f(0)n_d - \sigma n_d + \mu n_b, \tag{2.9.4}$$

$$\frac{\partial n_b}{\partial t} = g(0)n_b + \sigma n_d - \mu n_b. \tag{2.9.5}$$

Let $r_d = f(0)$ and $r_d = g(0)$. Rescale by setting $\tilde{t} = r_b t$, $\tilde{\mu} = \frac{\mu}{r_b}$, $\tilde{\sigma} = \frac{\sigma}{r_b}$ and $\tilde{x} = \frac{x}{\sqrt{\frac{D}{r_b}}}$. Dropping the tildes, we get the non-dimensionalized system

$$\frac{\partial n_d}{\partial t} = \frac{\partial^2 n_d}{\partial x^2} - v\frac{\partial n_d}{\partial x} + (r-\sigma)n_d - \sigma n_d + \mu n_b \tag{2.9.6}$$

$$\frac{\partial n_b}{\partial t} = (1-\mu)n_b + \sigma n_d. \tag{2.9.7}$$

Here, $r = \frac{r_d}{r_b}$. The coefficient $-\bar{\sigma} = r - \sigma$ represents the net growth in drift population, and can be negative, positive or zero. Note that the difference from (1.5.9) is that in (2.9.6) the coefficient of n_d is not equal to the coefficient of n_d in (2.9.7). As before, analyzing the second equation, we see that when $\mu < 1$ the persistence is guaranteed. As in the Introduction, we get the following.

Theorem 2.9.1 *The general solution of the system (2.9.1)-(2.9.2) has the following form:*

$$n_b(t,x) = e^{-(\mu-1)t}n_b(0,x) + \sigma e^{-(\mu-1)t}\int_0^t e^{(\mu-1)\tau}n_d(\tau,x)d\tau, \tag{2.9.8}$$

$$\begin{aligned} n_d(t,x) &= \textstyle\sum_{n=1}^{\infty}[c_1 m_{1n}e^{(m_{1n}-(\mu-1))t} + c_2 m_{2n}e^{(m_{2n}-(\mu-1))t}] \\ &\times[e^{\frac{vx}{2}}(a_1\cos(\tfrac{\sqrt{4\lambda_n - v^2}}{2}x) + a_2\sin(\tfrac{\sqrt{4\lambda_n-v^2}}{2}x))], \end{aligned} \tag{2.9.9}$$

where a_1, a_2 are constants, and

$$\begin{aligned} m_{1n} &= m_1(\lambda_n) = \tfrac{-(a+\lambda_n)+\sqrt{(a+\lambda_n)^2+4\mu\sigma}}{2}, \\ m_{2n} &= m_2(\lambda_n) = \tfrac{-(a+\lambda_n)-\sqrt{(a+\lambda_n)^2+4\mu\sigma}}{2}, \end{aligned} \tag{2.9.10}$$

$a = \bar{\sigma} - \mu + 1 = \sigma - r - \mu + 1$ and λ_n are the series of solutions $\lambda_n(v, L)$ with $\lambda_1 < \lambda_2 < \ldots$ which satisfy the following equation (obtained by applying the boundary conditions):

$$\frac{\sqrt{4\lambda - v^2}}{v} + \tan\left(\frac{\sqrt{4\lambda - v^2}}{2}L\right) = 0. \tag{2.9.11}$$

Note that in Theorem 1.5.2 we had $a = \sigma - \mu + 1$. In the case when $\mu > 1$, following the same technique as in Subsection 1.5.1 , we obtain the persistence condition

$$\lambda_1 < r + \frac{\sigma}{\mu - 1},$$

and the critical domain size is

$$L_c^* = \frac{2}{\sqrt{4(r + \frac{\sigma}{\mu-1}) - v^2}}\left(\pi - \arctan\left(\frac{1}{v}\sqrt{4\left(r + \frac{\sigma}{\mu - 1}\right) - v^2}\right)\right).$$

The critical domain size L_c^* goes to infinity when the advection speed approaches its critical value $v_c^* = 2\sqrt{r + \frac{\sigma}{\mu-1}}$. Interestingly, we found that $v_c^* > v_c = 2\sqrt{\frac{\sigma}{\mu-1}}$, where v_c is the critical advection speed in the case when growth only occurs on the benthos. Thus, the growth in the mobile compartment makes it easier for the population to persist.

2.10 Nonspatial approximation

Our goal in this section is to analyze the behavior of the diffusion-reaction-advection equation

$$\frac{\partial u}{\partial t} = d\frac{\partial^2 u}{\partial x^2} - q\frac{\partial u}{\partial x} + u(r - u) \tag{2.10.1}$$

with boundary conditions

$$d\frac{\partial u(0,t)}{\partial x} = qu(0,t), \quad \frac{\partial u}{\partial x}(L,t) = 0. \tag{2.10.2}$$

by reducing it to a nonspatial "approximation" of the form $\frac{\partial u}{\partial t} = \lambda u + u(1-u)$, where $\lambda < 0$ captures, in some sense, the effect of population loss at the boundary. At this point, the "approximation" is heuristic rather than rigorous. We provide some plausibility arguments and numerical simulations for the approximation. We use this approach in subsequent chapters and show by examples that it is quite valuable.

Note that the change in population density is due to movement and population growth (reaction). The flux through the boundary is a combination of fluxes due to random movement (equal to $-D\frac{\partial u}{\partial x}$, by Fick's Law) and due to advection (equal to qu). To account for population loss through the boundary, we replace the diffusion-advection operator with a term $\lambda_1 u$, where λ_1 is the leading eigenvalue of the linear equation for movement only:

$$\frac{\partial u}{\partial t} = d\frac{\partial^2 u}{\partial x^2} - q\frac{\partial u}{\partial x} \tag{2.10.3}$$

with the boundary conditions

$$d\frac{\partial u}{\partial x}(0,t) = qu(0,t),$$

$$\frac{\partial u}{\partial x}(L,t) = 0.$$

The corresponding eigenvalue problem

$$\begin{aligned} du'' - qu' &= \lambda u \\ du'(0) &= qu(0) \\ u'(L) &= 0. \end{aligned} \tag{2.10.4}$$

has a non-trivial solution only if $q^2 + 4\lambda d < 0$. In this case, the general solution of the above equation (for a fixed λ) has the form

$$u(x) = e^{\frac{qx}{2d}} A\cos\left(\frac{\sqrt{-q^2-4\lambda d}}{2d}x\right) + B\sin\left(\frac{\sqrt{-q^2-4\lambda d}}{2d}x\right).$$

Thus, a nontrivial solution that matches both boundary conditions requires

$$q\sqrt{-q^2-4\lambda d}\cos\left(\frac{\sqrt{-q^2-4\lambda d}}{2d}L\right)+(q^2+2\lambda d)\sin\left(\frac{\sqrt{-q^2-4\lambda d}}{2d}L\right)=0. \quad (2.10.5)$$

The roots of this equation form a decreasing sequence of eigenvalues $\lambda_1 > \lambda_2 > \ldots$, where $\lambda_1 < -\frac{q^2}{4d}$. The general solution of the "movement-only" boundary value problem (2.10.3) is then given as an infinite sum

$$u(t,x)=\sum_{k=1}^{\infty}e^{\lambda_k t}\left[A_k e^{\frac{qx}{2d}}\cos\left(\frac{\sqrt{-q^2-4\lambda_k d}}{2d}x\right)+B_k e^{\frac{qx}{2d}}\sin\left(\frac{\sqrt{-q^2-4\lambda_k d}}{2d}x\right)\right]$$
$$=e^{\lambda_1 t}u_1(x)+e^{\lambda_2 t}u_2(x)+....$$

Starting with any initial distribution, the population will be transported along the drift and leave through the downstream boundary, and its density will approach the zero steady state. The total population at time t is given by

$$U(t)=\int_0^L u(t,x)dx=e^{\lambda_1 t}U_1+e^{\lambda_2 t}U_2+...,$$

where the terms $U_k=\int_0^L u_k(x)dx$ are constant. Now, we have

$$U'(t)=\lambda_1 e^{\lambda_1 t}U_1+\lambda_2 e^{\lambda_2 t}U_2+...\le\lambda_1 U(t)$$

(with equality taking place when $U_k(x)=0$ for $k\ge 2$). Thus, $|\lambda_1|$ is the smallest possible rate of decay that a solution of (2.10.3) can have. In order to represent this removal of population from the domain due to diffusion and advection, we will introduce an additional "death term", $\lambda_1 u$, to the nonspatial logistic growth equation $u'=u(r-u)$.

Now we take a closer look at the behavior of λ_1 as a function of advection, q. To eliminate the advection term in (2.10.3), as before, we use the following transformation: $n(x,t)=u(x,t)e^{-\frac{qx}{2d}}$ (see Subsection 1.4.1). Then the advection-diffusion-reaction equation on $u(t,x)$ takes the form

$$\frac{\partial n}{\partial t} = d\frac{\partial^2 n}{\partial x^2} - \frac{q^2}{4d}n, \tag{2.10.6}$$

and boundary conditions are transformed into

$$\begin{cases} \frac{\partial n}{\partial x} - \frac{q}{2}n = 0, & x = 0 \\ \frac{\partial n}{\partial x} + \frac{q}{2}n = 0, & x = L. \end{cases} \tag{2.10.7}$$

The eigenvalues of (2.10.4) are precisely the eigenvalues of

$$\begin{aligned} &dn'' - qn' = \lambda n \\ &dn'(0) = \tfrac{q}{2}n(0) \\ &n'(L) = -\tfrac{q}{2}n(L). \end{aligned} \tag{2.10.8}$$

By Proposition 1.4.2, the principal eigenvalue is given by:

$$\lambda_1(q,d) = \frac{q^2}{4d} - \min_{\psi\in\Psi}\left\{\int_0^L d(\psi'(x))^2 dx + \left[\frac{q}{2}(\psi(0))^2 + \frac{q}{2}(\psi(L))^2\right]\right\}. \tag{2.10.9}$$

It follows, that for fixed diffusion d, $\lambda_1 = \lambda_1(q,d)$ is a decreasing function of advection. This is illustrated by numerics (see Figure 2.9).

To justify the use of the term $\lambda_1 u$ in our model, we first consider the reaction-diffusion-advection equation with the linear growth:

$$\frac{\partial u}{\partial t} = d\frac{\partial^2 u}{\partial x^2} - q\frac{\partial u}{\partial x} + ru, \tag{2.10.10}$$

with boundary conditions $d\frac{\partial u(0,t)}{\partial x} = qu(0,t)$, $\frac{\partial u}{\partial x}(L,t) = 0$. Persistence of a species with dynamics described by the above model is determined as follows: the infinitesimal amount of population will grow when $\lambda = r + \lambda_1 > 0$, and will decay when $\lambda = r + \lambda_1 < 0$ (here, λ_1 is the leading eigenvalue of (2.10.3)). The same is true for the solutions of the nonspatial model given by $\frac{\partial u}{\partial t} = (\lambda_1 + r)u$. Thus, in the linear case, the nonspatial approximation gives an accurate prediction of persistence conditions.

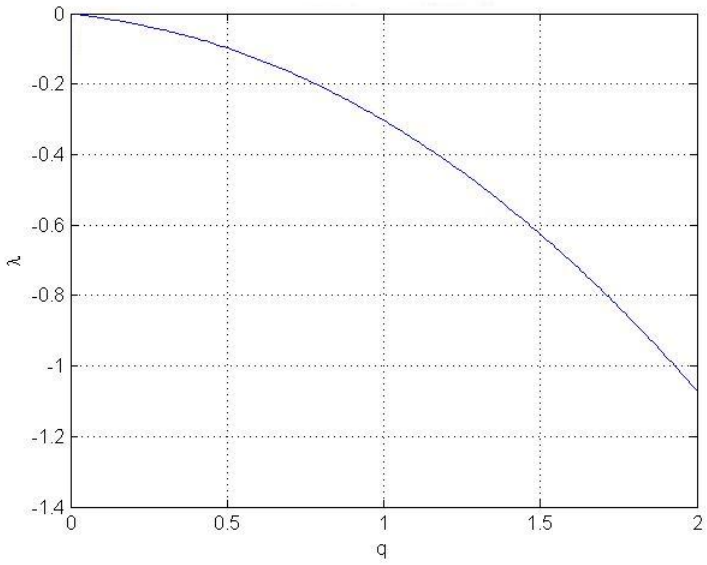

Figure 2.9: Principal eigenvalue as a function of advection, with $d = 1$.

In the case of the reaction-diffusion-advection model with logistically growing population described by

$$\frac{\partial u}{\partial t} = d\frac{\partial^2 u}{\partial x^2} - q\frac{\partial u}{\partial x} + u(r-u), \tag{2.10.11}$$

persistence is equivalent to growth at low density, i.e. the question reduces to growth in the linear model (2.10.10). Persistence is again equivalent to $r > -\lambda_1$ and decay happens when $r < -\lambda_1$. The same is true for the nonlinear equation

$$\frac{\partial u}{\partial t} = \lambda_1 u + u(r-u). \tag{2.10.12}$$

Indeed, (2.10.12) can be written as $\frac{\partial u}{\partial t} = u((r+\lambda_1) - u)$, and the stability analysis shows that the zero equilibrium state of the above equation is stable for $r+\lambda_1 < 0$ and unstable for $r+\lambda_1 > 0$. Thus, the dynamics of a single species boundary value problem is fairly well captured by the nonspatial equation (2.10.12). We will use this approach in our study of competition of two and three species in advective environment.

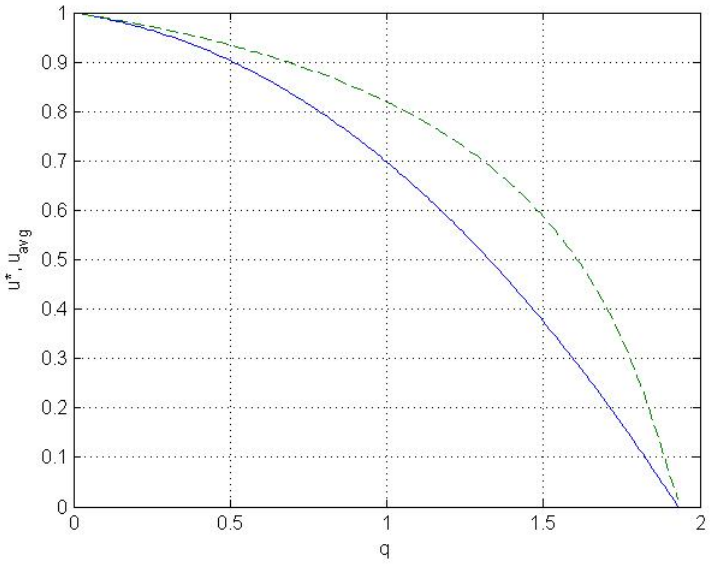

Figure 2.10: The solid curve represents the positive equilibrium of (2.10.12) $u^* = 1 + \lambda_1(q, 1)$; the dashed curve gives the average population density of the positive steady state of (2.10.11).

Further justification of validity of the nonspatial approximation for the diffusion-advection model with non-linear term is given in Figure 2.10. We compare the average value of the steady state solution of the spatial model (2.10.11) (subject to our boundary conditions) with the positive equilibrium of the corresponding nonspatial approximation (2.10.12), for different values of q and domain size $L = 10$.

Chapter 3

Two species

3.1 Introduction

The population dynamics of two competing species can be described by the classical Lotka-Volterra system in non-dimensional form:

$$\begin{cases} \frac{du_1}{dt} = u_1(1 - u_1 - \alpha u_2), \\ \frac{du_2}{dt} = u_2(r_2 - u_2 - \beta u_1). \end{cases} \tag{3.1.1}$$

where u_1, u_2 are the sizes or densities of two competing populations, $r_1 = 1$ and $r_2 > 0$ are the corresponding intrinsic growth rates, and $\alpha, \beta > 0$ are the interspecific competition coefficients. In Chapter 1, we gave a detailed description of possible competition outcomes in such a Lotka-Volterra model.

Figure 3.1 illustrates the dependence of the competition outcome on the choice of parameters, in the $\alpha\beta$-plane, for $r_2 = 1.15$.

Here, we consider a spatial version of the Lotka-Volterra competition model, first introduced in [30] to describe population dynamics in advective environments, such as streams, rivers, and other aquatic habitats with unidirectional flow. The new equations are obtained by introducing diffusion and advection terms in the classical Lotka-Volterra model. Let $u_1(t, x)$ and $u_2(t, x)$ be population densities of the two

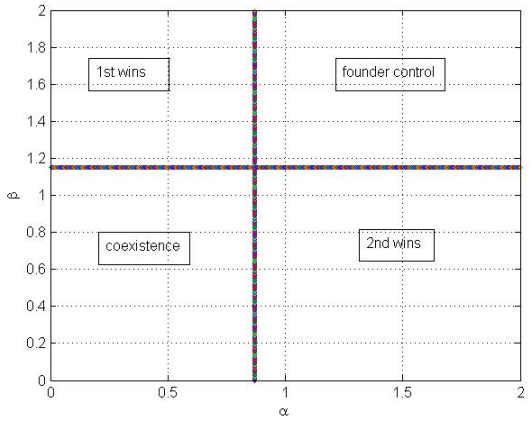

Figure 3.1: Four outcomes shown in the α-β-plane, for $r_2 = 1.15$.

species, at time t and point $x \in [0, L]$. The habitat is represented by the interval $[0, L]$, with $x = 0$ corresponding to the upstream boundary. We assume that the two species are subject to the same effective advection speed q [30]. The equations are:

$$\begin{cases} \frac{\partial u_1}{\partial t} = d_1 \frac{\partial^2 u_1}{\partial x^2} - q\frac{\partial u_1}{\partial x} + u_1(1 - u_1 - \alpha u_2), \\ \frac{\partial u_2}{\partial t} = d_2 \frac{\partial^2 u_2}{\partial x^2} - q\frac{\partial u_2}{\partial x} + u_2(r_2 - \beta u_1 - u_2), \end{cases} \tag{3.1.2}$$

where d_i are the diffusion coefficients for the two species. These equations are non-dimensionalized with respect to time and density, but do still carry the dimensions of space.

We use the same boundary conditions as in the case of a single species:

$$\begin{cases} d_i \frac{\partial u_i}{\partial x} = q u_i, \quad x = 0, \ i = 1, 2 \\ \frac{\partial u_i}{\partial x} = 0, \quad x = L. \end{cases} \tag{3.1.3}$$

Note that when $q = 0$, we have no-flux boundary conditions in (3.1.2)-(3.1.3), and the model has spatially constant steady states corresponding to the four outcomes of Lotka-Volterra competition. The goal of this chapter is to develop a theoretical framework for understanding how change in advection speed influences the outcome of competition in the spatial Lotka-Volterra model with advection.

As shown by numerical simulations in [30], the result of competition in (3.1.2)-(3.1.3) strongly depends on the advection speed. As an example, we fix parameters so that Species 1 is competitively superior, but Species 2 has the higher growth rate at low density, i.e. $0 < \alpha r_2 < 1 < \frac{\beta}{r_2}$ and $r_2 > 1$. Recall from Chapter 2 that, for any choice of the domain size L, there is a critical value of advection $q_c(L)$ such that, for $q > q_c(L)$, persistence is not possible. For $L \to \infty$, $q_c(L)$ approaches $q_c = 2\sqrt{d_i r_i}$. As observed in [30], Species 1 still outcompetes Species 2 in the case of low advection, the two species coexist (with Species 2 occupying the upstream boundary region) under intermediate advection, and Species 2 outcompetes Species 1 for higher values of advection. More details on these observations are given in Chapter 1.

In our analysis, we use a combination of analytical (linearization, variational principles) and numerical techniques. In Section 3.2, we analyze the mutual invasion conditions by linearizing the model (3.1.2)-(3.1.3) at equilibria $(\hat{u}_1(x), 0)$ and $(0, \hat{u}_2(x))$. Each of the equilibria is invadable by a competitor if it is unstable; i.e. if the principal eigenvalue of the corresponding eigenvalue problem for the invading species is positive.

Since the coefficients of the eigenvalue problems vary in space, obtaining an explicit formula for the principal eigenvalue is impossible. However, we use the variational formula (1.4.31) to analyze the properties of principal eigenvalues and to examine dependence of the eigenvalues and the invasion conditions on the biological parameters d_1, d_2, α, β, r_2 and q.

In Section 3.3, we assume that both species have the same motility ($d_1 = d_2$). We reduce (3.1.2) to a nonspatial "approximation" introduced in Chapter 2, by replacing the diffusion-advection operator with its principal eigenvalue (λ_1). The goal of Section 3.4 is to present the results of our numerical simulations, which complement and illustrate the analytical results obtained in previous sections. We build bifurcation diagrams for invasion in the β-r_2-plane (invasion by Species 2) and α-r_2-plane (invasion by Species 1) as well as in the q-r_2-plane (for both species). In the α-r_2- and

β-r_2-diagrams, we compare the "true" bifurcation diagrams (obtained numerically) with the ones obtained in Section 3.3 and find the latter give a good approximation.

3.2 Mutual invasibility of single species equilibria

We begin the mutual invasion analysis of our model by linearizing system (3.1.2) at the single species steady states $(\hat{u}_1(x), 0)$ and $(0, \hat{u}_2(x))$. In either case, the resulting linear equations decouple. We are interested in the possibility of invasion by one of the two species when it is rare, provided that the other species is at its steady state.

3.2.1 Linearization at single species equilibria

We start by setting

$$\begin{cases} u_1(x,t) = \hat{u}_1(x) + w_1(x,t) \\ u_2(x,t) = w_2(x,t), \end{cases} \tag{3.2.1}$$

where $w_1(x,t)$ and $w_2(x,t)$ are small perturbations from the single species steady state $(\hat{u}_1, 0)$. Substituting (3.2.1) into (3.1.2) and omitting higher order terms, we obtain

$$\frac{\partial w_1}{\partial t} = d_1 \frac{\partial^2 w_1}{\partial x^2} - q\frac{\partial w_1}{\partial x} + w_1(1 - 2\hat{u}_1(x)) - \alpha \hat{u}_1(x) w_2, \tag{3.2.2}$$

and

$$\frac{\partial w_2}{\partial t} = d_2 \frac{\partial^2 w_2}{\partial x^2} - q\frac{\partial w_2}{\partial x} + w_2(r_2 - \beta \hat{u}_1(x)), \tag{3.2.3}$$

with the same boundary conditions

$$\begin{cases} \frac{\partial w_i}{\partial x} = \frac{q}{d_i} w_i \quad (i = 1, 2), \quad x = 0 \\ \frac{\partial w_i}{\partial x} = 0 \quad (i = 1, 2), \quad x = L. \end{cases} \tag{3.2.4}$$

Note that equation (3.2.3) decouples from (3.2.2). Since we are mainly concerned with determining conditions under which the second species grows when it is rare, we omit the linearization of the first equation about $(\hat{u}_1(x), 0)$. As before, see Subsection 1.4.1 and Section 2.10. To eliminate the advection term in (3.2.3), we use the following transformation: $n_2(x,t) = w_2(x,t)e^{-\frac{qx}{2d_2}}$. We obtain

$$\frac{\partial n_2}{\partial t} = d_2 \frac{\partial^2 n_2}{\partial x^2} + \left(r_2 - \beta \hat{u}_1(x) - \frac{q^2}{4d_2} \right) n_2, \tag{3.2.5}$$

with boundary conditions

$$\begin{cases} \frac{\partial n_2}{\partial x} - \frac{q}{2d_2} n_2 = 0, & x = 0 \\ \frac{\partial n_2}{\partial x} + \frac{q}{2d_2} n_2 = 0, & x = L. \end{cases} \tag{3.2.6}$$

The second species will invade the first species' steady state exactly when the zero steady state of (3.2.5)-(3.2.6) is unstable; i.e. when the principal eigenvalue of the corresponding eigenvalue problem is positive.

Similarly, if we linearize (3.1.2) at the steady state $(0, \hat{u}_2(x))$ and follow the same steps as above, we obtain

$$\frac{\partial n_1}{\partial t} = d_1 \frac{\partial^2 n_1}{\partial x^2} + \left(1 - \alpha \hat{u}_2(x) - \frac{q^2}{4d_1} \right) n_1, \tag{3.2.7}$$

with boundary conditions

$$\begin{cases} \frac{\partial n_1}{\partial x} - \frac{q}{2d_1} n_1 = 0, & x = 0 \\ \frac{\partial n_1}{\partial x} + \frac{q}{2d_1} n_1 = 0, & x = L. \end{cases} \tag{3.2.8}$$

Thus, the first species will invade the second species' steady state exactly when the zero steady state of problem (3.2.7)-(3.2.8) is unstable; i.e. when the principal eigenvalue of the corresponding eigenvalue problem is positive.

Due to the presence of a spatially varying coefficient in the growth/reaction term in the above formulas, there is no explicit expression for the principal eigen-

value. However, a significant amount of information about its behavior with respect to parameters can be deduced from variational formulae, as presented in (1.4.31).

3.2.2 Invasion of the first species' steady state by the second species

We start by investigating the behavior of the principal eigenvalue of (3.2.5)-(3.2.6), corresponding to the case when the second species is at low density and trying to invade the single species steady state of the first species. By (1.4.31), we get

$$\sigma_2^* = \max_{\psi\in\Psi}\left\{-\int_0^L d_2(\psi'(x))^2dx + \int_0^L \left(r_2 - \beta\hat{u}_1(x) - \frac{q^2}{4d_2}\right)(\psi(x))^2dx \right.$$
$$\left. - \left[\frac{q}{2d_2}(\psi(0))^2 + \frac{q}{2d_2}(\psi(L))^2\right]\right\}, \tag{3.2.9}$$

where $\Psi = \{\psi \in W_2^1([0,L]) | \|\psi\|_2 = 1\}$, $\|\psi\|_2 = \int_0^L (\psi(x))^2dx$.

Taking into consideration that $\int_0^L (\psi(x))^2dx = 1$, we can separate the constants from the above expression, and rewrite it as $\sigma_2^* = r_2 - \frac{q^2}{4d_2} - \Gamma(\beta, q)$, where

$$\Gamma(\beta,q) = \min_{\psi\in\Psi}\left\{\int_0^L d_2(\psi'(x))^2dx + \left[\frac{q}{2d_2}(\psi(0))^2 + \frac{q}{2d_2}(\psi(L))^2\right] + \beta\int_0^L \hat{u}_1(x)\psi^2dx\right\}.$$

Note that $\Gamma(\beta, q) \geq 0$ for any $\beta \geq 0$. Next, we will analyze the dependence of Γ on parameters.

Proposition 3.2.1 *$\Gamma(\beta, q)$ is an increasing function of β (and therefore σ_2^* is a decreasing function of β).*

Proof: Suppose $\beta_1 < \beta_2$. Fix $0 \leq q < 2$, and let $\bar{\psi} \in \Psi$ be such that
$\Gamma(\beta_2, q) = \min_{\psi\in\Psi}\left\{\int_0^L d_2(\psi'(x))^2dx + \left[\frac{q}{2d_2}(\psi(0))^2 + \frac{q}{2d_2}(\psi(L))^2\right] + \beta_2\int_0^L \hat{u}_1(x)\psi^2dx\right\}$
$= \int_0^L d_2(\bar{\psi}'(x))^2dx + \left[\frac{q}{2d_2}(\bar{\psi}(0))^2 + \frac{q}{2d_2}(\bar{\psi}(L))^2\right] + \beta_2\int_0^L \hat{u}_1(x)(\bar{\psi}(x))^2dx$
$> \int_0^L d_2(\bar{\psi}'(x))^2dx + \left[\frac{q}{2d_2}(\bar{\psi}(0))^2 + \frac{q}{2d_2}(\bar{\psi}(L))^2\right] + \beta_1\int_0^L \hat{u}_1(x)(\bar{\psi}(x))^2dx$

$\geq \min_{\psi\in\Psi}\left\{\int_0^L d_2(\psi'(x))^2dx + \left[\frac{q}{2d_2}(\psi(0))^2 + \frac{q}{2d_2}(\psi(L))^2\right] + \beta_1\int_0^L \hat{u}_1(x)(\psi(x))^2dx\right\}$
$= \Gamma(\beta_1, q)$.

Here we used the fact that $\hat{u}_1(x) > 0$ on $[0, L]$, $\|\psi\|_2 = 1$, and therefore

$$\int_0^L \hat{u}_1(x)(\psi(x))^2dx$$

is positive. ∎

Proposition 3.2.2 *(a)* $\Gamma(0, q) \leq \frac{d_2\pi^2}{L^2}$. *(b)* $\Gamma(\beta, 0) = \beta$

Proof: (a) First note that for any choice of ψ,

$$\int_0^L d_2(\psi'(x))^2dx + \left[\frac{q}{2d_2}(\psi(0))^2 + \frac{q}{2d_2}(\psi(L))^2\right] \geq 0.$$

We can choose ψ to be $\psi(x) = \sqrt{\frac{2}{L}}\sin\left(\frac{\pi x}{L}\right)$, then $\|\psi\|_2 = 1, \psi(0) = \psi(L) = 0$, and

$$\int_0^L d_2(\psi'(x))^2dx = \frac{d_2\pi^2}{L^2}.$$

It follows that

$$\Gamma(0, q) = \min_{\psi\in\Psi}\left\{\int_0^L d_2(\psi'(x))^2dx + \left[\frac{q}{2d_2}(\psi(0))^2 + \frac{q}{2d_2}(\psi(L))^2\right]\right\} \leq \frac{d_2\pi^2}{L^2}.$$

(b) First note that, for $q = 0$, $\hat{u_1}(x) \equiv 1$. Thus, we have

$$\Gamma(\beta, 0) = \min_{\psi\in\Psi}\left\{\int_0^L d_2(\psi'(x))^2dx + \beta\right\} \geq \beta.$$

Taking $\psi \equiv \frac{1}{\sqrt{L}}$ we have

$$\int_0^L d_2(\psi'(x))^2dx + \beta = \beta.$$

Therefore, $\Gamma(\beta, 0) = \beta$.

The trivial steady state of the second species is stable if the dominant eigenvalue σ_2^* is negative, and otherwise the steady state is unstable. Thus, the invasion condition takes the form

$$r_2 > \frac{q^2}{4d_2} + \Gamma(\beta, q).$$

For $\beta = 0$, the second species is independent of the first. Hence, the invasion condition $r_2 > \frac{q^2}{4d_2} + \Gamma(0, q)$ is precisely the single species persistence condition. For $L \to \infty$, by Proposition 3.2.2(a), the invasion condition becomes $r_2 > \frac{q^2}{4d_2}$ which is equivalent to $q < q_c$, where $q_c = 2\sqrt{d_2 r_2}$ is the critical advection in the single species case. Note that, since there is no influence from the first competitor, the second equation in (3.1.2) decouples from the first one.

In the case of zero advection $q = 0$, by Proposition 3.2.2(b), the invasion condition takes the form $r_2 > \beta$, which is exactly the nonspatial invasion condition for the second species.

The stability boundary can be found by setting $\sigma_2^* = 0$, or

$$r_2 = r_2(\beta, q) = \frac{q^2}{4d_2} + \Gamma(\beta, q). \tag{3.2.10}$$

By Propositions 3.2.1 and 3.2.2, this curve is a graph of an increasing function in the first quadrant of the β-r_2-plane, with the r_2-intercept approaching $\frac{q^2}{4d_2}$ for large L, see Figure 3.2. The invasion region of the β-r_2-plane is located above the stability boundary.

We will now use the invasion conditions to describe (qualitatively) possible transitions between the competition outcomes due to advection. First we show that, for $q > 0$, the second species invasion boundary (in the β-r_2-plane) lies below the nonspatial invasion boundary $r_2 = \beta$ for large enough β.

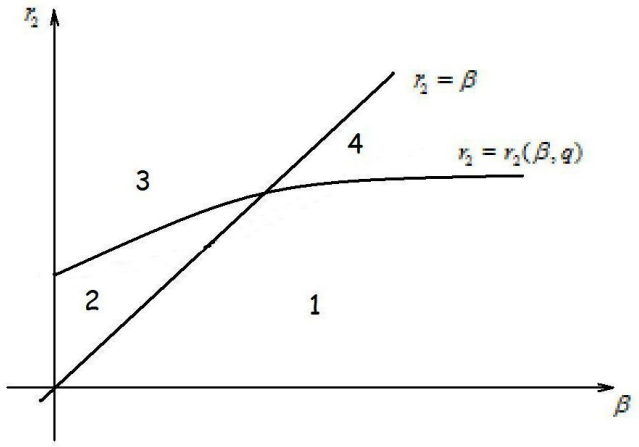

Figure 3.2: Four regions describing the effect of advection q on invasion by second species:
Region 1: no invasion for $q = 0 \rightarrow$ no invasion for $q > 0$;
Region 2: invasion for $q = 0 \rightarrow$ no invasion for $q > 0$;
Region 3: invasion for $q = 0 \rightarrow$ invasion for $q > 0$;
Region 4: no invasion for $q = 0 \rightarrow$ invasion for $q > 0$.
In the nonspatial model, Species 2 can invade for parameters above the line $r_2 = \beta$. In the spatial model, invasion is possible for parameter combinations above the curve $r_2 = r_2(\beta, q)$.

Proposition 3.2.3 *Let $q > 0$. Then $r_2(\beta, q) < \beta$ for*

$$\beta > \frac{\frac{q^2}{4d_2} + \frac{q}{d_2 L}}{1 - \frac{\int_0^L \hat{u}_1(x)dx}{L}}.$$

Proof: First note that

$$r_2(\beta, q) = \frac{q^2}{4d_2} + \Gamma(\beta, q) = \frac{q^2}{4d_2}$$

$$+ \min_{\psi \in \Psi} \left\{ \int_0^L d_2(\psi'(x))^2 dx + \left[\frac{q}{2d_2}(\psi(0))^2 + \frac{q}{2d_2}(\psi(L))^2 \right] + \beta \int_0^L \hat{u}_1(x)(\psi(x))^2 dx \right\}.$$

Taking $\psi(x) \equiv \frac{1}{\sqrt{L}}$, and using that $\int_0^L \hat{u}_1(x)dx < L$ for $q > 0$, we get

$$\begin{aligned} r_2(\beta, q) &\leq \frac{q^2}{4d_2} + 0 + \frac{q}{2d_2}\left(\frac{1}{L} + \frac{1}{L}\right) + \frac{\beta}{L}\int_0^L \hat{u}_1(x)dx \\ &= \frac{q^2}{4d_2} + \frac{q}{d_2 L} + \frac{\beta}{L}\int_0^L \hat{u}_1(x)dx \\ &< \beta \end{aligned}$$

for

$$\beta > \frac{\frac{q^2}{4d_2} + \frac{q}{d_2 L}}{1 - \frac{\int_0^L \hat{u}_1(x)dx}{L}}.$$

∎

Note that for β close to 0 (and $q > 0$), the invasion boundary lies above $r_2 = \beta$. Thus, the spatial and nonspatial boundaries intersect.

As shown in Figure 3.2, the β-r_2-plane is divided into four regions, characterized by the the effect the advection has on the invasion by the second species.

For example, if we take parameters from Region 4, then the second competitor, which could not grow at low density in the nonspatial case, is able to invade the first one in the case of advection q.

Remark 3.2.4 When $q > 0$, the eigenvalue σ_2^* also depends on the values of the diffusion coefficients d_1 and d_2 (the implicit dependence on d_1 is due to the term $\hat{u}_1$). Note that $\Gamma(\beta, q)$ increases as a function of d_2. As $d_2 \to 0$, $\Gamma(\beta, q)$ is bounded, while $-\frac{q^2}{4d_2} \to -\infty$, and thus $\sigma_2^* < 0$. Hence, the second competitor cannot invade. For large d_2, the situation is not as clear, but taking $\psi(x) = \frac{1}{\sqrt{L}}$ as above, and using $\hat{u}_1(x) \leq 1$, we get $\sigma_2^* \geq r_2 - \frac{q^2}{4d_2} - \frac{q}{d_2 L} - \beta$. Thus if $d_2 \to \infty$ and $L \to \infty$, then $r_2 > \beta$ is sufficient for invasion by the second species (Region 2 in Figure 3.2 disappears).

Now we prove that, if $d_1 = d_2$, the spatial and nonspatial invasion boundaries intersect at the point $(\beta, r_2) = (1, 1)$, and our numerical simulations suggest that this is the only intersection point.

Proposition 3.2.5 *If $d_1 = d_2 = d$, then $r_2(1, q) = 1$ for all $q \geq 0$; i.e. the invasion boundary passes through $(\beta, r_2) = (1, 1)$.*

Proof: The eigenvalue problem associated with equation (3.2.3) and boundary conditions (3.2.4) with $\beta = 1$ has the following form

$$\sigma w = dw'' - qw' + w(r_2 - \hat{u}_1(x)), \tag{3.2.11}$$

$$dw'(0) = qw(0), \quad w'(L) = 0. \tag{3.2.12}$$

Let $w(x) = \hat{u}_1(x)$. Then we have

$$d\hat{u}_1'' - q\hat{u}_1' + \hat{u}_1(r_2 - \hat{u}_1) = d\hat{u}_1'' - q\hat{u}_1' + \hat{u}_1(1 - \hat{u}_1) + (r_2 - 1)\hat{u}_1 = (r_2 - 1)\hat{u}_1.$$

Thus, $w(x) = \hat{u}_1(x)$ is an eigenfunction corresponding to $\sigma_2^* = r_2 - 1$. Since the positive eigenfunction always corresponds to the principal eigenvalue [10], and $\hat{u}_1(x) > 0$, we conclude that $\sigma_2^* = r_2 - 1$ is the principal eigenvalue. Therefore, the invasion condition for the second species, $\sigma_2^* > 0$, takes the form $r_2 > 1$. This means that $r_2(1, q) = 1$, i.e. the point $(\beta, r_2) = (1, 1)$ lies on the invasion boundary. ∎

3.2.3 Invasion of the second species steady state by the first species

We will now look at the behavior of the principal eigenvalue σ_1^* that corresponds to the case when the first species is at low density and tries to invade the single species steady state of the second species.

As before, we can write

$$\sigma_1^* = 1 - \frac{q^2}{4d_1} - \Delta(\alpha, r_2, q), \tag{3.2.13}$$

where

$$\Delta(\alpha, r_2, q) = \min_{\psi \in \Psi} \left\{ \int_0^L d_1(\psi'(x))^2 dx + \left[\frac{q}{2d_1}(\psi(0))^2 + \frac{q}{2d_1}(\psi(L))^2 \right] + \alpha \int_0^L \hat{u}_2(x)\psi^2 dx \right\}.$$

Unlike the previous case, there is an implicit dependence on r_2, due to $\hat{u}_2(x)$ being a solution of

$$u'' - qu' + r_2 u(1-u) = 0.$$

Note that $\Delta(\alpha, r_2, q) \geq 0$ for any $\alpha \geq 0$.

Proposition 3.2.6 *$\Delta(\alpha, r_2, q)$ is increasing with respect to α and r_2, and therefore σ_1^* is decreasing with respect to α and r_2.*

Proof: The proof of increase with respect to α is the same as in Proposition 3.2.1. The proof for r_2 follows the same argument and uses monotonicity of the single species steady state with respect to its growth rate r (see Chapter 2, Theorem 2.7.6). ∎

Proposition 3.2.7 *(a) $\Delta(0, r_2, q) = \Delta(\alpha, 0, q) \leq \frac{d_1\pi^2}{L^2}$. (b) $\Delta(\alpha, r_2, 0) = \alpha r_2$.*

Proof: (a) Note first that if one of α or r_2 is zero, the term $\alpha \int_0^L \hat{u}_2(x)(\psi(x))^2 dx$ in the definition of Δ vanishes. Then one follows the proof in Proposition 3.2.2.

(b) Note that when $q = 0$, we have $\hat{u}_2 \equiv r_2$. Thus, taking $\psi \equiv \frac{1}{\sqrt{L}}$, we obtain $\Delta(\alpha, r_2, 0) = \min_{\psi\in\Psi}\left\{\int_0^L d_1(\psi'(x))^2 dx + \alpha r_2\right\} = \alpha r_2$. ∎

The invasion condition for the first species therefore takes form

$$\Delta(\alpha, r_2, q) < 1 - \frac{q^2}{4d_1}.$$

If $\alpha = 0$, there is no influence from the second competitor. If $r_2 = 0$, the second competitor is absent. In either case, the equation for the first species decouples from the equation for the second species, and the invasion condition coincides with the persistence condition for a single species. Note also that in both cases, as $L \to \infty$, by Proposition 3.2.7(a), the invasion condition becomes $\frac{q^2}{4d_1} < 1$, which is equivalent to $q < q_c$ in the single species case with $r = 1$.

In a non-advective environment ($q = 0$), by Proposition 3.2.7(b), the invasion condition takes the form $\alpha r_2 < 1$, which coincides with the nonspatial invasion condition for the first species.

Remark 3.2.8 The function $\Delta(\alpha, r_2, q)$ increases with respect to both α and r_2. Therefore, the invasion region in the α-r_2-plane is bounded by the α- and r_2-axes and the level curve $\Delta(\alpha, r_2, q) = 1 - \frac{q^2}{4d_1}$ (stability boundary).

We also obtain the following lower bound for $\sigma_1^*(\alpha, r_2, q)$.

Proposition 3.2.9 $\sigma_1^*(\alpha, r_2, q) > 1 - \frac{q^2}{4d_1} - \frac{q}{d_1 L} - \alpha r_2$.

Proof: Recall that

$$\Delta(\alpha, r_2, q) = \min_{\psi\in\Psi}\left\{\int_0^L d_1(\psi'(x))^2 dx + \left(\frac{q}{2d_1}(\psi(0))^2 + \frac{q}{2d_1}(\psi(L))^2\right) + \alpha\int_0^L \hat{u}_2(x)(\psi(x))^2 dx\right\}.$$

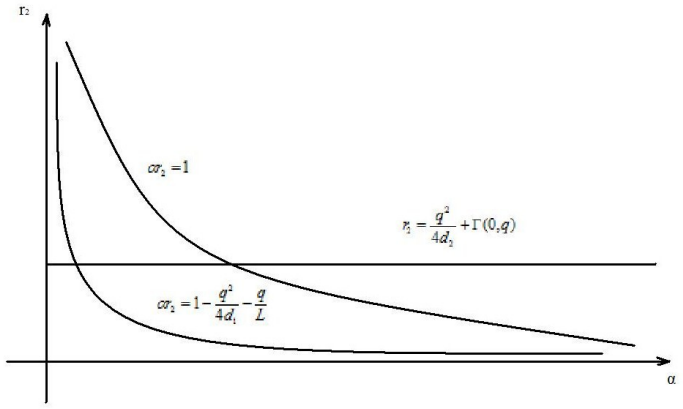

Figure 3.3: In the nonspatial model, the first species can invade for parameters below the curve $\alpha r_2 = 1$. In the spatial model, a sufficient condition for invasion by the first species is given by the curve $\alpha r_2 = 1 - \frac{q^2}{4d_1} - \frac{q}{d_1 L}$ (invasion is guaranteed if the point (α, r_2) is below the curve). If parameters are chosen below the horizontal line $r_2 = \frac{q^2}{4d_2} + \Gamma(0, q)$, the second species cannot persist even without competition.

Taking $\psi(x) \equiv \frac{1}{\sqrt{L}}$ and noticing that $\int_0^L \hat{u}_2(x)dx < r_2 L$, we get

$$\Delta(\alpha, r_2, q) \leq \frac{q}{d_1 L} + \frac{\alpha}{L}\int_0^L \hat{u}_2(x)dx < \frac{q}{d_1 L} + \alpha r_2,$$

and hence $\sigma_1^*(\alpha, r_2, q) > 1 - \frac{q^2}{4d_1} - \frac{q}{d_1 L} - \alpha r_2$. ∎

Thus,

$$\alpha r_2 < 1 - \frac{q^2}{4d_1} - \frac{q}{d_1 L}$$

is a sufficient (but not necessary) condition for invasion by the first species. In the case when $q = 0$, the above expression reads as $\alpha r_2 < 1$ which corresponds to condition for invasion by the first competitor in the nonspatial case.

Note also that, for $r_2 < \frac{q^2}{4d_2} + \Gamma(0, q)$, the second species is absent, and therefore the first species persists, regardless of the value of α (for advection less than critical

for domain size L). Thus, the actual first species invasion boundary $\Delta(\alpha, r_2, q) = 1 - \frac{q^2}{4d_1}$ lies above both the horizontal line $r_2 = \frac{q^2}{4d_2} + \Gamma(0, q)$ and the curve $\alpha r_2 = 1 - \frac{q^2}{4d_1} - \frac{q}{d_1 L}$ (see Figure 3.3). The existence of an intersection point between the "true" spatial and the nonspatial invasion boundaries is confirmed numerically in Section 4, and thus, also gives rise to four regions, as in the case of invasion by the second species. When the two species have equal diffusivities, we conjecture that the invasion boundary passes through the point $(1, 1)$, similarly to the case of invasion by Species 2 (confirmed numerically in Section 4). Note however, that the same proof does not work here.

Remark 3.2.10 Similarly to σ_2^*, the value of σ_1^* also depends on the values of d_1 and d_2 for $q > 0$. Note that $\Delta(\alpha, r_2, q)$ increases as a function of d_1. As $d_1 \to 0$, $\Delta(\alpha, r_2, q)$ is bounded, while $-\frac{q^2}{4d_1} \to -\infty$, and thus $\sigma_1^* < 0$, and the first competitor cannot invade. Also, by Proposition 3.2.9, if $d_1 \to \infty$ and $L \to \infty$, the condition $\alpha r_2 < 1$ becomes sufficient for invasion by the first species.

3.2.4 Summary of analytic results on mutual invasibility

When considering the β-r_2-bifurcation diagram, we see that, for $q > 0$, the invasion boundary $r_2 = \frac{q^2}{4d_2} + \Gamma(\beta, q)$ is the graph of an increasing function with a positive r_2-intercept (which rises with increase in advection). The curve stays below $r_2 = \beta$ for large enough β. If two species have equal diffusivities ($d_1 = d_2$), then the graph always passes through $(1, 1)$. These observations provide an analytical explanation of the numerical simulations made in [30], where Species 2 was able to coexist with, or even outcompete Species 1 for large enough advection.

Species 1 invades the single species equilibrium of Species 2 if and only if $\Delta(\alpha, r_2, q) < 1 - \frac{q^2}{4d_1}$, where $\Delta(\alpha, r_2, q)$ is a non-negative function that increases with respect to both α and r_2 (with $\Delta(\alpha, r_2, 0) = \alpha r_2$). We have also observed the α-r_2-invasion boundary $\Delta(\alpha, r_2, q)$ is bounded from below by the horizontal line $r_2 = \frac{q^2}{4d_2} + \Gamma(0, q)$

and curve $\alpha r_2 = 1 - \frac{q^2}{4d_1} - \frac{q}{d_1 L}$.

3.3 A nonspatial approximation of the spatial model

In this section, we assume that the species have equal diffusivities $d_1 = d_2 = d$. Our goal is to analyze the behavior of the spatial competition model (3.1.2) by reducing it to a nonspatial "approximation", as described in Chapter 2. We will therefore analyze the behavior of the nonspatial competition model by replacing the diffusion-advection term with $\lambda_1 u$ in both equations:

$$\begin{aligned} \tfrac{du_1}{dt} &= \lambda_1 u_1 + u_1(1 - u_1 - \alpha u_2) \\ \tfrac{du_2}{dt} &= \lambda_1 u_2 + u_2(r_2 - u_2 - \beta u_1). \end{aligned} \tag{3.3.1}$$

The effect of adding the terms with λ_1 (which is non-positive) is the reduction of single species carrying capacities by $-\lambda_1$:

$$\begin{aligned} \tfrac{du_1}{dt} &= u_1(1 + \lambda_1 - u_1 - \alpha u_2) \\ \tfrac{du_2}{dt} &= u_2(r_2 + \lambda_1 - u_2 - \beta u_1). \end{aligned} \tag{3.3.2}$$

Note that, in our previous analysis, to obtain the mutual invasion conditions, we substituted the steady-state solution of one species into the equation for its competitor. Here, we substitute the modified (shifted by λ_1) carrying capacity of a single species instead of its steady state. System (3.3.2) is, of course, just a Lotka-Volterra system with slightly renewed parameters. Hence, the results presented in the Introduction apply and give the following.

The first species can invade the equilibrium $(0, r_2 + \lambda_1)$ if and only if $1 + \lambda_1 > \alpha(r_2 + \lambda_1)$ or $r_2 < \frac{1+\lambda_1}{\alpha} - \lambda_1$;
The second species can invade the equilibrium $(1 + \lambda_1, 0)$ if and only if $r_2 + \lambda_1 > \beta(1 + \lambda_1)$ or $r_2 > (1 + \lambda_1)\beta - \lambda_1$.

Note that the first invasion boundary in (α-r_2-space) is a hyperbola with asymptotes $r_2 = -\lambda_1$ and $\alpha = 0$, and the second (in β-r_2-space) is a straight line with r_2-intercept $-\lambda_1$ and slope $1+\lambda_1$. Since λ_1 is decreasing as we increase q, we observe that the horizontal asymptote of the first boundary is rising, while the slope of the second one is decreasing and its r_2 intercept increases. Note also that both boundaries always pass through point $(1, 1)$.
Using general Lotka-Volterra theory, we conclude that if

1. $1+\lambda_1 > \alpha(r_2+\lambda_1)$ and $r_2+\lambda_1 < \beta(1+\lambda_1)$ then the first competitor wins;

2. $1+\lambda_1 < \alpha(r_2+\lambda_1)$ and $r_2+\lambda_1 > \beta(1+\lambda_1)$ then the second competitor wins;

3. $1+\lambda_1 > \alpha(r_2+\lambda_1)$ and $r_2+\lambda_1 > \beta(1+\lambda_1)$ then there is the coexistence between two species;

4. $1+\lambda_1 < \alpha(r_2+\lambda_1)$ and $r_2+\lambda_1 < \beta(1+\lambda_1)$ then there is a founder control situation. Figures 3.4 and 3.5 show the effect of advection, as we increase q from 0 to 1.5 (or decrease λ_1 from 0 to -0.625).

3.4 Bifurcation analysis of invasibility

In this section we build bifurcation diagrams for our model (3.1.2) in the β-r_2-, α-r_2-, and q-r_2-planes. We use both, spatial and nonspatial, approaches. We assume $d_1 = d_2 = 1$ and $L = 10$. In the spatial approach, for a fixed choice of parameters, we determine invasibility of a single species steady state by its competitor. First, we find the numerical approximation of the steady-state solution (using an implicit finite difference scheme). Then we iterate the linearization of diffusion-reaction-advection operator at the steady state, to determine the sign of its principal eigenvalue. Once

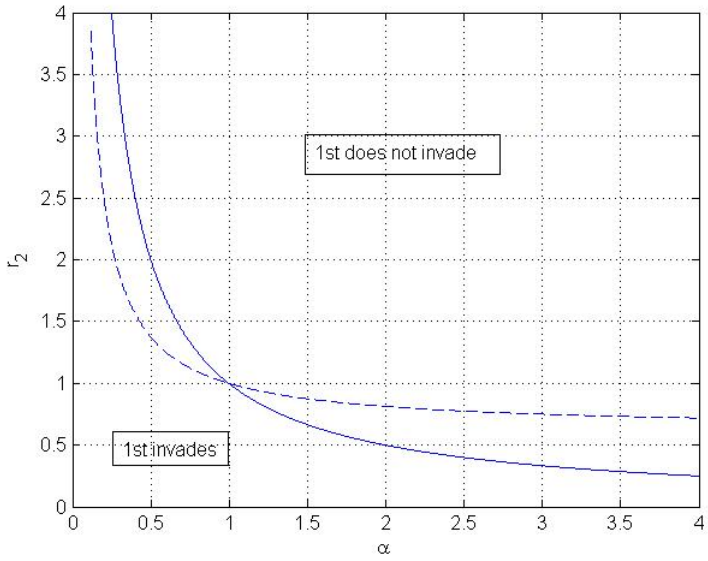

Figure 3.4: The plot shows the invasion boundary for the first species, for $\lambda_1 = 0$, corresponding to $q = 0$ (solid), and for $\lambda_1 = -0.625$, corresponding to $q = 1.5$ (dashed), obtained using nonspatial approximation.

the invasibility outcome is determined, we move on to the next choice of parameters, in such a way that we follow the invasion boundary on the corresponding parameter plane (e.g. qr_2-plane, β-r_2-plane etc).

3.4.1 Bifurcation in the β-r_2-plane

First, we obtain bifurcation diagrams for invasion by the second species in the β-r_2-plane. The invasion condition is given by $r_2 > r_2(\beta, q)$ (as defined in Section 3.2, equation (3.2.10)).

In each diagram, we fix $q > 0$ and show three curves: the nonspatial invasion boundary $r_2 = \beta$ (for $q = 0$) (thin solid line); the spatial boundary obtained numerically $r_2 = r_2(\beta, q)$ (dashed line); and the approximation of the invasion boundary given by $r_2 = (1 + \lambda_1(q, 1))\beta - \lambda_1$ (thick line, obtained in Section 3.3).
Note that all three curves pass through the point $(1, 1)$ of the β-r_2-plane. The last

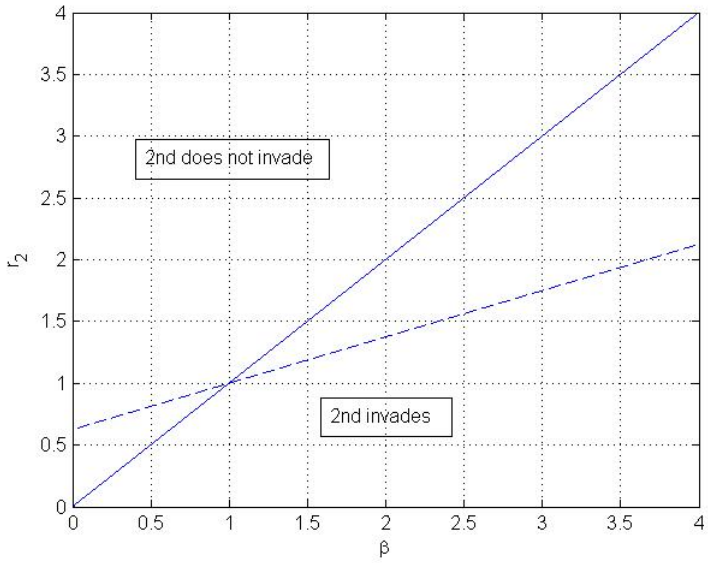

Figure 3.5: The plot shows the invasion boundary for the second species, for $\lambda_1 = 0$, corresponding to $q = 0$ (solid), and for $\lambda_1 = -0.625$, corresponding to $q = 1.5$ (dashed), obtained using nonspatial approximation.

observation is justified by Proposition 3.2.5.

As it is seen in Figure 3.6, both $r_2 = r_2(\beta, q)$ and its approximation $r_2 = (1 + \lambda_1(q, 1))\beta - \lambda_1$ are increasing functions of β (which agrees with Proposition 3.2.1). Moreover, there is always an intersection between the spatial and nonspatial ($r_2 = \beta$) invasion boundaries. This gives rise to four regions mentioned in the previous section (see Proposition 3.2.3). If there is no influence from the first species ($\beta = 0$), then the r_2-intercept is given by $r_2 = -\lambda_1(q, 1)$ and it increases with advection. In addition, we observe that, if flow becomes faster, then the slope of the approximation $r_2 = (1 + \lambda_1(q, 1))\beta - \lambda_1$ decreases, and the curve itself flattens. Note that the same behavior is true for the persistence boundaries obtained by numerics and our predictions obtained from the variational formula.

The diagrams support the numerical results obtained in [30]. For example, if we use the invasion boundaries obtained numerically (dashed curves), then we can

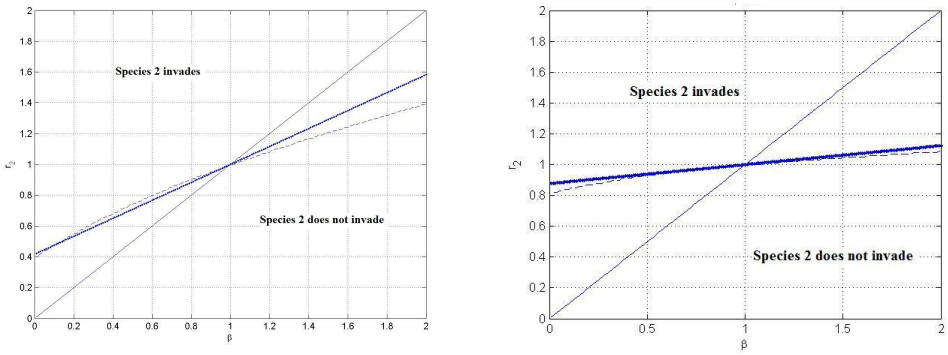

Figure 3.6: Bifurcation in the β-r_2-plane, $q = 1.2$ (left panel) and $q = 1.8$ (right panel). Thin solid lines are given by $\beta = r_2$, corresponding to the non-advective case. Dashed curves are the invasion boundaries in the advective case, obtained numerically. Thick solid lines are given by the nonspatial approximation.

observe the following. In case of intermediate flow $q = 1.2$ and high interspecific coefficient $\beta = 1.8$, the second species needs a growth rate higher than approximately 1.3 in order to persist. On the other hand, for high advection $q = 1.8$ and the same interspecific coefficient $\beta = 1.8$ the second competitor survives even if its growth rate is 1.1. See Figure 3.6.

3.4.2 Bifurcation in the α-r_2-plane

Next, we obtain bifurcation diagrams in the α-r_2-plane showing the conditions for invasion by the first species. As noted above, in the case of zero advection, the invasion condition is given by $\alpha r_2 < 1$. In Figure 3.7, we show the corresponding nonspatial stability boundary $\alpha r_2 = 1$, the stability boundary given by $\Delta(\alpha, r_2, q) = \frac{q^2}{4} - 1$ (dashed curve, obtained numerically), and its approximation $r_2 = \frac{1+\lambda_1(q,1)}{\alpha} - \lambda_1(q, 1)$ (thick curve), for $q = 0.9$ and $q = 1.8$. We notice that, as we increase q, the invasion curve keeps the same shape. However, its upper part (for $r_2 > 1$) gets more narrow, which means that the first species becomes less competitive. This observation agrees

with [30]. The lower part of the invasion region (for $r_2 < 1$) expands (i.e. its boundary rises). This can be explained by extinction of the second species due to advection higher than critical for given growth rate r_2. Namely, when $r_2 < -\lambda_1(q, 1)$, the second species is absent, and thus the area under the line $r_2 = -\lambda_1(q, 1)$ is always included in the invasion region. Moreover $r_2 = -\lambda_1(q, 1)$ appears to be the horizontal asymptote of the spatial invasion boundary $\Delta(\alpha, r_2, q) = \frac{q^2}{4} - 1$. As noted in the previous section, all this is true for our approximation $r_2 = \frac{1+\lambda_1(q,1)}{\alpha} - \lambda_1(q, 1)$.

We can also observe that the spatial and nonspatial boundaries intersect at $(1, 1)$, so the curves divide the first quadrant into four regions.

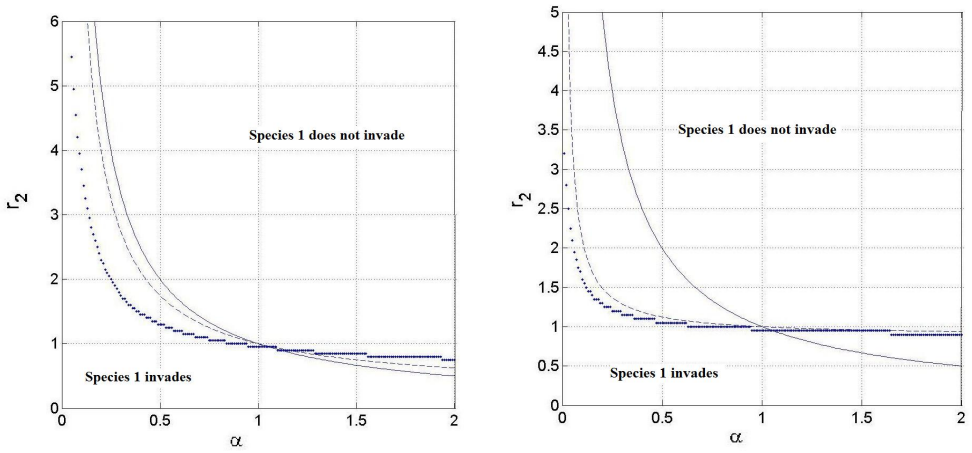

Figure 3.7: Bifurcation in the α-r_2-plane, $q = 0.9$ (left panel), $q = 1.8$ (right panel). Thin solid curves are given by $\alpha r_2 = 1$, corresponding to the non-advective case. Dashed curves are the invasion boundaries in the advective case, obtained numerically. Thick curves are given by the nonspatial approximation.

3.4.3 Bifurcation in the q-r_2-plane: invasion by second species

Since the persistence condition for the second competitor is $r_2 + \lambda_1(q) > 0$, the invasion region is bounded from below by the curve $r_2 = -\lambda_1(q)$ (see Figure 3.8). This curve approaches the parabola $r_2 = \frac{q^2}{4}$ as $L \to \infty$. The invasion region lies above the

curves corresponding to different values of β. These curves are obtained numerically, by analyzing the eigenvalue problem associated with the linearization of our model at the non-trivial equilibrium of the first species. At $\beta = 0$, we are dealing with a single species situation, and thus the invasion boundary coincides with the curve $r_2 = -\lambda_1(q)$. As we increase β (i.e. the first species becomes stronger), the invasion boundary is raised and the invasion region shrinks. For each curve, the r_2-intercept is given by $(0, \beta)$; indeed, when $q = 0$, we have the nonspatial case, where the invasion condition is $r_2 > \beta$.

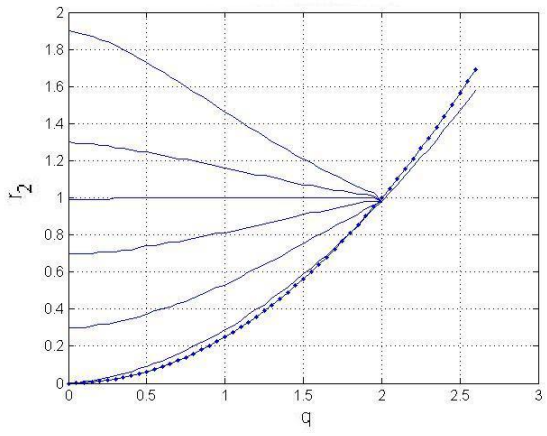

Figure 3.8: The plot shows invasion boundaries for the second species, for $L = 10$, $d_1 = d_2 = 1$, $\beta = 0, 0.3, 0.7, 1, 1.3, 1.9$ (thin curves, obtained numerically). The r_2-intercepts of these curves are given by $(0, \beta)$. The second species invades for the parameters chosen above the corresponding boundary. The dotted curve is the persistence boundary for the second species with no competitor, given by $r_2 = -\lambda_1(q)$, corresponding to the case when $\beta = 0$.

3.4.4 Bifurcation in the q-r_2-plane: invasion by first species

Figure 3.9 gives the invasion boundaries for the first competitor for different values of α. The invasion region lies below the curve. Since the value of the critical velocity for the first species is $q^* \approx 1.9$ as above (corresponding to $L = 10$), the invasion region

is bounded from the right by the line $q = q^*$. When $q = 0$ the invasion condition is $r_2\alpha < 1$, and thus the r_2-intercept of the boundary is given by $(0, \frac{1}{\alpha})$. As we increase α, the invasion boundary is lowered, and thus the invasion region shrinks.

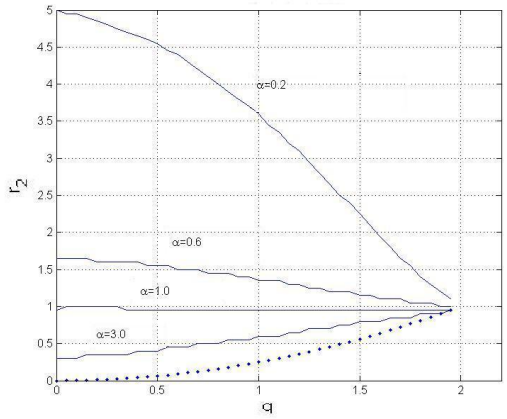

Figure 3.9: The plot shows invasion boundaries for the first species, for $L = 10$, $d_1 = d_2 = 1$, $\alpha = 0.2, 0.6, 1, 3$. Invasion by the first species occurs below the corresponding boundary. The dotted curve is the persistence boundary for the second species with no competitor, given by $r_2 = -\lambda_1(q)$.

3.4.5 Bifurcation in the q-r_2-plane via nonspatial approximation

An alternative way to obtain the bifurcation diagram and analyze the dependence of competition on parameters q and r_2 is to use the invasion conditions formulated in terms of the nonspatial approximation used in Section 3.3.

Recall that the invasion conditions formulated in terms of r_2 and λ_1 are given by:

$r_2 > (1 + \lambda_1)\beta - \lambda_1 = -\lambda_1(\beta - 1) + \beta$ for invasion of the first species equilibrium by the second species;

$r_2 < \frac{1+\lambda_1}{\alpha} - \lambda_1 = -\lambda_1(1 - \frac{1}{\alpha}) + \frac{1}{\alpha}$ for invasion of the equilibrium of the second

species by the first species.

Recall also that λ_1 is a decreasing function of q, where $\lambda_1(0) = 0$, $\lambda_1(q^*) = -1$, and $0 < q^* < 2$ is the critical advection corresponding to $L = 10$, $d = 1$ and $r = 1$.

The bifurcation diagram in the $(-\lambda_1)$-r_2-plane is presented in Figure 3.10. Note that all the invasion boundaries are straight lines.

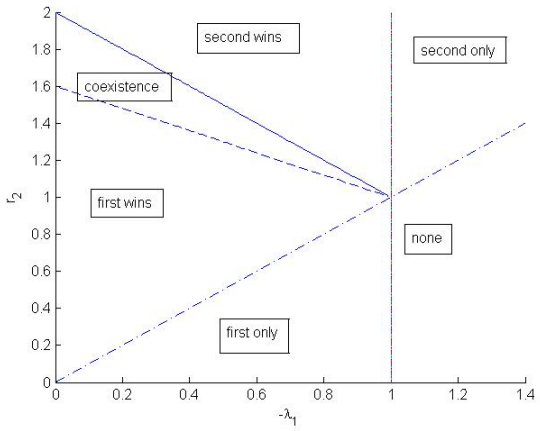

Figure 3.10: The dashed line corresponds to the invasion boundary for the second competitor. The solid line represents the invasion boundary for the first species. To the right of the vertical line the first competitor is absent, since the persistence condition is violated in this whole region. The dashed-dotted line stands for the persistence boundary for the second species in the absence of the first one. Here $\alpha = 0.5$, $\beta = 1.6$, $L = 10$, $d_1 = d_2 = 1$.

Now, we obtain a bifurcation diagram in the q-r_2-plane (see Figure 3.11) by applying the change of variables $\lambda_1 = \lambda_1(q)$ to the diagram in $(-\lambda_1)$-r_2-plane. We observe that the line $r_2 = -\lambda_1$ becomes a curve $r_2 = -\lambda_1(q)$, which is close to the parabola $r_2 = \frac{q^2}{4}$, and the line $-\lambda_1 = 1$ becomes $q = q^* \approx 1.9$. In addition, the other two lines (corresponding to the invasion conditions) transform into decreasing non-intersecting curves, both of which pass through $(q^*, 1)$. The same can be observed from our numerical plots (see also Figures 3.8, 3.9).

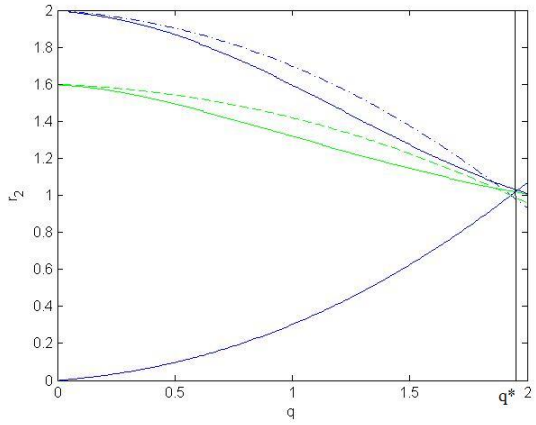

Figure 3.11: The bottom curve is $r_2 = -\lambda_1(q)$, the persistence boundary for the second species. The vertical line corresponds to $q = q^*$, the persistence boundary for the first species. The dashed and dashed-dotted curves are the invasion boundaries for the second and first species, respectively, obtained from nonspatial approximation. The two solid curves next to them are the corresponding invasion boundaries obtained numerically using linearizations at steady states. Here $\alpha = 0.5$, $\beta = 1.6$, $L = 10$, $d_1 = d_2 = 1$.

3.4.6 Effects of increasing advection: two cases

Putting together our observations and using the nonspatial approximation approach, we describe two possible cases. As was shown above, the invasion boundaries of two competitors intersect only at one point $(q^*, 1)$ in q-r_2-plane. We assume that $r_2 > 1$ (otherwise the first species always dominates).

Case 1. If $\beta < \frac{1}{\alpha}$ (see Figure 3.12), then there is a coexistence region between the two curves. The possible scenarios as we increase advection are:

- For $r_2 < \beta$, we have exclusion by first species, followed by coexistence, followed by exclusion by second species.
- For $\beta < r_2 < \frac{1}{\alpha}$, we have coexistence, followed by exclusion by second species.
- For $r_2 > \frac{1}{\alpha}$, we have exclusion by second species.

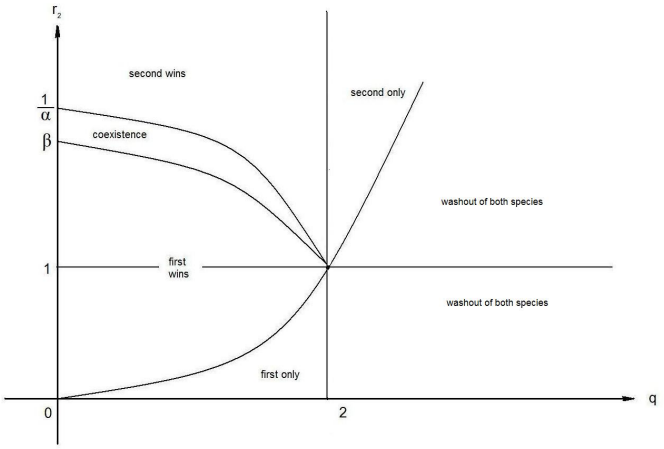

Figure 3.12: Bifurcation diagram in the q-r_2-plane, coexistence case.

Case 2. If $\frac{1}{\alpha} < \beta$ (see Figure 3.13), then there exists a founder control region between the two curves. The possible scenarios as we increase advection are:

- For $r_2 < \frac{1}{\alpha}$, we have exclusion by first species, followed by founder control, followed by exclusion by second species.
- For $\frac{1}{\alpha} < r_2 < \beta$, we have founder control, followed by exclusion by second species.
- For $r_2 > \beta$, we have exclusion by second species.

In both cases, because of monotonicity of the invasion boundaries in the qr_2-plane, the only transitions possible due to increase in advection are

- first wins $\rightarrow$ coexistence
- coexistence $\rightarrow$ second wins
- first wins $\rightarrow$ founder control
- founder control $\rightarrow$ second wins

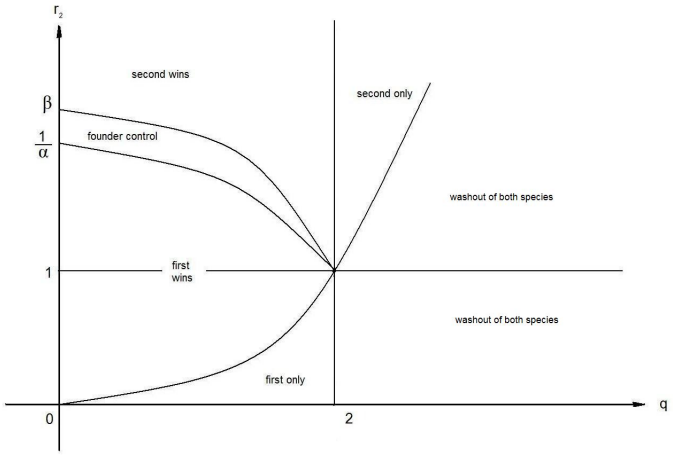

Figure 3.13: Bifurcation diagram in the q-r_2 plane, founder control case.

3.4.7 Steady states vs. advection in nonspatial model.

In the following series of diagrams, we use yet another way to show the effect of advection on the competition outcome in the context of the nonspatial approximation, outlined in Figures 3.12 and 3.13.

In all the diagrams, the solid and the dashed curves show the values of the populations of first and second species, respectively, when they reach an equilibrium, for a given value of q. Namely, for each value of q we compute $\lambda_1(q)$, and using the four inequalities at the end of Section 3.3, we determine the competitive outcome (competitive exclusion by first or second species, coexistence, or founder control). We indicate the equilibrium values for both species:

1. Competitive exclusion by first species: $u_1^* = 1 + \lambda_1(q)$, $u_2^* = 0$
2. Competitive exclusion by second species: $u_1^* = 0$, $u_2^* = r_2 + \lambda_1(q)$).
3. Coexistence:

$u_1^* = (1 + \lambda_1) - \frac{\alpha\beta(1-\lambda_1)-\alpha(r_2+\lambda_1)}{\alpha\beta-1}$

$u_2^* = \frac{\beta(1+\lambda_1)-(r_2+\lambda_1)}{\alpha\beta-1}$.

4. Founder control: we indicate both $u_1^* = 1 + \lambda_1(q)$ and $u_2^* = r_2 + \lambda_1(q)$, as well as highlight the zero value, to emphasize the fact that the outcome is either

$(1 + \lambda_1(q), 0)$ or $(0, r_2 + \lambda_1(q))$, depending on the initial conditions.

In Figure 3.14, we fix interspecific coefficients as $\alpha = 0.6$, $\beta = 1.9$, and use $r_2 = 0.7, 1.4, 1.8, 2.1$, observing four different scenarios, as predicted by Figure 3.13: with possible transitions from domination by the first species to founder control, or from founder control to domination by the second species.

In Figure 3.15, we fix interspecific coefficients as $\alpha = 0.5$, $\beta = 1.4$, and use $r_2 = 0.7, 1.1, 1.5, 2.2$. Again, we observe four scenarios, as predicted by Figure 3.12. The possible transitions are from domination by the first species to coexistence, and from coexistence to domination by the second species.

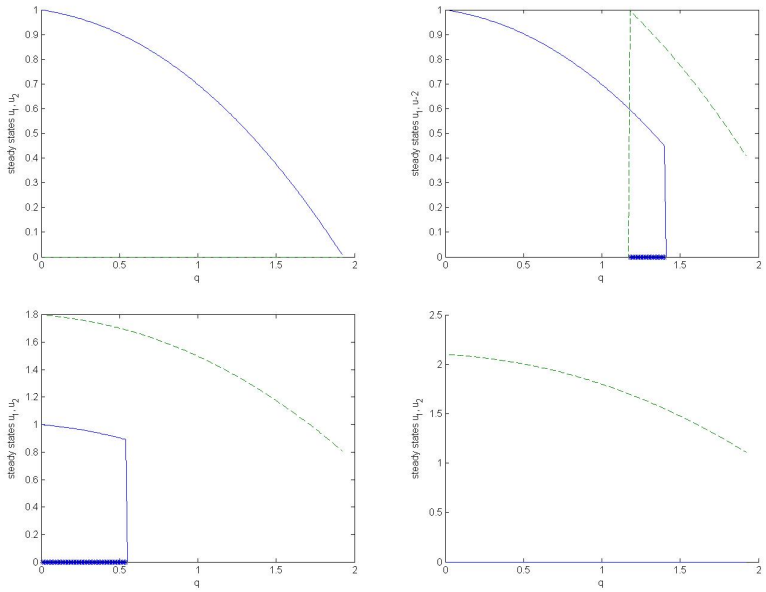

Figure 3.14: Solid curve represents the first species, dashed curve represents the second species. In all four cases, $\alpha = 0.6$, $\beta = 1.9$. *Upper left panel*: competitive exclusion by the first species, $r_2 = 0.7$. *Upper right panel*: competitive exclusion by the first species, followed by founder control ($q \approx 1.2 - 1.4$), followed by competitive exclusion by the second species, $r_2 = 1.4$. *Lower left panel*: Founder control ($q \approx 0 - 0.5$), followed by competitive exclusion by the second species, $r_2 = 1.8$. *Lower right panel*: competitive exclusion by the second species, $r_2 = 2.1$.

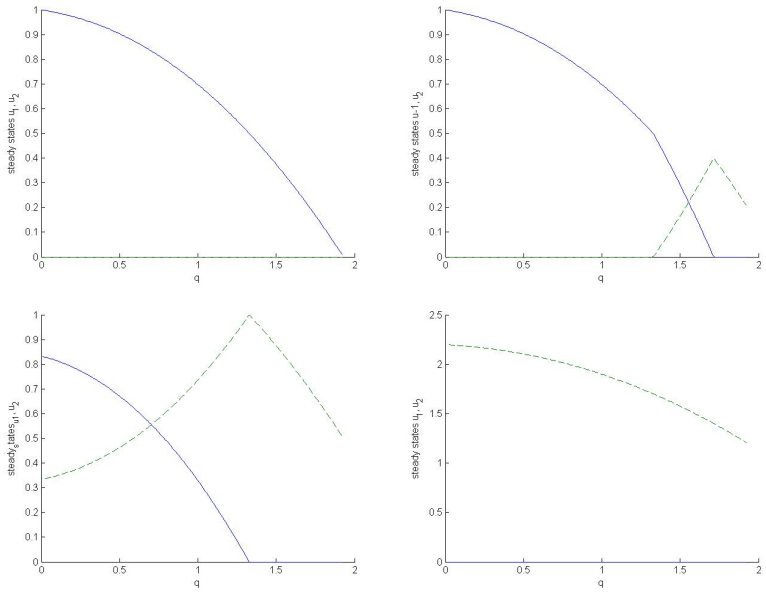

Figure 3.15: Solid curve represents the first species, dashed curve represents the second species. In all four cases, $\alpha = 0.5$, $\beta = 1.4$. *Upper left panel*: competitive exclusion by the first species, $r_2 = 0.7$. *Upper right panel*: competitive exclusion by the first species, followed by coexistence ($q \approx 1.35-1.7$), followed by competitive exclusion by the second species, $r_2 = 1.1$. *Lower left panel*: coexistence ($q \approx 0 - 1.35$), followed by competitive exclusion by the second species, $r_2 = 1.5$. *Lower right panel*: competitive exclusion by the second species, $r_2 = 2.2$.

3.4.8 Bifurcation in the α-β-plane: an example

Note that when q and r_2 are fixed, the invasion conditions for both species are determined by the values of interspecific coefficients: α for invasion by the first species, and β for invasion by the second species. In Figure 3.16, we show the effect of increasing advection from $q = 0$ to $q = 1.5$ on the competition outcome in the α-β-plane, using the nonspatial approximation. In this case, when we change q to 1.5, the new critical values of α and β are $\alpha = 0.7$ and $\beta = 1.4$ and the regions shift as well. Namely, the "1st wins" region shrinks, the "2nd wins" region expands, while the other two change in shape. We can clearly see possible transitions, e.g. from coexistence to domination

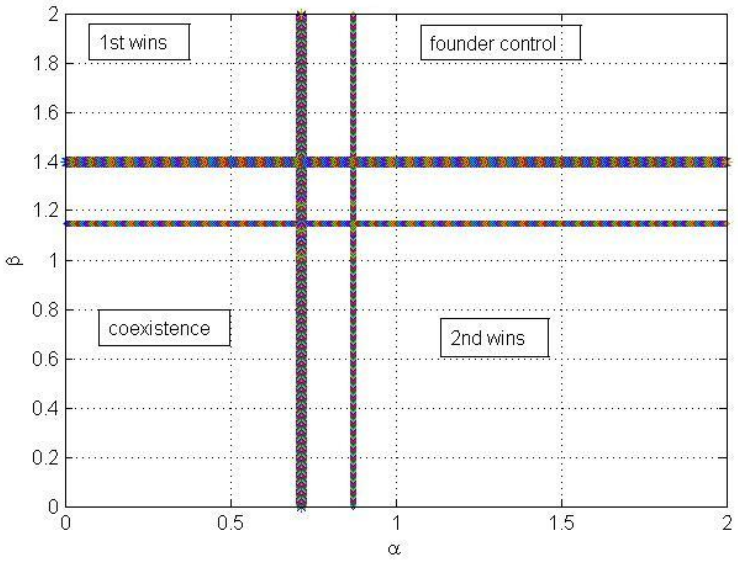

Figure 3.16: Invasion boundaries in the α-β-plane for $q = 0$ (thinner lines) and $q = 1.5$ (thicker lines).

of the second species, from domination of the first species to founder control, etc.

Chapter 4

Three species

4.1 Introduction

In this chapter, we study the dynamics of three competing species in an advective environment. This addition of a third competitor is not just a slight extension of the situation in Chapter 3, but rather a fundamental change. The brief review of the behavior of the nonspatial three-species competition model in Chapter 1 already demonstrated how much richer the dynamics of three compared to two species are. In spatial models of three competing species, even more patterns can be observed; for example diffusion-driven instabilities [23]. The mathematical reason for this increase in complexity is that a 3-species competition model is not monotone, whereas a two-species model is. See [45] for more details on monotone systems. There are a few articles on spatial models for three competing species (e.g. [11], [9], [12]) concerned with the non-advective case (reaction-diffusion only) in a finite habitat with the hostile boundary conditions.

When analyzing the behavior of a three species model, it is natural to start by looking at its two-species submodels. In Chapter 3, we have established that under the assumption of competitive exclusion, the increase in advection speed may affect

the competition outcome: if the competitively weaker species has higher growth rate, it will be a winner under sufficiently high advection. To make our three species setting compatible with that of Chapter 3, we choose the population dynamics parameters so that in the absence of diffusion and advection, each of the three two-species submodels are in the competitive exclusion situation, i.e. no two-species subsystem has a coexistence state or a founder control (in the absence of diffusion and advection) Depending on the outcome of competition in two-species submodels in the absence of advection, there are two cases to investigate: cyclic and non-cyclic. In the non-cyclic case, there is an "absolute loser", i.e. the species who loses the two-species competition with each of the other two species. In the non-cyclic setting, we assume that the weaker competitor always has the higher growth rate, as was the case in Chapter 3 and [30] (otherwise, advection will not change the outcome). In the cyclic setting, the species are arranged in the "rock-paper-scissors" manner, i.e. Species 2 beats Species 1, Species 3 beats Species 2, Species 1 beats Species 3, or in the opposite direction. Two cyclic cases (I and II) differ according to arrangement of growth rates among three competitors. Due to the large number of parameters, we simplify our model even further. Namely, in both cyclic and non-cyclic cases we assume that the competition matrices have specific forms, thus reducing the parameters to the growth rates r_1, r_2, r_3 and interspecific coefficients α and β. While increasing advection eventually leads to changes of outcome in two-species subsystems, the key issue is the effect of advection on the existence and stability of an interior fixed point. We describe and classify several possible scenarios as we increase advection.

4.2 Spatial case

We now formulate the spatial version of system (1.2.6) in an advective environment. The system takes the form

$$\begin{cases} \frac{\partial u_1}{\partial t} = d\frac{\partial^2 u_1}{\partial x^2} - q\frac{\partial u_1}{\partial x} + u_1(r_1 - a_{11}u_1 - a_{12}u_2 - a_{13}u_3), \\ \frac{\partial u_2}{\partial t} = d\frac{\partial^2 u_2}{\partial x^2} - q\frac{\partial u_2}{\partial x} + u_2(r_2 - a_{21}u_1 - a_{22}u_2 - a_{23}u_3), \\ \frac{\partial u_3}{\partial t} = d\frac{\partial^2 u_3}{\partial x^2} - q\frac{\partial u_3}{\partial x} + u_3(r_3 - a_{31}u_1 - a_{32}u_2 - a_{33}u_3), \end{cases} \tag{4.2.1}$$

where $u_i(t,x)$ is the density of the i-th species at time t and at point x of the finite domain $[0,L]$, d is the diffusivity coefficient and q is the advection speed (assumed to be the same for all three species). In addition to the above equations, we consider the same boundary conditions as in the previous chapters, i.e.

$$\begin{cases} d\frac{\partial u_i}{\partial x} = qu_i, \quad x = 0, \ i = 1,2,3 \\ \frac{\partial u_i}{\partial x} = 0, \quad x = L, \ i = 1,2,3. \end{cases} \tag{4.2.2}$$

To analyze the behavior of our model, we use the approach from Chapter 3, where we replaced the diffusion-advection term in the two-species analogue of (4.2.1) by λu, where λ is the leading eigenvalue of the diffusion-advection operator subject to our boundary conditions (it was denoted by λ_1 in Chapter 2 and Chapter 3). This "nonspatial approximation" reduces our spatial model to a nonspatial system

$$\begin{cases} \frac{du_1}{dt} = \lambda u_1 + u_1(r_1 - a_{11}u_1 - a_{12}u_2 - a_{13}u_3), \\ \frac{du_2}{dt} = \lambda u_2 + u_2(r_2 - a_{21}u_1 - a_{22}u_2 - a_{23}u_3), \\ \frac{du_3}{dt} = \lambda u_3 + u_3(r_3 - a_{31}u_1 - a_{32}u_2 - a_{33}u_3). \end{cases} \tag{4.2.3}$$

It was observed in Chapters 2 and 3 that such an approximation gave an accurate enough prediction of the behavior of the corresponding single and two species spatial models.

As we have seen before, $\lambda = \lambda(d,q)$ is a non-positive, decreasing function of q for fixed d, and $\lambda(d,0) = 0$. Thus, we are interested in the behavior of (4.2.3) as we decrease λ starting at $\lambda = 0$.

It was shown numerically in [30] and partially confirmed analytically in Chapter 3 that an increase in advection may change the competitive outcome in a two-species Lotka-Volterra spatial model. Namely, the weaker competitor (in the case of low advection) wins in the case of faster flow, provided it has a higher intrinsic growth rate.

Since the behavior of the three-species model is partially determined by the dynamics of its two-species subsystems, we will use the results from Chapter 3 in our setting. We assume that in each of the two species subsystems, one species competitively excludes the other. This restriction leaves only two possible arrangements between three competitors (up to permutation): 2 beats 1, 3 beats 2, 1 beats 3 (cyclic), or 1 beats 2, 2 beats 3, 1 beats 3 (non-cyclic).

4.3 Cyclic case

In the cyclic case, system (4.2.3) admits a heteroclinic cycle when $\lambda = 0$; i.e. in the absence of one competitor, the model has a competitive exclusion outcome, and the "winners" and "losers" are arranged in a cyclic "rock-paper-scissors" [19] manner, as described above. We assume that the growth rates are arranged as follows: $r_1 > r_2 > r_3 > 0$, and the two species subsystems satisfy one of the two orderings: 2 outcompetes 1, 3 outcompetes 2, 1 outcompetes 3 (case I) or the reverse arrangement, i.e. 1 outcompetes 2, 2 outcompetes 3, 3 outcompetes 1 (case II). By symmetry of the outcomes, this assumption does not limit generality, except for the case of equal growth rates (we exclude the case when $r_i = r_j$, since in that case advection does not change the competitive outcome for the two species).

In order to further simplify our model, we assume that the competition matrix

in (1.2.6) has the form

$$A = \begin{pmatrix} r_1 & r_1\alpha & r_1\beta \\ r_2\beta & r_2 & r_2\alpha \\ r_3\alpha & r_3\beta & r_3 \end{pmatrix},$$

where $0 < \beta < 1 < \alpha$ (case I) or $0 < \alpha < 1 < \beta$ (case II), and $\alpha\beta < 1$. The first condition (in both cases) ensures the "rock-paper-scissors" arrangement, and the second assumption excludes the possibility of founder control in any of the two-species subsystems by Remark 1.2.6, no matter what the growth rates are. In the case $r_1 = r_2 = r_3 = 1$, this model is known as May-Leonard model (see [10]).

System (4.2.3) can be rewritten as

$$\begin{cases} \dfrac{du_1}{dt} = r_1 u_1 \left[\left(1 + \dfrac{\lambda}{r_1}\right) - u_1 - \alpha u_2 - \beta u_3 \right], \\ \dfrac{du_2}{dt} = r_2 u_2 \left[\left(1 + \dfrac{\lambda}{r_2}\right) - \beta u_1 - u_2 - \alpha u_3 \right], \\ \dfrac{du_3}{dt} = r_3 u_3 \left[\left(1 + \dfrac{\lambda}{r_3}\right) - \alpha u_1 - \beta u_2 - u_3 \right]. \end{cases} \tag{4.3.1}$$

Our first goal is to investigate persistence of system (4.3.1) as we vary $\lambda \leq 0$. Thus, we need to check the three conditions in Theorem 1.2.5. We start with the following observation.

Lemma 4.3.1 *(a)* $\alpha^2 - \alpha\beta + \beta^2 - \alpha - \beta + 1 > 0$

(b) $\det \begin{pmatrix} 1 & \alpha & \beta \\ \beta & 1 & \alpha \\ \alpha & \beta & 1 \end{pmatrix} > 0.$

Proof: (a) We have $\alpha^2 - \alpha\beta + \beta^2 - \alpha - \beta + 1 = \frac{3}{4}(\alpha - \beta)^2 + \frac{1}{4}(\alpha + \beta - 2)^2 > 0$.

(b) The determinant is given by

$$\alpha^3 + \beta^3 - 3\alpha\beta + 1 \quad =$$

$$\begin{aligned}(\alpha+\beta)^3-3\alpha^2\beta-3\alpha\beta^2-3\alpha\beta+1 &= \\ (\alpha+\beta)^3+1-3\alpha\beta(\alpha+\beta+1) &= \\ (\alpha+\beta+1)(\alpha^2+2\alpha\beta+\beta^2-\alpha-\beta+1)-3\alpha\beta(\alpha+\beta+1) &= \\ (\alpha+\beta+1)(\alpha^2-\alpha\beta+\beta^2-\alpha-\beta+1).\end{aligned}$$

The statement now follows from $\alpha+\beta+1>0$ and (a).

∎

In a series of lemmas, we determine conditions for which model (4.3.1) has an interior fixed point, i.e. a fixed point with all coordinates positive.

Lemma 4.3.2 *(a) For $\lambda=0$, system (4.3.1) admits a unique interior fixed point $(u_1^0,u_2^0,u_3^0)=(\gamma,\gamma,\gamma)$, where $\gamma=\dfrac{1}{1+\alpha+\beta}$.*
(b) For $\lambda<0$, system (4.3.1) admits a unique fixed point $(u_1^\lambda,u_2^\lambda,u_3^\lambda)=$
$\left(\gamma+\frac{\lambda}{\Delta}\left(\frac{1-\alpha\beta}{r_1}+\frac{\beta^2-\alpha}{r_2}+\frac{\alpha^2-\beta}{r_3}\right),\gamma+\frac{\lambda}{\Delta}\left(\frac{1-\alpha\beta}{r_2}+\frac{\beta^2-\alpha}{r_3}+\frac{\alpha^2-\beta}{r_1}\right),\gamma+\frac{\lambda}{\Delta}\left(\frac{1-\alpha\beta}{r_3}+\frac{\beta^2-\alpha}{r_1}+\frac{\alpha^2-\beta}{r_2}\right)\right)$,
where

$$\Delta=\det\begin{pmatrix}1&\alpha&\beta\\ \beta&1&\alpha\\ \alpha&\beta&1\end{pmatrix}=\alpha^3+\beta^3-3\alpha\beta+1.$$

Proof: (a) Clearly, (u_1^0,u_2^0,u_3^0) is an interior fixed point. Uniqueness follows from Lemma 4.3.1(b).

(b) This can be easily shown by Cramer's rule, using the fact that

$$\alpha^3+\beta^3-3\alpha\beta+1=(\alpha+\beta+1)(\alpha^2-\alpha\beta+\beta^2-\alpha-\beta+1).$$

∎

Proposition 4.3.3 *System (4.3.1) is persistent iff all three of the following inequalities hold:*

$$\lambda\left(\frac{1-\alpha\beta}{r_1}+\frac{\beta^2-\alpha}{r_2}+\frac{\alpha^2-\beta}{r_3}\right)+\alpha^2-\alpha\beta+\beta^2-\alpha-\beta+1>0, \tag{4.3.2}$$

$$\lambda\left(\frac{1-\alpha\beta}{r_2}+\frac{\beta^2-\alpha}{r_3}+\frac{\alpha^2-\beta}{r_1}\right)+\alpha^2-\alpha\beta+\beta^2-\alpha-\beta+1>0, \tag{4.3.3}$$

$$\lambda\left(\frac{1-\alpha\beta}{r_3}+\frac{\beta^2-\alpha}{r_1}+\frac{\alpha^2-\beta}{r_2}\right)+\alpha^2-\alpha\beta+\beta^2-\alpha-\beta+1>0. \tag{4.3.4}$$

Proof: Lemma 4.3.1 implies that the second condition in Theorem 1.2.5 is satisfied for any λ. As we noted above, the condition $\alpha\beta < 1$ excludes the founder control outcome in any of the three two-species subsystems, as long as $\lambda > -r_3$ (see Remark 1.2.6), hence the third condition in Theorem 1.2.5 is true as well. Thus, the only condition we have to check is that the fixed point is indeed in $\mathbb{R}^3_+$. The rest follows by Lemma 4.3.2(b).

∎

Note that if system (4.3.1) is persistent, then it has an interior fixed point $(u_1^\lambda, u_2^\lambda, u_3^\lambda)$, with $u_i^\lambda > 0$ for $i = 1, 2, 3$. Thus, by definition of the interior fixed point, we have

$$\begin{pmatrix} 1 & \alpha & \beta \\ \beta & 1 & \alpha \\ \alpha & \beta & 1 \end{pmatrix} \begin{pmatrix} u_1^\lambda \\ u_2^\lambda \\ u_3^\lambda \end{pmatrix} = \begin{pmatrix} 1+\frac{\lambda}{r_1} \\ 1+\frac{\lambda}{r_2} \\ 1+\frac{\lambda}{r_3} \end{pmatrix}. \tag{4.3.5}$$

Since all components of the matrix are positive, the right-hand side above has positive components as well. Thus, in order for system to be persistent, the value of λ has to be greater than $-r_3$.

By Lemma 4.3.1(a), if $\lambda = 0$ then inequalities (4.3.2), (4.3.3), (4.3.4) hold, and we have an interior fixed point. In addition, each of the inequalities is linear with

respect to λ. Therefore, there exists a persistence boundary $\lambda_c < 0$ such that at least one of the inequalities becomes an equality when $\lambda = \lambda_c$, but all three inequalities hold (and the system is persistent) for $\lambda \in (\lambda_c, 0]$.

Note that $\lambda_c > -r_3$. Clearly, if $\lambda_c \leq -r_3$ then the third component of the right-hand side of (4.3.5) is non-positive. Therefore, at least one of the coordinates of the fixed point must be negative (since all three cannot be equal to zero, otherwise the right-hand side of (4.3.5) becomes zero which cannot happen). Thus, at least one of the inequalities (4.3.2), (4.3.3), (4.3.4) is reversed when $\lambda = \lambda_c$. However, this contradicts the definition of λ_c. Therefore, $\lambda_c \in (-r_3, 0)$.

Now, we will find explicit formulas for λ_c in the two cases.

Case I.

Here, we assume $0 < \beta < 1 < \alpha$. We start by proving the following technical lemmas.

Lemma 4.3.4 *Assume that* $0 < \beta < 1 < \alpha$, $\alpha\beta < 1$ *and* $r_1 > r_2 > r_3 > 0$. *Then the following inequalities hold*

(a) $$\frac{1-\alpha\beta}{r_2} + \frac{\beta^2-\alpha}{r_3} + \frac{\alpha^2-\beta}{r_1} < \frac{\alpha^2-\alpha\beta+\beta^2-\alpha-\beta+1}{r_3};$$

(b) $$\frac{1-\alpha\beta}{r_3} + \frac{\beta^2-\alpha}{r_1} + \frac{\alpha^2-\beta}{r_2} > \frac{\alpha^2-\alpha\beta+\beta^2-\alpha-\beta+1}{r_1} > 0.$$

Proof: The result follows from $\alpha > 1 > \beta > 0$ and $r_1 > r_2 > r_3$, and Lemma 4.3.1(a). ∎

Lemma 4.3.5 *Inequality (4.3.3) holds for* $\lambda = \lambda_c$, *i.e.*

$$\lambda_c \left(\frac{1-\alpha\beta}{r_2} + \frac{\beta^2-\alpha}{r_3} + \frac{\alpha^2-\beta}{r_1} \right) + \alpha^2 - \alpha\beta + \beta^2 - \alpha - \beta + 1 > 0.$$

Proof: Since $-r_3 < \lambda_c < 0$, by Lemma 4.3.4(a) and Lemma 4.3.1(a) we get

$$\lambda_c \left(\frac{1-\alpha\beta}{r_2} + \frac{\beta^2-\alpha}{r_3} + \frac{\alpha^2-\beta}{r_1} \right) + \alpha^2 - \alpha\beta + \beta^2 - \alpha - \beta + 1 >$$

$$\lambda_c \frac{\alpha^2-\alpha\beta+\beta^2-\alpha-\beta+1}{r_3} + \alpha^2-\alpha\beta+\beta^2-\alpha-\beta+1 >$$
$$-r_3 \frac{\alpha^2-\alpha\beta+\beta^2-\alpha-\beta+1}{r_3} + \alpha^2-\alpha\beta+\beta^2-\alpha-\beta+1 = 0.$$

∎

Proposition 4.3.6 *The critical value of λ in Case I is given by*

$$\lambda_c = -\frac{\alpha^2-\alpha\beta+\beta^2-\alpha-\beta+1}{\max\{\frac{1-\alpha\beta}{r_1}+\frac{\beta^2-\alpha}{r_2}+\frac{\alpha^2-\beta}{r_3}, \frac{1-\alpha\beta}{r_3}+\frac{\beta^2-\alpha}{r_1}+\frac{\alpha^2-\beta}{r_2}\}}.$$

Proof: By definition of λ_c, one of the inequalities (4.3.2), (4.3.3) and (4.3.4) must turn into an equality. Lemma 4.3.5 excludes the second one. Thus, we have either

$$\lambda_c\left(\frac{1-\alpha\beta}{r_1}+\frac{\beta^2-\alpha}{r_2}+\frac{\alpha^2-\beta}{r_3}\right)+\alpha^2-\alpha\beta+\beta^2-\alpha-\beta+1=0$$

or

$$\lambda_c\left(\frac{1-\alpha\beta}{r_3}+\frac{\beta^2-\alpha}{r_1}+\frac{\alpha^2-\beta}{r_2}\right)+\alpha^2-\alpha\beta+\beta^2-\alpha-\beta+1=0.$$

Thus, either

$$\lambda_c = \lambda_{c,1} = -\frac{\alpha^2-\alpha\beta+\beta^2-\alpha-\beta+1}{\frac{1-\alpha\beta}{r_1}+\frac{\beta^2-\alpha}{r_2}+\frac{\alpha^2-\beta}{r_3}}$$

or

$$\lambda_c = \lambda_{c,2} = -\frac{\alpha^2-\alpha\beta+\beta^2-\alpha-\beta+1}{\frac{1-\alpha\beta}{r_3}+\frac{\beta^2-\alpha}{r_1}+\frac{\alpha^2-\beta}{r_2}}.$$

By Lemma 4.3.1(a), the numerator in both fractions is positive. By Lemma 4.3.5(b), the denominator of the second fraction is positive as well. Thus $\lambda_{c,2} < 0$. If $\lambda_{c,1} < 0$ as well, then λ_c is the larger of the two. Otherwise $\lambda_c = \lambda_{c,2}$. Thus we get the required formula, and λ_c is well defined and is negative for any choice of $\alpha > 1 > \beta > 0$ and $r_1 > r_2 > r_3 > 0$. ∎

Case II.

Next we obtain critical threshold value of λ for the second arrangement in the Cyclic case.

Lemma 4.3.7 *Assume that* $0 < \alpha < 1 < \beta$, $\alpha\beta < 1$ *and* $r_1 > r_2 > r_3 > 0$. *Then the following inequalities hold*

(a) $\dfrac{1-\alpha\beta}{r_2} + \dfrac{\beta^2-\alpha}{r_3} + \dfrac{\alpha^2-\beta}{r_1} > 0$;

(b) $\dfrac{1-\alpha\beta}{r_1} + \dfrac{\beta^2-\alpha}{r_2} + \dfrac{\alpha^2-\beta}{r_3} < \dfrac{1-\alpha\beta}{r_2} + \dfrac{\beta^2-\alpha}{r_3} + \dfrac{\alpha^2-\beta}{r_1}$;

(c) $\dfrac{1-\alpha\beta}{r_3} + \dfrac{\beta^2-\alpha}{r_1} + \dfrac{\alpha^2-\beta}{r_2} < \dfrac{1-\alpha\beta}{r_2} + \dfrac{\beta^2-\alpha}{r_3} + \dfrac{\alpha^2-\beta}{r_1}$.

Proof: (a) It follows from the assumptions that

$$\frac{1-\alpha\beta}{r_2}+\frac{\beta^2-\alpha}{r_3}+\frac{\alpha^2-\beta}{r_1} > \frac{1-\alpha\beta}{r_1}+\frac{\beta^2-\alpha}{r_1}+\frac{\alpha^2-\beta}{r_1} = \frac{\alpha^2-\alpha\beta+\beta^2-\alpha-\beta+1}{r_1} > 0.$$

(b) The inequality holds term-by-term.

(c) Taking the difference, we get

$$\begin{aligned}
&\frac{1-\alpha\beta}{r_2} + \frac{\beta^2-\alpha}{r_3} + \frac{\alpha^2-\beta}{r_1} - \frac{1-\alpha\beta}{r_3} - \frac{\beta^2-\alpha}{r_1} - \frac{\alpha^2-\beta}{r_2} \\
&= \frac{\alpha^2-\beta-\beta^2+\alpha}{r_1} + \frac{1-\alpha\beta-\alpha^2+\beta}{r_2} + \frac{\beta^2-\alpha-1+\alpha\beta}{r_3} \\
&= \frac{(\alpha-\beta)(\alpha+\beta+1)}{r_1} + \frac{(1-\alpha)(\alpha+\beta+1)}{r_2} + \frac{(\beta-1)(\alpha+\beta+1)}{r_3} \\
&> \frac{(\alpha-\beta)(\alpha+\beta+1)+(1-\alpha)(\alpha+\beta+1)+(\beta-1)(\alpha+\beta+1)}{r_1} = 0,
\end{aligned}$$

as needed.

∎

Lemma 4.3.7 implies that, in Case II, inequality (4.3.3) is always the first to fail when we decrease $\lambda < 0$. Thus, we get

Proposition 4.3.8 *The critical value of* λ *for persistence in Case II is given by*

$$\lambda_c = -\frac{\alpha^2-\alpha\beta+\beta^2-\alpha-\beta+1}{\frac{1-\alpha\beta}{r_2}+\frac{\beta^2-\alpha}{r_3}+\frac{\alpha^2-\beta}{r_1}}.$$

We now turn our attention to the question of permanence. By Theorem 1.2.7, with our assumptions, system (4.3.1) with $\lambda = 0$ is permanent iff it is persistent and satisfies

$$(\alpha - 1)^3 < (1 - \beta)^3,$$

or, equivalently,

$$\alpha + \beta < 2.$$

Note that if the system is permanent, then either the interior fixed point is stable, or it is unstable and there exists a stable interior limit cycle. We investigate the stability of the interior fixed point when $\lambda = 0$ and when λ approaches λ_c (i.e. the interior fixed point approaches the boundary).

First, we show that if $\lambda = 0$ and the permanence condition $\alpha + \beta < 2$ is satisfied, then the interior fixed point is stable (so there is no stable limit cycle). Namely, we prove the following.

Proposition 4.3.9 *Suppose $r_1, r_2, r_3 > 0$, $\alpha, \beta > 0$ and $\alpha + \beta < 2$. Then the interior fixed point (γ, γ, γ) (where $\gamma = \frac{1}{1+\alpha+\beta}$) of*

$$\begin{cases} \dfrac{du_1}{dt} = r_1 u_1 \left(1 - u_1 - \alpha u_2 - \beta u_3\right), \\ \dfrac{du_2}{dt} = r_2 u_2 \left(1 - \beta u_1 - u_2 - \alpha u_3\right), \\ \dfrac{du_3}{dt} = r_3 u_3 \left(1 - \alpha u_1 - \beta u_2 - u_3\right). \end{cases} \tag{4.3.6}$$

is stable.

Proof: The Jacobian at the fixed point is given by

$$J_{r_1 r_2 r_3} = \frac{1}{1 + \alpha + \beta} \begin{pmatrix} -r_1 & -r_1\alpha & -r_1\beta \\ -r_2\beta & -r_2 & -r_2\alpha \\ -r_3\alpha & -r_3\beta & -r_3 \end{pmatrix}.$$

In the case $r_1 = r_2 = r_3 = r > 0$, the eigenvalues of J have negative real parts. Namely, J_{rrr} has eigenvalue $\mu_1 = -r$ (with eigenvector $(1,1,1)$) and trace $\mathrm{tr}(J) = -\frac{3r}{1+\alpha+\beta}$. Let μ_2, μ_3 be the other two eigenvalues. Thus, $-\frac{3r}{1+\alpha+\beta} = \mu_1 + \mu_2 + \mu_3 = -r + \mu_2 + \mu_3$, and therefore $\mu_2 + \mu_3 = -\frac{3r}{1+\alpha+\beta} + r = \frac{r(\alpha+\beta-2)}{1+\alpha+\beta} < 0$, by assumption $\alpha + \beta < 2$. Hence, $\mu_2 + \mu_3 < 0$. On the other hand, $\mu_1\mu_2\mu_3 = \det J_{rrr} < 0$. Since $\mu_1 < 0$, this implies that $\mu_2\mu_3 > 0$. Together with $\mu_2 + \mu_3 < 0$, this implies that $Re(\mu_2), Re(\mu_3) < 0$. Thus, all the eigenvalues have negative real parts, which, Grobman-Hartman Theorem (see, for example, [39]), implies asymptotic stability of (γ, γ, γ) in the case $r_1 = r_2 = r_3 = r > 0$.

Now, suppose for some $r_1, r_2, r_3 > 0$ the fixed point is unstable. Then at least one of the eigenvalues of J has positive real part. Note that eigenvalues of $J_{r_1 r_2 r_3}$ depend continuously on its entries (and therefore on r_1, r_2, r_3), and there is a continuous path from (r, r, r) to (r_1, r_2, r_3) in the first octant. Travelling along this path from (r, r, r) to (r_1, r_2, r_3), we take the first point (r_1^*, r_2^*, r_3^*) at which the real part of at least one eigenvalue becomes zero (such a point exists by continuity). This means that either we have three real eigenvalues (with at least one eigenvalue which is zero) or a negative real eigenvalue and two purely imaginary eigenvalues. Since, $\det(J_{r_1^* r_2^* r_3^*}) = r_1^* r_2^* r_3^* \det(J_{111}) \neq 0$, only the second possibility remains: $\mu_1 < 0$, $\mu_2 = bi$, and $\mu_3 = -bi$.

The characteristic polynomial of $J_{r_1^* r_2^* r_3^*}$ is given by

$$p(\mu) = \det(\mu I - J_{r_1^* r_2^* r_3^*}) = \det\left(\mu I + \frac{1}{1+\alpha+\beta}\begin{pmatrix} r_1^* & r_1^*\alpha & r_1^*\beta \\ r_2^*\beta & r_2^* & r_2^*\alpha \\ r_3^*\alpha & r_3^*\beta & r_3^* \end{pmatrix}\right)$$

$$= (\mu - \mu_1)(\mu^2 + b^2) = \mu^3 - \mu_1\mu^2 + b^2\mu - \mu_1 b^2.$$

Expanding the determinant and equating all the coefficients, we get:

$$-\mu_1 = \frac{1}{1+\alpha+\beta}(r_1^* + r_2^* + r_3^*),$$

$$b^2 = \frac{1}{(1+\alpha+\beta)^2}(1-\alpha\beta)(r_1^*r_2^* + r_1^*r_3^* + r_2^*r_3^*),$$

$$-\mu_1 b^2 = \frac{1}{(1+\alpha+\beta)^3} r_1^*r_2^*r_3^*(1+\alpha^3+\beta^3-3\alpha\beta).$$

Thus, we have

$$\frac{(r_1^*+r_2^*+r_3^*)(r_1^*r_2^*+r_1^*r_3^*+r_2^*r_3^*)}{r_1^*r_2^*r_3^*} = \frac{1+\alpha^3+\beta^3-3\alpha\beta}{1-\alpha\beta}.$$

Note that

$$\frac{(r_1^*+r_2^*+r_3^*)(r_1^*r_2^*+r_1^*r_3^*+r_2^*r_3^*)}{r_1^*r_2^*r_3^*} = 3 + \frac{r_1^*}{r_2^*} + \frac{r_2^*}{r_1^*} + \frac{r_1^*}{r_3^*} + \frac{r_3^*}{r_1^*} + \frac{r_2^*}{r_3^*} + \frac{r_3^*}{r_2^*} \geq 9,$$

since $x + \frac{1}{x} \geq 2$ for any $x > 0$.

Then

$$\frac{1+\alpha^3+\beta^3-3\alpha\beta}{1-\alpha\beta} \geq 9,$$

and since $\alpha\beta < 1$, we get

$$1+\alpha^3+\beta^3-3\alpha\beta \geq 9-9\alpha\beta,$$

or

$$\alpha^3+\beta^3+6\alpha\beta \geq 8.$$

But since $\alpha+\beta<2$, we have:

$$\alpha^3+\beta^3+6\alpha\beta = (\alpha+\beta)(\alpha^2-\alpha\beta+\beta^2)+6\alpha\beta < 2(\alpha^2-\alpha\beta+\beta^2)+6\alpha\beta = 2(\alpha+\beta)^2 < 8,$$

a contradiction.

∎

Next, we show that when λ approaches λ_c, the interior fixed point is stable as well (regardless of whether $\alpha+\beta<2$ is true or not). We make an additional "generic" assumption: when the interior fixed point reaches the boundary of $\mathbb{R}^3_+$, only one of its coordinates becomes zero. The case when the assumption fails is biologically unlikely.

Proposition 4.3.10 *Suppose $r_1, r_2, r_3 > 0$, $\alpha, \beta > 0$. Let $(u_1^\lambda, u_2^\lambda, u_3^\lambda)$ be the interior fixed point of (4.3.1) where $\lambda < 0$. Assume that $(u_1^{\lambda_c}, u_2^{\lambda_c}, u_3^{\lambda_c})$ has only one zero component. Then the interior fixed point $(u_1^\lambda, u_2^\lambda, u_3^\lambda)$ of (4.3.1) is stable for $\lambda \in (\lambda_c, \lambda_c + \varepsilon)$ for some $\varepsilon > 0$.*

Proof: Let $\lambda_c < \lambda \leq 0$. The Jacobian of (4.3.1) at the fixed point $(u_1^\lambda, u_2^\lambda, u_3^\lambda)$ is given by

$$J^\lambda = \begin{pmatrix} -r_1 u_1^\lambda & -r_1\alpha u_1^\lambda & -r_1\beta u_1^\lambda \\ -r_2\beta u_2^\lambda & -r_2 u_2^\lambda & -r_2\alpha u_2^\lambda \\ -r_3\alpha u_3^\lambda & -r_3\beta u_3^\lambda & -r_3 u_3^\lambda \end{pmatrix}.$$

Note that by Lemma 4.3.1,

$$\det(J^\lambda) = -r_1 r_2 r_3 u_1^\lambda u_2^\lambda u_3^\lambda \det \begin{pmatrix} 1 & \alpha & \beta \\ \beta & 1 & \alpha \\ \alpha & \beta & 1 \end{pmatrix} < 0.$$

Therefore, the determinant of the Jacobian at the interior fixed point is always negative. As we decrease λ, the interior fixed point approaches one of the $u_i u_j$-planes; i.e. one of its coordinates u_k^λ approaches zero. We may assume that u_3^λ approaches 0 as λ approaches λ_c and therefore $(u_1^\lambda, u_2^\lambda, u_3^\lambda)$ approaches $(u_1^{\lambda_c}, u_2^{\lambda_c}, 0)$. By our assumption, $u_1^{\lambda_c}$ and $u_2^{\lambda_c}$ are positive. Thus,

$$J^{\lambda_c} = \begin{pmatrix} -r_1 u_1^{\lambda_c} & -r_1\alpha u_1^{\lambda_c} & -r_1\beta u_1^{\lambda_c} \\ -r_2\beta u_2^{\lambda_c} & -r_2 u_2^{\lambda_c} & -r_2\alpha u_2^{\lambda_c} \\ 0 & 0 & 0 \end{pmatrix}.$$

At $\lambda = \lambda_c$, the two species subsystem of (4.3.1) consisting of Species 1 and 2 has a stable coexistence outcome $(u_1^{\lambda_c}, u_2^{\lambda_c})$, since the founder control outcome is not possible for $\lambda > \lambda_c$, by the assumption $\alpha\beta < 1$ and Remark 1.2.6 (see also the

bifurcation diagram in Figure 3.10). The Jacobian is given by

$$\begin{pmatrix} -r_1 u_1^{\lambda_c} & -r_1 \alpha u_1^{\lambda_c} \\ -r_2 \beta u_2^{\lambda_c} & -r_2 u_2^{\lambda_c} \end{pmatrix}.$$

This Jacobian has two negative real eigenvalues μ_1, μ_2 (from the general Lotka-Volterra theory). The eigenvalues of J^{λ_c} are given by μ_1, μ_2 and $\mu_3 = 0$.

Since the eigenvalues of J^{λ} depend continuously on λ, for λ close enough to λ_c, J^{λ} has two eigenvalues with negative real parts, and one other real eigenvalue. On the other hand, we know that for $\lambda > \lambda_c$, $\det(J^{\lambda}) < 0$. Since the determinant of a matrix is equal to the product of its eigenvalues, it follows that the third eigenvalue is negative. Thus, for λ close enough to λ_c, the interior fixed point of (4.3.1) is stable.

∎

In summary, we have the following possible scenarios as we decrease λ from 0 to λ_c:

1. if $\alpha + \beta < 2$, the system starts and ends with a stable interior fixed point. Numerical simulations (see Section 4.5) suggest that it remains stable for intermediate values of λ);

2. if $\alpha + \beta \geq 2$, the system starts with a stable heteroclinic cycle (and unstable interior fixed point), and ends with a stable interior fixed point; numerical simulations show that the transition occurs via a stable interior limit cycle (namely, the heteroclinic cycle loses its stability before the interior fixed point becomes stable).

4.4 Non-cyclic case

In the non-cyclic case, when $\lambda = 0$, system (4.3.1) does not admit a heteroclinic cycle. Without loss of generality, we arrange the competitors in the following manner: 1 outcompetes 2, 2 outcompetes 3, 1 outcompetes 3. We also arrange the growth

rates as follows: $0 < r_1 < r_2 < r_3$. This makes our model a natural generalization of the two-species competition model from Chapter 3: in each of the two-species subsystems, the stronger competitor has a lower growth rate. Note also that Species 3 is the absolute "loser", but has the highest growth rate among the three, while Species 1 outcompetes each of the other two, but has the lowest growth rate.

In order to simplify our model, we assume that the competition matrix in (1.2.6) has form

$$A = \begin{pmatrix} r_1 & r_1\beta & r_1\beta \\ r_2\alpha & r_2 & r_2\beta \\ r_3\alpha & r_3\alpha & r_3 \end{pmatrix},$$

where $0 < \beta < 1 < \alpha$ and $\alpha\beta < 1$. The first condition ensures the given arrangement, and the second assumption excludes the possibility of founder control in any of the two-species subsystems by Remark 1.2.6, no matter what the growth rates are.

Now, system (4.3.1) can be rewritten as

$$\begin{cases} \dfrac{du_1}{dt} = r_1u_1\left[\left(1+\dfrac{\lambda}{r_1}\right) - u_1 - \beta u_2 - \beta u_3\right], \\ \dfrac{du_2}{dt} = r_2u_2\left[\left(1+\dfrac{\lambda}{r_2}\right) - \alpha u_1 - u_2 - \beta u_3\right], \\ \dfrac{du_3}{dt} = r_3u_3\left[\left(1+\dfrac{\lambda}{r_3}\right) - \alpha u_1 - \alpha u_2 - u_3\right]. \end{cases} \tag{4.4.1}$$

Lemma 4.4.1 *Assume $0 < \beta < 1 < \alpha$ and $\alpha\beta < 1$. Then*

$$\det\begin{pmatrix} 1 & \beta & \beta \\ \alpha & 1 & \beta \\ \alpha & \alpha & 1 \end{pmatrix} = \alpha\beta(\alpha+\beta-3)+1 = \alpha^2\beta + \alpha\beta^2 - 3\alpha\beta + 1 > 0.$$

Proof: It suffices to prove that $\beta\alpha^2 + (\beta^2 - 3\beta)\alpha + 1 > 0$ for all $0 < \beta < 1$. It is enough to show that the discriminant $D = (\beta^2 - 3\beta)^2 - 4\beta = \beta^4 - 6\beta^3 + 9\beta^2 - 4\beta$ is negative for all $0 < \beta < 1$. Equivalently, $f(\beta) = \beta^3 - 6\beta^2 + 9\beta - 4 < 0$ for all

$0 < \beta < 1$. Note that $f(1) = f'(1) = 0$, $f'(\beta) = 3(\beta-1)(\beta-3)$ and $f''(1) < 0$. Hence $\beta = 1$ is a local maximum, and $f(\beta) < 0$ for all $\beta < 1$, as needed.

∎

Next, we investigate the question of existence of an interior fixed point for (4.4.1). The following is an easy application of Cramer's rule.

Lemma 4.4.2 *System (4.4.1) has a unique fixed point* $(u_1^\lambda, u_2^\lambda, u_3^\lambda)$*, where*

$$u_1^\lambda = \lambda\left(\frac{1-\alpha\beta}{r_1} + \frac{\beta(\alpha-1)}{r_2} + \frac{\beta(\beta-1)}{r_3}\right) + (\beta-1)^2,$$

$$u_2^\lambda = \lambda\left(\frac{\alpha(\beta-1)}{r_1} + \frac{1-\alpha\beta}{r_2} + \frac{\beta(\alpha-1)}{r_3}\right) + (\alpha-1)(\beta-1),$$

$$u_3^\lambda = \lambda\left(\frac{\alpha(\alpha-1)}{r_1} + \frac{\alpha(\beta-1)}{r_2} + \frac{1-\alpha\beta}{r_3}\right) + (\alpha-1)^2.$$

Note that $u_2^0 = (\alpha-1)(\beta-1) < 0$, and thus for $\lambda = 0$ (non-advective case), there is no interior fixed point; i.e. the system is non-persistent (no coexistence). In fact, it has a stable exclusion state $(1, 0, 0)$.

As we decrease $\lambda < 0$ (increase advection), system (4.4.1) may admit an interior fixed point and thus become persistent (or even permanent), under certain conditions outlined in the following proposition.

Proposition 4.4.3 *System (4.4.1) is persistent iff all three of the following inequalities hold:*

$$\lambda\left(\frac{1-\alpha\beta}{r_1} + \frac{\beta(\alpha-1)}{r_2} + \frac{\beta(\beta-1)}{r_3}\right) + (\beta-1)^2 > 0, \tag{4.4.2}$$

$$\lambda\left(\frac{\alpha(\beta-1)}{r_1} + \frac{1-\alpha\beta}{r_2} + \frac{\beta(\alpha-1)}{r_3}\right) + (\alpha-1)(\beta-1) > 0, \tag{4.4.3}$$

$$\lambda\left(\frac{\alpha(\alpha-1)}{r_1}+\frac{\alpha(\beta-1)}{r_2}+\frac{1-\alpha\beta}{r_3}\right)+(\alpha-1)^2>0. \tag{4.4.4}$$

Proof: The proof is analogous to the proof of Proposition 4.3.3.

∎

In the following lemma, we show that the coefficient of λ in inequality (4.4.3) is always negative; therefore, although the inequality fails for $\lambda = 0$, it will hold for sufficiently negative λ. We also show that the coefficient of λ in inequality (4.4.2) is always positive; therefore, for sufficiently negative λ, this inequality will be violated. Note that we cannot obtain a similar result regarding inequality (4.4.4), since the sign of the corresponding coefficient of λ depends on the choice of parameters.

Lemma 4.4.4 *The inequalities*

(a) $\frac{\alpha(\beta-1)}{r_1}+\frac{1-\alpha\beta}{r_2}+\frac{\beta(\alpha-1)}{r_3}<0$

(b) $\frac{1-\alpha\beta}{r_1}+\frac{\beta(\alpha-1)}{r_2}+\frac{\beta(\beta-1)}{r_3}>0$

hold for any $\alpha>1>\beta>0$ *and* $0<r_1<r_2<r_3$.

Proof: (a)

$$\frac{\alpha(\beta-1)}{r_1}+\frac{1-\alpha\beta}{r_2}+\frac{\beta(\alpha-1)}{r_3}<$$

$$\frac{\alpha(\beta-1)}{r_1}+\frac{1-\alpha\beta}{r_1}+\frac{\beta(\alpha-1)}{r_1}=\frac{(1-\alpha)(1-\beta)}{r_1}<0.$$

(b)

$$\frac{1-\alpha\beta}{r_1}+\frac{\beta(\alpha-1)}{r_2}+\frac{\beta(\beta-1)}{r_3}>$$

$$\frac{1-\alpha\beta}{r_3}+\frac{\beta(\alpha-1)}{r_3}+\frac{\beta(\beta-1)}{r_3}=\frac{(\beta-1)^2}{r_3}>0.$$

∎

Let

$$\lambda_{s2} = \frac{(\alpha-1)(1-\beta)}{\frac{\alpha(\beta-1)}{r_1} + \frac{1-\alpha\beta}{r_2} + \frac{\beta(\alpha-1)}{r_3}}. \tag{4.4.5}$$

Then, by Lemma 4.4.4(a), $\lambda_{s2} < 0$. Note that (4.4.3) holds exactly when $\lambda < \lambda_{s2}$.

Lemma 4.4.5 *Let $\alpha > 1 > \beta > 0$, $0 < r_1 < r_2 < r_3$. Then inequalities (4.4.2) and (4.4.4) are satisfied for $\lambda = \lambda_{s2}$.*

Proof: Substituting $\lambda = \lambda_{s2}$ into (4.4.2), we get

$$\frac{(\alpha-1)(1-\beta)}{\frac{\alpha(\beta-1)}{r_1} + \frac{1-\alpha\beta}{r_2} + \frac{\beta(\alpha-1)}{r_3}} \left(\frac{1-\alpha\beta}{r_1} + \frac{\beta(\alpha-1)}{r_2} + \frac{\beta(\beta-1)}{r_3} \right) + (\beta-1)^2 > 0.$$

Since the denominator is negative and $\beta < 1$, this is equivalent to

$$(\alpha-1)\left(\frac{1-\alpha\beta}{r_1} + \frac{\beta(\alpha-1)}{r_2} + \frac{\beta(\beta-1)}{r_3} \right) < (\beta-1)\left(\frac{\alpha(\beta-1)}{r_1} + \frac{1-\alpha\beta}{r_2} + \frac{\beta(\alpha-1)}{r_3} \right),$$

or

$$(\alpha-1)(r_2r_3 - \alpha\beta r_2r_3 + \alpha\beta r_1r_3 - \beta r_1r_3 + \beta^2 r_1r_2 - \beta r_1r_2) <$$

$$(\beta-1)(\alpha\beta r_2r_3 - \alpha r_2r_3 + r_1r_3 - \alpha\beta r_1r_3 + \alpha\beta r_1r_2 - \beta r_1r_2).$$

Simplifying, we get

$$r_2r_3(-\alpha^2\beta - \alpha\beta^2 + 3\alpha\beta - 1) + r_1r_3(\alpha^2\beta + \alpha\beta^2 - 3\alpha\beta + 1) - r_1r_2\alpha\beta^2 < 0,$$

or

$$r_3(r_1 - r_2)(\alpha\beta(\alpha+\beta-3)+1) - r_1r_2\alpha\beta^2 < 0.$$

This inequality holds since $r_1 < r_2$ and, by Lemma 4.4.1, $\alpha\beta(\alpha+\beta-3)+1 > 0$. Similarly, plugging $\lambda = \lambda_{s2}$ into (4.4.3) and simplifying, we get

$$(1-\beta)(\alpha^2 r_2r_3 - \alpha r_2r_3 + \alpha\beta r_1r_3 - \alpha r_1r_3 + r_1r_2 - \alpha\beta r_1r_2) >$$

$$(\alpha-1)(\alpha\beta r_2r_3 - \alpha r_2r_3 + r_1r_3 - \alpha\beta r_1r_3 + \alpha\beta r_1r_2 - \beta r_1r_2),$$

or

$$(\alpha\beta^2 + \alpha^2\beta - 3\alpha\beta + 1 + \alpha)r_1r_3 + (-\alpha\beta^2 - \alpha^2\beta + 3\alpha\beta - 1 - \beta)r_1r_2 > 0.$$

This can be rewritten as

$$r_1(r_3 - r_2)(\alpha\beta(\alpha + \beta - 3) + 1) + r_1(r_3\alpha - r_2\beta) > 0,$$

which holds by Lemma 4.4.1 and the assumptions $r_2 < r_3$ and $\alpha > \beta$. ∎

Let

$$\lambda_{s1} = \max\left(-\frac{(\beta-1)^2}{\frac{1-\alpha\beta}{r_1} + \frac{\beta(\alpha-1)}{r_2} + \frac{\beta(\beta-1)}{r_3}}, -\frac{(\alpha-1)^2}{\frac{\alpha(\alpha-1)}{r_1} + \frac{\alpha(\beta-1)}{r_2} + \frac{1-\alpha\beta}{r_3}}\right). \tag{4.4.6}$$

By Lemma 4.4.4(b), λ_{s1} is well-defined and $\lambda_{s1} < 0$. Note that one of the inequalities (4.4.2) and (4.4.4) fails exactly when $\lambda < \lambda_{s1}$. Also, by Lemma 4.4.5, $\lambda_{s1} < \lambda_{s2}$. Note that $\lambda_{s1} > -r_1$, since for $\lambda \leq -r_1$ the first species will not persist.
Summarizing our results we have the following.

Proposition 4.4.6 *System (4.4.1) is persistent exactly when* $\lambda_{s1} < \lambda < \lambda_{s2}$.

Next, we investigate under which conditions system (4.4.1) admits a heteroclinic cycle. Recall that $\alpha < \frac{1}{\beta}$. In the following lemma, we establish conditions under which a two species subsystem has three different outcomes.

Lemma 4.4.7 *Let* $1 \leq i < j \leq 3$ *and* $\lambda \in (-r_1, 0]$. *Then, in the two species subsystem consisting of* i *and* j, *we have*

(a) i *outcompetes* j *iff* $\frac{1+\frac{\lambda}{r_j}}{1+\frac{\lambda}{r_i}} < \alpha$,

(b) i *coexists with* j *iff* $\alpha < \frac{1+\frac{\lambda}{r_j}}{1+\frac{\lambda}{r_i}} < \frac{1}{\beta}$,

(c) j *outcompetes* i *iff* $\frac{1+\frac{\lambda}{r_j}}{1+\frac{\lambda}{r_i}} > \frac{1}{\beta}$.

Proof: Follows from Lotka-Volterra theory.

∎

Note that for $\lambda \in (-r_1, 0)$ the following inequalities hold:

$$\frac{1+\frac{\lambda}{r_2}}{1+\frac{\lambda}{r_1}}, \quad \frac{1+\frac{\lambda}{r_3}}{1+\frac{\lambda}{r_2}} < \frac{1+\frac{\lambda}{r_3}}{1+\frac{\lambda}{r_1}}.$$

Proposition 4.4.8 *Let $\lambda \in (-r_1, 0)$. Then a heteroclinic cycle occurs iff the following inequalities take place*

$$\frac{1+\frac{\lambda}{r_3}}{1+\frac{\lambda}{r_2}}, \frac{1+\frac{\lambda}{r_2}}{1+\frac{\lambda}{r_1}} < \alpha$$

and

$$\frac{1+\frac{\lambda}{r_3}}{1+\frac{\lambda}{r_1}} > \frac{1}{\beta}.$$

Proof: Follows from Lemma 4.4.7.

∎

Observe that all these fractions

$$\frac{1+\frac{\lambda}{r_3}}{1+\frac{\lambda}{r_2}}, \quad \frac{1+\frac{\lambda}{r_2}}{1+\frac{\lambda}{r_1}} \quad \text{and} \quad \frac{1+\frac{\lambda}{r_3}}{1+\frac{\lambda}{r_1}}$$

increase as we decrease λ. Thus, we have a "race" between the three quantities above as we decrease λ. A heteroclinic cycle happens when $\frac{1+\frac{\lambda}{r_3}}{1+\frac{\lambda}{r_1}}$ exceeds $\frac{1}{\beta}$, while $\frac{1+\frac{\lambda}{r_3}}{1+\frac{\lambda}{r_2}}$, $\frac{1+\frac{\lambda}{r_2}}{1+\frac{\lambda}{r_1}}$ still have not reached α. Setting

$$\frac{1+\frac{\lambda}{r_3}}{1+\frac{\lambda}{r_2}} = \alpha \text{ and } \frac{1+\frac{\lambda}{r_2}}{1+\frac{\lambda}{r_1}} = \alpha$$

we can find the "critical values" of λ. Taking the larger of the two, we denote

$$\lambda_{hc1} = \max\left(\frac{r_2 r_3(\alpha-1)}{r_2 - \alpha r_3}, \frac{r_1 r_2(\alpha-1)}{r_1 - \alpha r_2}\right). \tag{4.4.7}$$

Setting

$$\frac{1+\frac{\lambda}{r_3}}{1+\frac{\lambda}{r_1}} = \frac{1}{\beta}$$

we find

$$\lambda_{hc2} = \frac{r_1 r_3(1-\beta)}{\beta r_1 - r_3}. \tag{4.4.8}$$

Note that $\lambda > -r_1$ is the necessary and sufficient condition for all three species to persist in the absence of their competitors. The next lemma shows that it is satisfied for λ_{hc2}.

Lemma 4.4.9 $\lambda_{hc2} > -r_1$.

Proof: Suppose $\lambda_{hc2} \leq -r_1$. Then $r_3(1-\beta) \geq -\beta r_1 + r_3$ or $\beta(r_1 - r_3) \geq 0$. The latter contradicts the assumption $r_1 < r_3$.

∎

To determine the condition for the existence of a heteroclinic cycle, using Proposition 4.4.8, we substitute the expression for λ_{hc2} into

$$\frac{1+\frac{\lambda}{r_3}}{1+\frac{\lambda}{r_2}}, \frac{1+\frac{\lambda}{r_2}}{1+\frac{\lambda}{r_1}} < \alpha.$$

After performing some algebraic simplifications, we obtain the equivalent conditions

$$\frac{\beta r_1(r_2 - r_3) + r_3(r_1 - r_2)}{\beta r_2(r_1 - r_3)} < \alpha, \tag{4.4.9}$$

$$\frac{r_2(r_1 - r_3)}{\beta r_1(r_2 - r_3) + r_3(r_1 - r_2)} < \alpha. \tag{4.4.10}$$

Note that these two inequalities are equivalent to $\lambda_{hc1} < \lambda_{hc2}$.

Now, we prove that the left-hand sides of the two inequalities (4.4.9), (4.4.10) are greater than 1 but less than $\frac{1}{\beta}$.

Lemma 4.4.10

$$1 < \frac{\beta r_1(r_2 - r_3) + r_3(r_1 - r_2)}{\beta r_2(r_1 - r_3)} < \frac{1}{\beta},$$

$$1 < \frac{r_2(r_1 - r_3)}{\beta r_1(r_2 - r_3) + r_3(r_1 - r_2)} < \frac{1}{\beta}.$$

Proof: First, note that, for any $\lambda < 0$,

$$\frac{1 + \frac{\lambda}{r_3}}{1 + \frac{\lambda}{r_2}}, \frac{1 + \frac{\lambda}{r_2}}{1 + \frac{\lambda}{r_1}} > 1.$$

In particular, this holds for $\lambda = \lambda_{hc2}$. Next, we want to show that $\frac{\beta r_1(r_2 - r_3) + r_3(r_1 - r_2)}{\beta r_2(r_1 - r_3)} < \frac{1}{\beta}$, or $\beta r_1(r_2 - r_3) > r_1(r_2 - r_3)$ which is equivalent to $\beta < 1$.

For the second inequality, let $x = \frac{r_2(r_1 - r_3)}{\beta r_1(r_2 - r_3) + r_3(r_1 - r_2)}$. Then, by the first inequality,

$$1 < \frac{1}{\beta x} < \beta,$$

or $1 < x < \frac{1}{\beta}$, as needed.

∎

Thus, a heteroclinic cycle exists (i.e. it is admissible) if we choose parameter α between 1 and $\frac{1}{\beta}$.

In the case when a heteroclinic cycle is admissible we can also determine its attractiveness (same as non-permanence of the system) by using Theorem 1.2.7. The condition for attractiveness of the heteroclinic cycle takes the form

$$(\alpha r_3(r_1 + \lambda) - r_1(r_3 + \lambda))(\beta r_1(r_2 + \lambda) - r_2(r_1 + \lambda))(\beta r_2(r_3 + \lambda) - r_3(r_2 + \lambda)) >$$

$$(r_1(r_2 + \lambda) - \alpha r_2(r_1 + \lambda))(r_2(r_3 + \lambda) - \alpha r_3(r_2 + \lambda))(r_3(r_1 + \lambda) - \beta r_1(r_3 + \lambda)). \tag{4.4.11}$$

Summarizing our results, we obtain the following proposition.

Proposition 4.4.11 *Given* $0 < r_1 < r_2 < r_3$, $0 < \beta < 1 < \alpha$, *such that* $\alpha\beta < 1$, *then system (4.4.1) is persistent exactly when* $\lambda_{s1} < \lambda < \lambda_{s2}$. *In addition, if inequalities (4.4.9) and (4.4.10) hold, then*

(a) $\lambda_{s1} \leq \lambda_{hc1} < \lambda_{hc2} \leq \lambda_{s2}$

(b) system (4.4.1) admits a heteroclinic cycle for $\lambda_{hc1} < \lambda < \lambda_{hc2}$

(c) if (4.4.11) holds, then the heteroclinic cycle is attractive.

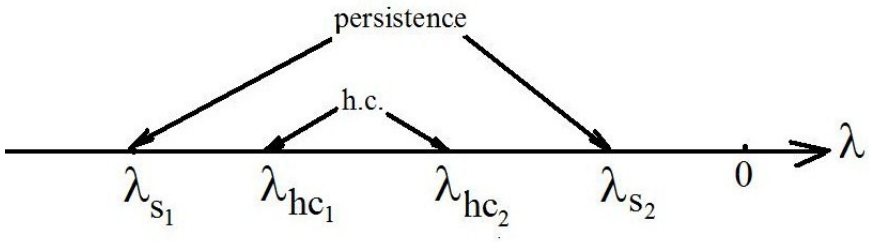

Figure 4.1: Persistence interval and interval with admissible heteroclinic cycle, from Proposition 4.4.11.

Figure 4.1 illustrates the above proposition. Thus, depending on the choice of parameters, we may have a subinterval of $(\lambda_{hc1}, \lambda_{hc2})$ where any solution will approach a stable heteroclinic cycle. If the inequality above fails for $\lambda \in (\lambda_{hc1}, \lambda_{hc2})$, then the heteroclinic cycle is unstable and therefore the system is permanent (i.e. we have stable coexistence of all three species).

4.5 Numerical Results

In this section, we classify the possible effects of advection on the competition of three species in our settings. We consider both cases, cyclic and non-cyclic.

4.5.1 Cyclic case

We use the following spatial model:

$$\begin{cases} \frac{\partial u_1}{\partial t} = d\frac{\partial^2 u_1}{\partial x^2} - q\frac{\partial u_1}{\partial x} + r_1 u_1(1 - u_1 - \alpha u_2 - \beta u_3), \\ \frac{\partial u_2}{\partial t} = d\frac{\partial^2 u_2}{\partial x^2} - q\frac{\partial u_2}{\partial x} + r_2 u_2(1 - \beta u_1 - u_2 - \alpha u_3), \\ \frac{\partial u_3}{\partial t} = d\frac{\partial^2 u_3}{\partial x^2} - q\frac{\partial u_3}{\partial x} + r_3 u_3(1 - \alpha u_1 - \beta u_2 - u_3), \end{cases} \tag{4.5.1}$$

and its nonspatial approximation (4.3.1). An increase of advection in (4.5.1) is equivalent to a decrease of $\lambda \leq 0$ in (4.3.1). Our numerous simulations show that changes in the behavior of these two models are qualitatively identical. Thus, we will mostly concentrate on description of results for the nonspatial models. However, when it is appropriate, we add comments and plots illustrating simulations for the corresponding spatial models.

To illustrate the different cases, we will use triangular diagrams representing relations between three competitors. Arrows on the sides correspond to the outcomes of the two-species subsystems (so an arrow from 1 to 2 means that the second species outcompetes the first in the absence of the third species). Two arrows meeting on an edge represent coexistence outcome in the corresponding two-species subsystem. A square indicates the stable equilibrium of the full model. Its location indicates whether it is an interior coexistence point (meaning permanence), coexistence of two species only, or an exclusion state (in the last two cases, the system loses its persistence). Note that the two species subsystems are guaranteed to exclude the founder control outcome for any $\lambda > \lambda_c$; see Remark 1.2.6 (see also the bifurcation diagram in Figure 3.10). As before, we have $r_1 > r_2 > r_3$ and $\alpha\beta < 1$.

4.5.2 Cyclic Case I

Here we choose parameters so that Species 2 beats Species 1, Species 3 beats Species 2, and Species 1 beats Species 3. Thus, $\alpha > 1 > \beta > 0$.

Cyclic Permanent Case I. The nonspatial system (4.3.1) is permanent iff $\alpha + \beta < 2$. We start with $\lambda = 0$ (zero advection in the corresponding spatial model).

As shown in the leftmost diagram in Figures 4.2, 4.5 species are arranged in a cyclic manner. There is an interior fixed point $(\frac{1}{\alpha+\beta+1}, \frac{1}{\alpha+\beta+1}, \frac{1}{\alpha+\beta+1})$; by Proposition 4.3.9, it is stable. Thus, we start with all three species coexisting in a stable equilibrium. As we decrease $\lambda < 0$ (equivalently, increase advection), this coexistence lasts until one of the inequalities (4.3.2) or (4.3.4) is violated.

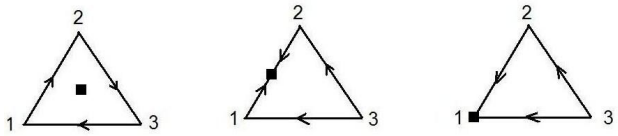

Figure 4.2: Effect of advection on competition in the Cyclic Permanent Case I (a).

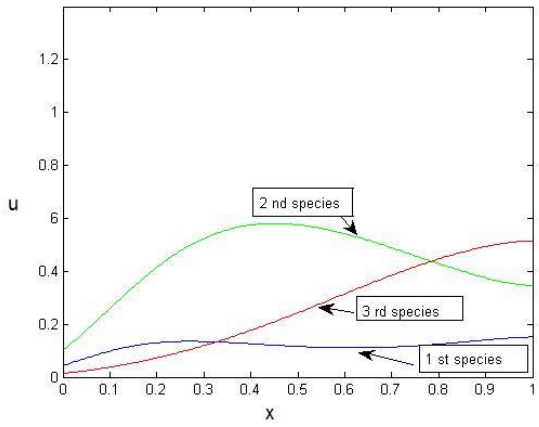

Figure 4.3: Steady state of the spatial model (4.5.1) for $\alpha = 1.5, \beta = 0.4, r_1 = 1.8, r_2 = 1.3, r_3 = 1, d = 1, L = 10$ and advection $q = 1.3$, Cyclic Permanent case I. All three species are present throughout the habitat.

Cyclic Permanent Case I (a): If inequality (4.3.4) becomes violated first (meaning $\lambda_c = \lambda_{c2}$), then Species 3 is first to disappear. For example, this is the case for $r_1 = 1.8, r_2 = 1.3, r_3 = 1, \alpha = 1.5, \beta = 0.4$: $\lambda_c = \max(\lambda_{c1}, \lambda_{c2}) = \max(-0.8738, -0.8437) = -0.8437$. The effect of further decrease of λ (increase of advection) is summarized in Figure 4.2. Once Species 3 disappears, we are left with the two-species competition,

studied in [30] and Chapter 3. Namely, we have a competitively superior Species 2, with lower growth rate. As we increase advection even further, Species 1 gradually replaces Species 2, as predicted in [30] and Chapter 3.

The spatial model goes through the same stages as we increase the advection. The coexistence of three species (see Figure 4.3) is replaced by coexistence of the first and second species (see Figure 4.4), with the first species winning under sufficiently high advection. A more detailed description of the spatial patterns at steady state is given in Subsection 4.5.5.

Remark 4.5.1 Performing spatial model simulations with increasing values of advection speed q (with a patch of size $L = 10$), we notice that the third species disappears when q reaches the value of ≈ 1.53. The principal eigenvalue corresponding to $q = 1.53$ is $\lambda_1 \approx -0.6482$ (see Section 2.10), which is greater than the value of $\lambda_c = -0.8437$ (which corresponds to the disappearance of the third species in the nonspatial approximation).

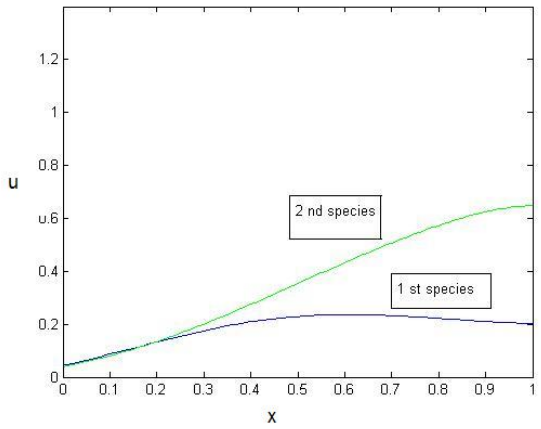

Figure 4.4: The third species has disappeared first in the Cyclic Permanent Case I (a) ($q = 1.6$, $r_1 = 1.8$, $r_2 = 1.3$, $r_3 = 1$, $\alpha = 1.5$, $\beta = 0.4$).

Cyclic Permanent Case I (b): If inequality (4.3.2) is violated first (meaning $\lambda_c = \lambda_{c1}$), then Species 1 is first to disappear. This happens, for example, for $r_1 =$

$1.6, r_2 = 1.3, r_3 = 1, \alpha = 1.5, \beta = 0.4$,: $\lambda_c = \max(\lambda_{c1}, \lambda_{c2}) = \max(-0.8511, -0.9233) = -0.8511$. Figure 4.5 summarizes the effect of decreasing λ (increase of advection): coexistence of Species 2 and 3 is replaced by domination of Species 2, then coexistence of Species 1 and 2, with an eventual domination by Species 1.

Remark 4.5.2 As in case (a), increasing q in the spatial model, we notice that the first species almost disappears (as noted above) when q reaches the value of ≈ 1.62. The principal eigenvalue corresponding to $q = 1.62$ is $\lambda_1 \approx -0.7287$, which is again greater than the value of $\lambda_c = -0.8511$ (which corresponds to the disappearance of the first species in the nonspatial approximation). We observe that in this particular case the nonspatial approximation fails: Species 1 is not completely gone for intermediate values of advection, but is clearly dominated by Species 2 and 3, as seen in Figure 4.6. This demonstrates the limitations of the nonspatial approach.

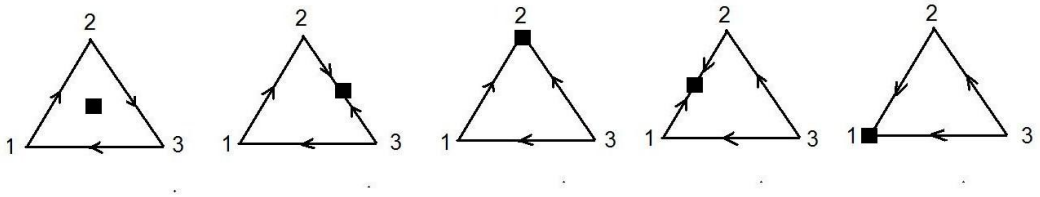

Figure 4.5: Effect of advection on competition in the Cyclic Permanent case I (b).

Note that in both cases (a) and (b), the dot representing the fixed point moves counterclockwise around the triangle. We also observe that if the subsystem involving Species 1 and 2 is the first subsystem to reach the coexistence stage, then we are in case (a). This may happen, for example, when the values r_2 and r_3 are closer to each other than r_1 and r_2. In this case, the effect of advection on the competition of

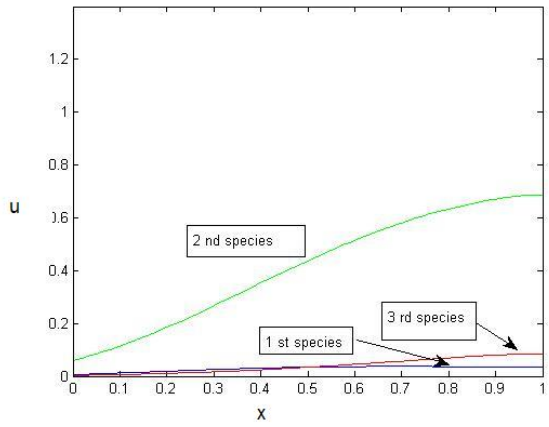

Figure 4.6: The first species is almost gone for the spatial model in the Cyclic Permanent Case I (b).

Species 2 and 3 is not as strong (their competition outcome is mainly determined by interspecific coefficients), while advection forces Species 1 and 2 to coexist.

Non-permanent Cyclic Case I:

The nonspatial system (4.3.1) is non-permanent with $\lambda = 0$ iff $\alpha+\beta \geq 2$. An example of this situation is given by the following choice of parameters: $r_1 = 1.6$, $r_2 = 1.3$, $r_3 = 1$, $\alpha = 1.6$, $\beta = 0.5$, $L = 10$, $d = 1$. For $-0.66 < \lambda < 0$ the solution approaches a heteroclinic cycle (by Theorem 16.1.1 of [19], this solution is an attractor): one competitor almost reaches its carrying capacity while the other two remain at almost zero density, then the next competitor takes the place of the first one, and the process repeats. Here, the single species states lasting longer and getting closer to the fixed points $(1, 0, 0)$, $(0, 1, 0)$ and $(0, 0, 1)$. For $-0.68 < \lambda < -0.66$, we observe a limit cycle behavior: all three species oscillate above the zero density. Our numerous simulations suggest that these oscillations last indefinitely, without approaching any steady state. It corresponds to the case when the system becomes permanent (the heteroclinic cycle loses its stability), but the interior fixed point has not yet become stable. As we decrease λ even further, the oscillations eventually stabilize at a coexistence steady

state. When λ is increased even further, the behavior of the model follows one of the two permanent cases described above ((a) and (b)). Figure 4.7 illustrates the first three stages: species 1, 2 and 3 alternating in a heteroclinic cycle followed by limit cycle followed by coexistence of 1, 2 and 3.

Similar changes in behavior of the spatial system are observed when we increase advection. Namely, for low advection, we are in a heteroclinic cycle setting: e.g. for $q = 0.8$, we observe an oscillatory behavior for all three species, with alternating dominations by each of the species. Over time, the single species stages become longer, as can be seen in Figures 4.8 and 4.9. The figures show the spatial distribution of the first species at different times, for $q = 0.8$. Similar pictures describe dynamics of the other two competitors. For $q = 0.87$, the solution approaches a limit cycle, see Figures 4.10, 4.11.

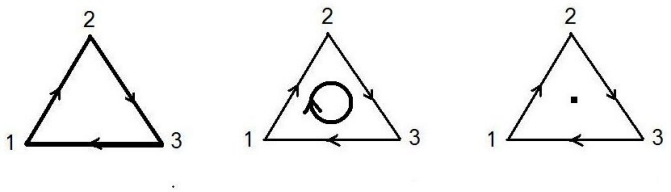

Figure 4.7: Effect of advection on competition in the Non-permanent Cyclic case I.

4.5.3 Cyclic Case II

Here, we choose parameters so that Species 1 beats Species 2, Species 2 beats Species 3, Species 3 beats Species 1. Thus, $\beta > 1 > \alpha > 0$.

Cyclic Permanent Case II.

As before, we begin with $\lambda = 0$ (zero advection in corresponding spatial model). There is an interior fixed point $(\frac{1}{\alpha+\beta+1}, \frac{1}{\alpha+\beta+1}, \frac{1}{\alpha+\beta+1})$. By Proposition 4.3.9, it is

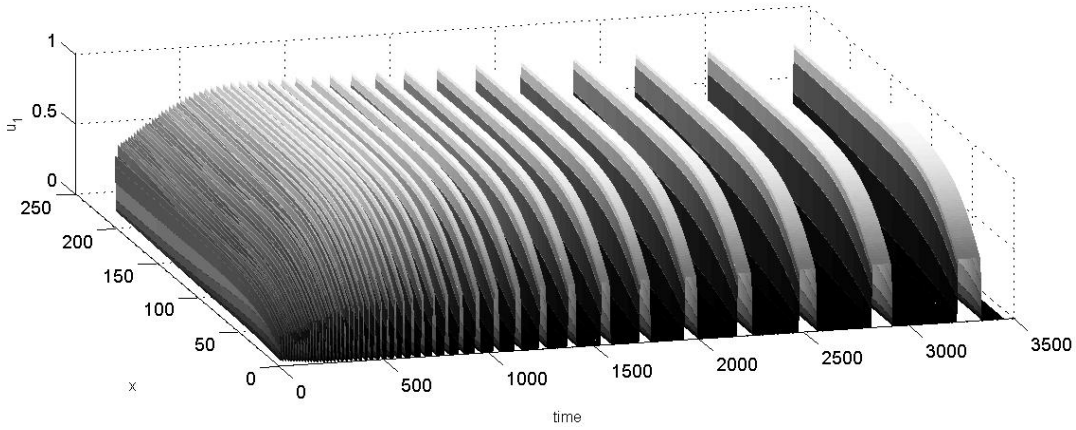

Figure 4.8: The 3D plot shows the spatial profile of the first competitor for times from $t = 0$ to $t = 340$, with the time and space steps equal to 0.1. Here, $q = 0.8$, $r_1 = 1.6$, $r_2 = 1.3$, $r_3 = 1$, $\alpha = 1.6$, $\beta = 0.5$, $L = 10$ and $d = 1$. Notice the increase in the width of the peaks and the distance between the peaks. This happens because the solution approaches the single-species steady states and the time it spends at each monocultural state approaches infinity.

stable. Thus, we start with all three species coexisting in a stable equilibrium. As we decrease $\lambda < 0$ (equivalently, increase advection), coexistence lasts until inequality (4.3.3) is violated and we get coexistence between Species 1 and Species 3. Note that outcomes in the two-species subsystems "one-two" and "two-three" stay the same. Further decrease of advection leads to competitive exclusion by the first species (see Figure 4.12). For instance, if $r_1 = 1.6, r_2 = 1.3, r_3 = 1$, and $\alpha = 0.4$, $\beta = 1.5$, then for $\lambda = -0.68$ the second species disappears, and coexistence between 1 and 3 can be clearly seen. As we increase advection, the spatial model for Cyclic case II goes through the same stages as the nonspatial model. In Figure 4.14, we observe coexistence of the three competitors with the second species being pushed downstream by the other two competitors.

Non-permanent Cyclic Case II:

We observe the same stages as in Non-permanent Cyclic Case I. Namely, as we increase

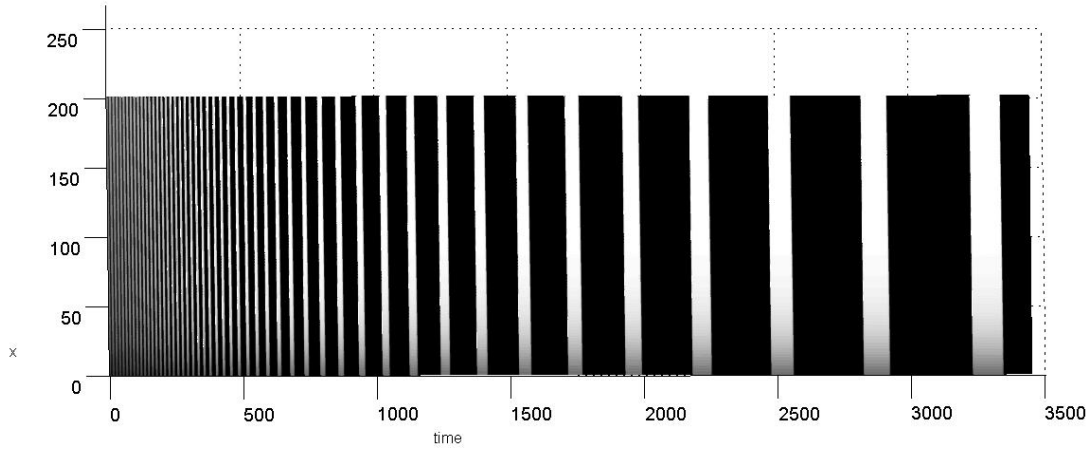

Figure 4.9: The same plot as in the previous figure, viewed from above (time vs. space). The dark stripes represent zero density, white stripes correspond to positive density. Again, notice the increase in the width of both stages as time increases.

advection, the heteroclinic cycle is followed by the limit cycle, and the process ends at the stable, interior point. After that, we follow Permanent Cyclic Case II steps; see Figures 4.13, 4.12. We relate Figures 4.8, 4.9 and 4.10, 4.11 to the Non-permanent Cyclic Case II as well, since the dynamics of each of the three competitors in this case are identical to the dynamics of all species in the Non-permanent Cyclic Case I: (a heteroclinic cycle followed by limit cycle followed by a stable coexistence of 1, 2 and 3) for both spatial and nonspatial case.

Remark 4.5.3 Performing spatial model simulations with increasing values of advection speed q (with a patch of size $L = 10$), we notice that the second species is gone when q reaches the value of ≈ 1.38. The principal eigenvalue corresponding to $q = 1.38$ is $\lambda_1 \approx -0.5366$ (see Section 2.10, Section 4.3), which is greater than the value of $\lambda_c = -0.69$ (which corresponds to the disappearance of the second species in the nonspatial approximation).

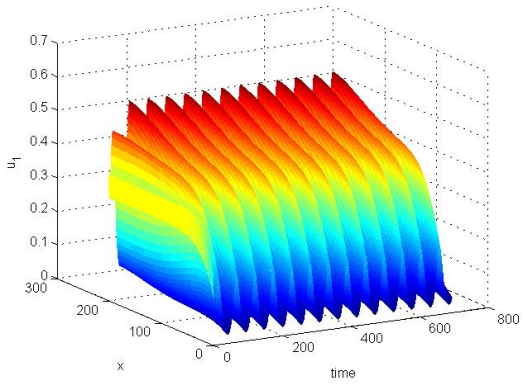

Figure 4.10: The 3D plot shows the spatial profile of the first competitor for times from $t = 0$ to $t = 340$, with the time and space steps equal to 0.1. Here, $q = 0.87$, $r_1 = 1.6$, $r_2 = 1.3$, $r_3 = 1$, $\alpha = 1.6$, $\beta = 0.5$, $L = 10$ and $d = 1$. Notice that the width of the peaks and the distance between the peaks stays approximately the same, since we are in a limit cycle situation.

4.5.4 Non-cyclic Case

In the non-cyclic case, for $\lambda = 0$, the system is non-persistent, with a stable single species steady state (i.e. the only species present is Species 1, with the lowest growth rate). As we decrease λ (increase advection), the system becomes persistent (for $\lambda_{s1} < \lambda < \lambda_{s2}$), then loses persistence and finishes with the domination of the species with the highest growth rate (Species 3). Depending on the existence and stability of a heteroclinic cycle within the "persistence interval", there are three possible cases outlined below. In all three cases, numerical simulations show that with our choice of parameters, as we increase advection, the spatial model goes through the same stages as the nonspatial approximation does when we decrease λ.

Non-cyclic Case (a): no heteroclinic cycle.

In this case, throughout the persistence interval $(\lambda_{s1}, \lambda_{s2})$ the three species coexist in stable equilibrium (fixed point). For example, let $r_1 = 1, r_2 = 1.2, r_3 = 1.5$, $\alpha = 1.2$, $\beta = 0.5$. Then, using formulas (4.4.6, 4.4.5, 4.4.7, 4.4.8), we find $\lambda_{hc1} = -0.5455$,

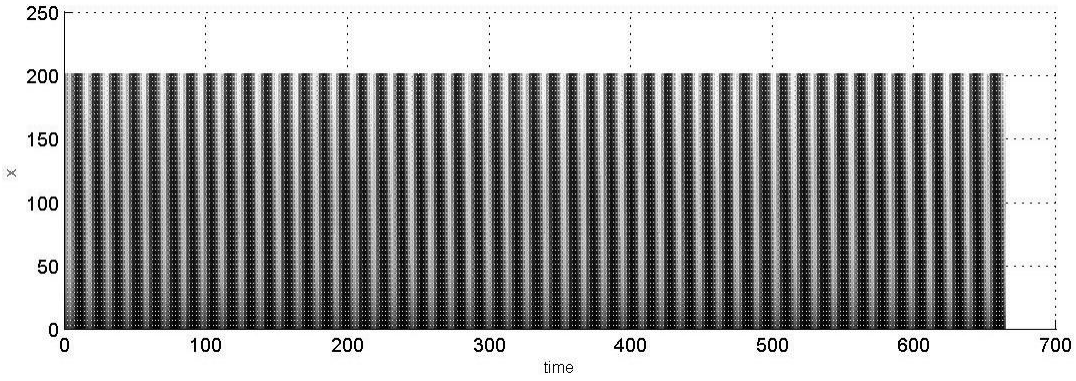

Figure 4.11: The same plot as in the previous figure, viewed from above (time vs. space). The dark stripes represent zero density, white stripes correspond to positive density. Again, notice that the width of the stages stays the same.

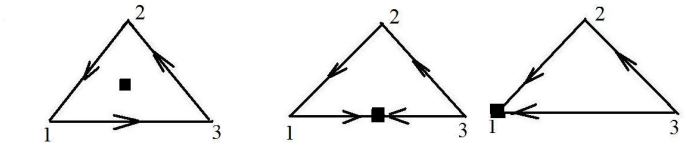

Figure 4.12: The second species has disappeared first in the Permanent Cyclic Case II.

$\lambda_{hc2} = -0.75$, $\lambda_{s1} = -0.7895$, $\lambda_{s2} = -0.5$. Note that $\lambda_{hc1} > \lambda_{hc2}$ means that the heteroclinic cycle is never admissible; i.e. the arrangement of winners and losers in two-species subsystems is non-cyclic for any $\lambda < 0$. The system is permanent throughout the persistence interval $-0.7895 < \lambda < -0.5$. As we decrease λ from 0 to -1.1, we observe the following transitions (see Figure 4.15):

First wins, followed by coexistence of 1 and 3, followed by coexistence of 1,2, and 3 (for $-0.7895 < \lambda < -0.5$), followed by coexistence of 2 and 3 followed by third wins.

Notice that in the middle triangle (corresponding to $\lambda = -0.7$) we have a stable interior fixed point for the three species model, as well as stable coexistence states for each of the three two-species subsystems. Of course, the two-species coexistence

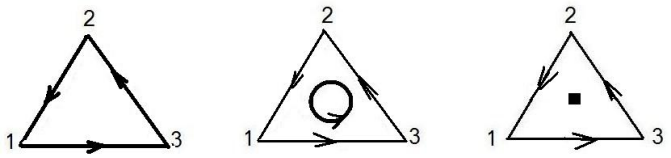

Figure 4.13: Effect of advection on competition in the Non-permanent Cyclic Case II.

states are unstable from the point of view of the full three-species model. With a different choice of parameters, we may see a slightly different picture. Namely, we may have only one or two of the two-species subsystems in the coexistence state, but we are only interested in the behavior of the full system.

Remark 4.5.4 Note that, in the nonspatial approximation, we have persistence for $-0.7895 < \lambda < -0.5$. In the spatial model ($L = 10$), persistence takes place for $1.09 < q < 1.55$. This corresponds to principal eigenvalues λ_1 in the interval $(-0.6639, -0.3515)$. Comparing with the "nonspatial" persistence interval above, we can observe that both endpoints are shifted to the right in the spatial case.

Non-cyclic Case (b): unstable heteroclinic cycle.

In this case, inside the persistence interval there is an interval for which the two-species subsystems are arranged in a cyclic manner; however, the heteroclinic cycle is never an attractor. Let $r_1 = 1, r_2 = 1.4, r_3 = 2.2$, $\alpha = 1.7$, $\beta = 0.5$. Then by formulas (4.4.6), (4.4.5), (4.4.7), (4.4.8), we have $\lambda_{hc1} = -0.7101$, $\lambda_{hc2} = -0.6471$, $\lambda_{s1} = -0.7526$, $\lambda_{s2} = -0.5996$. Note that, since $\lambda_{hc1} < \lambda_{hc2}$, the heteroclinic cycle exists for $\lambda_{hc1} < \lambda < \lambda_{hc2}$. However, for any such λ, inequality (4.4.11) fails, and thus the heteroclinic cycle never becomes stable.

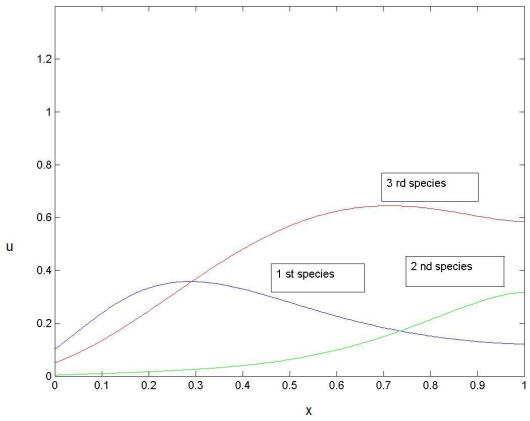

Figure 4.14: Steady state of the spatial model (4.5.1) for $\alpha = 0.4, \beta = 1.5, r_1 = 1.6, r_2 = 1.3, r_3 = 1, d = 1, L = 10$ and advection $q = 1.3$, Cyclic Permanent Case II. All three species are present throughout the habitat.

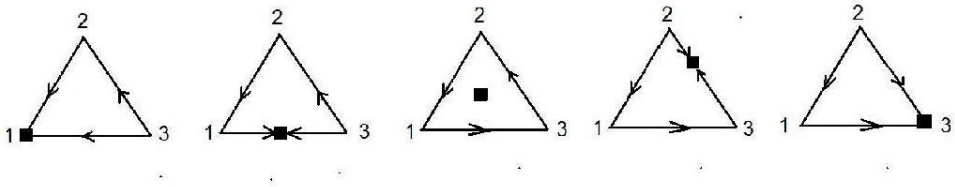

Figure 4.15: Effect of advection on competition in the Non-cyclic case (a).

As we decrease λ, we observe the following (see Figure 4.16):

first wins followed by coexistence of 1 and 3 followed by coexistence of 1,2 and 3 with no heteroclinic cycle followed by stable coexistence of 1,2 and 3, with two-species subsystems forming a heteroclinic cycle followed by coexistence of 1,2 and 3 with no heteroclinic cycle → coexistence of 1 and 2 followed by second wins followed by coexistence of 2 and 3 followed by third wins.

With a different choice of parameters, the system may skip the stages shown in brackets, so we can have two possible scenarios, as in cyclic cases (a) and (b), depending on which coordinate of the interior fixed point becomes zero first. However, the end result is always the same: Species 3 (with the highest growth rate) is the winner.

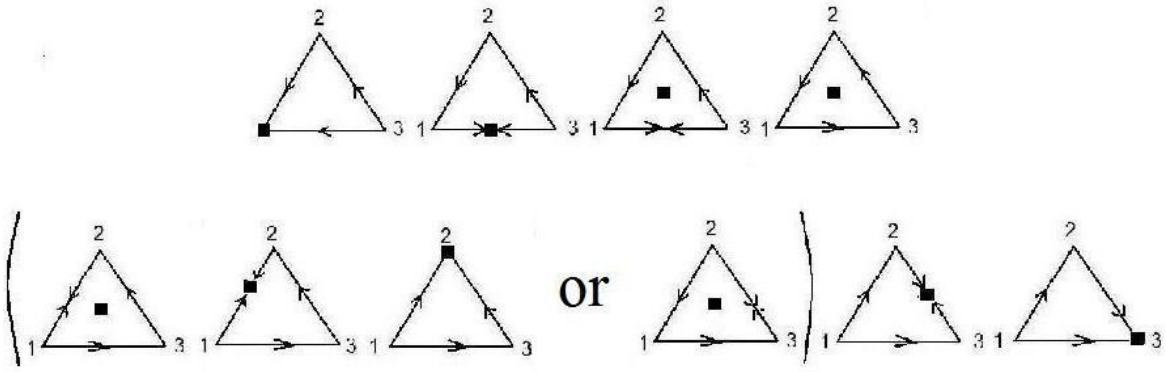

Figure 4.16: Effect of advection on competition in the Non-cyclic Case (b). Stages in brackets may or may not occur for different choices of parameters.

We can compare the results regarding the behavior of the nonspatial model with simulations of the spatial model. Namely, we can find the persistence interval in terms of advection q.

Remark 4.5.5 In the nonspatial model, we have persistence for $-0.7529 < \lambda < -0.5996$. In the spatial model, persistence takes place for $1.22 < q < 1.53$. This corresponds to principal eigenvalues λ_1 in the interval $(-0.6482, -0.4295)$. We again observe that the "spatial" persistence interval is shifted to the right.

Non-cyclic Case (c): stable heteroclinic cycle.

In this case (which is not easy to capture, but it is nevertheless quite interesting), within the persistence interval, there is an interval where the system has a cyclic arrangement of two-species subsystems, and inside that interval there is a subinterval for which the heteroclinic cycle is actually stable. This means that for certain intermediate values of λ (intermediate advection), the system switches from a stable coexistence equilibrium to stable heteroclinic cycle, and then back to stable coexistence.

Let $r_1 = 1, r_2 = 1.5, r_3 = 2.7$, $\alpha = 2$, $\beta = 0.49$. Then $\lambda_{hc1} = -0.75$, $\lambda_{hc2} = -0.6231$, $\lambda_{s1} = -0.7533$, $\lambda_{s2} = -0.618$. Note that, since $\lambda_{hc1} < \lambda_{hc2}$, the heteroclinic cycle exists for $\lambda_{hc1} < \lambda < \lambda_{hc2}$. Moreover, for $-0.76 < \lambda < -0.63$, inequality (4.4.11) holds, and thus the heteroclinic cycle is stable.

As we decrease λ, we observe the following:

first wins followed by coexistence of 1 and 3 followed by coexistence of 1,2 and 3 with no heteroclinic cycle followed by coexistence of 1,2 and 3 with two-species subsystems forming a heteroclinic cycle followed by Species 1,2 and 3 alternating in a heteroclinic cycle → coexistence of 1,2 and 3 with two-species subsystems forming a heteroclinic cycle followed by coexistence of 1,2 and 3 with no heteroclinic cycle → coexistence of 1 and 2 followed by second wins followed by coexistence of 2 and 3 followed by third wins.

Figure 4.17 gives a summary of these transitions. As in case (b), the system may skip the bracketed stages for different parameter values. This is the second time when the nonspatial approximation does not completely agree with the spatial simulations. Namely, we were not able to obtain the stable heteroclinic cycle for the spatial model.

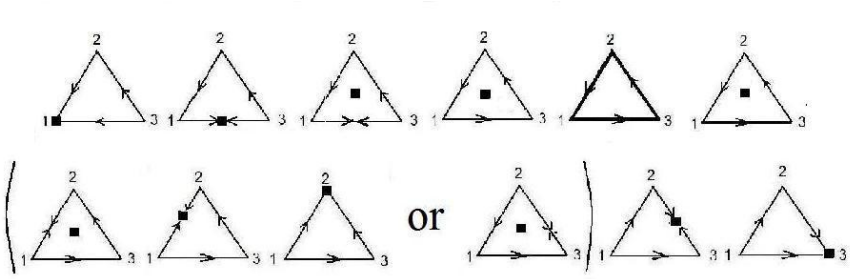

Figure 4.17: Effect of advection on competition in the Non-cyclic Case (c).

Remark 4.5.6 Note that, in the nonspatial approximation, we have persistence for $-0.7533 < \lambda < -0.618$. In the spatial model ($L = 10$), persistence takes place for $1.25 < q < 1.51$. This corresponds to principal eigenvalues λ_1 in the interval

$(-0.6327, -0.4486)$. Comparing with the "nonspatial" persistence interval above, we can observe that both endpoints are shifted to the right in the spatial case.

Based on the observations in Remarks 4.5.1, 4.5.2, 4.5.4, 4.5.5 and 4.5.6, we make the following conjecture.

Conjecture: Let $(\lambda_{p1}, \lambda_{p2})$ be the persistence interval for the nonspatial approximation model (in cyclic or non-cyclic case). Let (q_1, q_2) be the interval of the values of advection for which the corresponding spatial system (for a fixed L) is persistent. Let $\lambda_1(q_1)$ and $\lambda_1(q_2)$ be the principal eigenvalues corresponding to q_1 and q_2 respectively. Then $\lambda_1(q_1) \geqslant \lambda_{p1}$ and $\lambda_2(q_2) \geqslant \lambda_{p2}$.

4.5.5 Spatial distribution of species at the coexistence states

To get an insight into the actual spatial distribution of three competing species in a stable coexistence equilibrium, we perform numerical simulations for a reasonably long domain $L = 100$ and $d = 1$.

Cyclic Case I. In all three cyclic cases (permanent (a), (b) and non-permanent), we observe that when the system is at such a steady state (i.e. for relatively small advection in cases (a), (b), and for intermediate advection in the non-permanent case), there is a common pattern of alternating patches where one of the three species seems to dominate. The pattern starts in the upstream region, where it is most distinguished. In all the cases, the leftmost part of the upstream region is dominated by Species 2, followed by Species 3, and then Species 1. Then the pattern repeats as we move downstream, but with decreasing amplitude, almost disappearing downstream. The number of alternations seem to increase with advection (see Figures 4.18, 4.19).

From the biological viewpoint, these observations mean that the species with the intermediate growth rate and intermediate "strength" occupies the top of the stream, followed by the species with the lowest growth rate, and then the species with the highest growth rate, and then the alternating pattern continues as we move

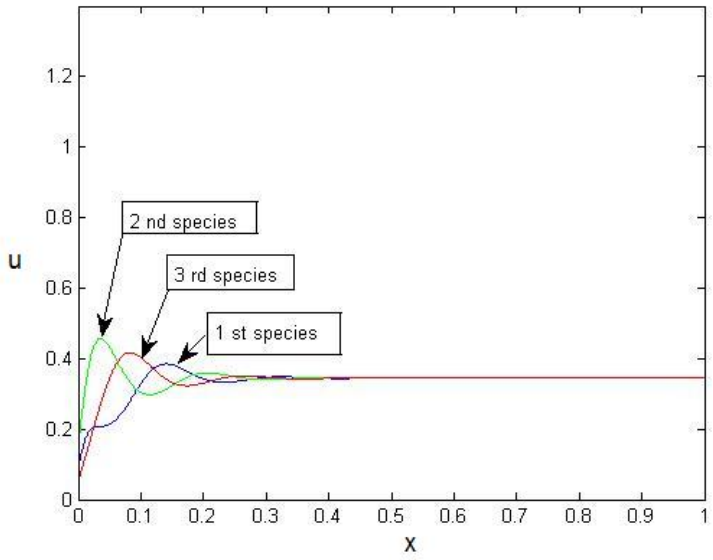

Figure 4.18: Spatial profile of coexistence state for Cyclic Permanent case I(a), $q = 1$, $r_1 = 1.8$, $r_2 = 1.3$, $r_3 = 1$, $\alpha = 1.5$, $\beta = 0.4$.

downstream, with each the "domination intervals" of approximately equal length. Domination becomes less dramatic and almost disappears as we move downstream. Thus, the competition is most prominent upstream, and is almost invisible downstream. We also find it intriguing that the species with intermediate growth rate has the advantage in the upstream region.

Cyclic Case II. As in Cyclic Case I, we observe that all three species are distributed throughout the habitat in a similar manner. Namely, as before, we see alternating patches, starting at the upstream border. However, in this case, we see the first competitor, followed by the third and the second one located at the end of each patch.

Non-cyclic case. In any of the the non-cyclic cases, the stable coexistence state is characterized by the presence of all three species in the upstream region, with the rest of the habitat occupied by Species 1 only (with the lowest growth rate). Several examples are given in Figures 4.20, 4.21, 4.22 and 4.23. There is no alternation

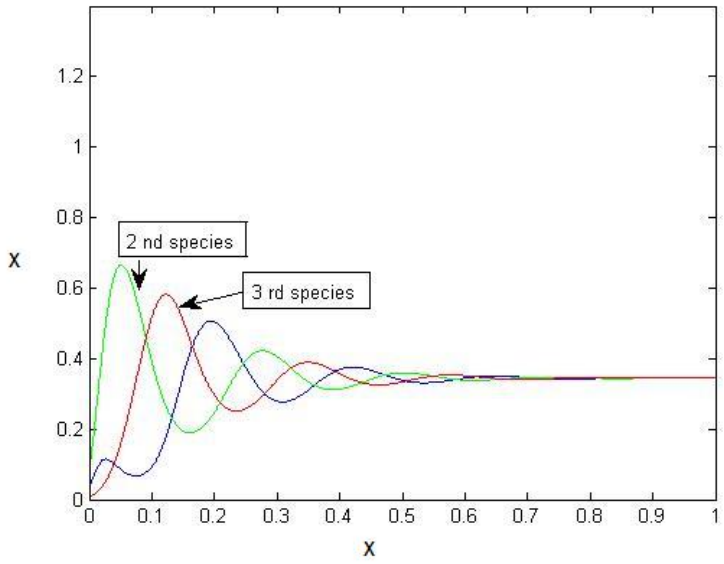

Figure 4.19: Spatial profile of coexistence state for Cyclic Permanent case I(a), $q = 1.4$, $r_1 = 1.8$, $r_2 = 1.3$, $r_3 = 1$, $\alpha = 1.5$, $\beta = 0.4$.

pattern as in the cyclic case. In fact, the situation is quite similar to the two species case: the species with the lower growth rate occupies the downstream part of the habitat, leaving the upstream region to its competitor(s).

It is also worth noting that we do not have any chaotic behavior of solutions in our settings, see also [48].

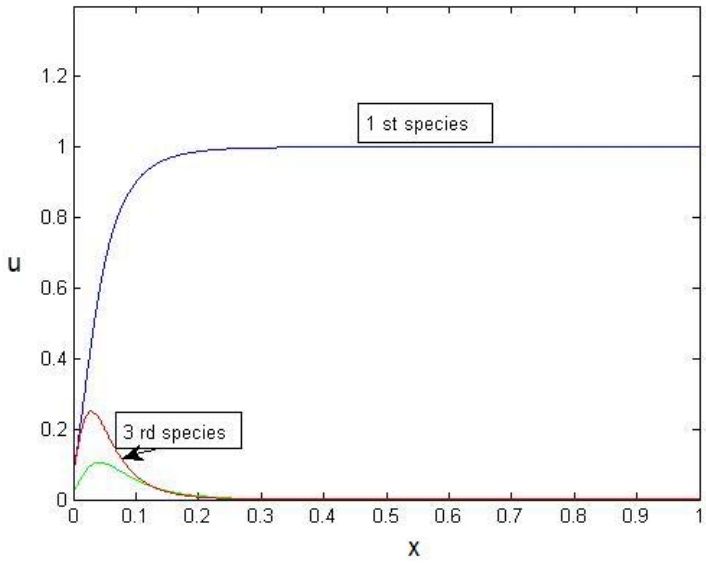

Figure 4.20: Spatial profile of coexistence state for Non-cyclic Case (a), for $q = 1.2$, $r_1 = 1$, $r_2 = 1.2$, $r_3 = 1.5$, $\alpha = 1.2$ and $\beta = 0.5$.

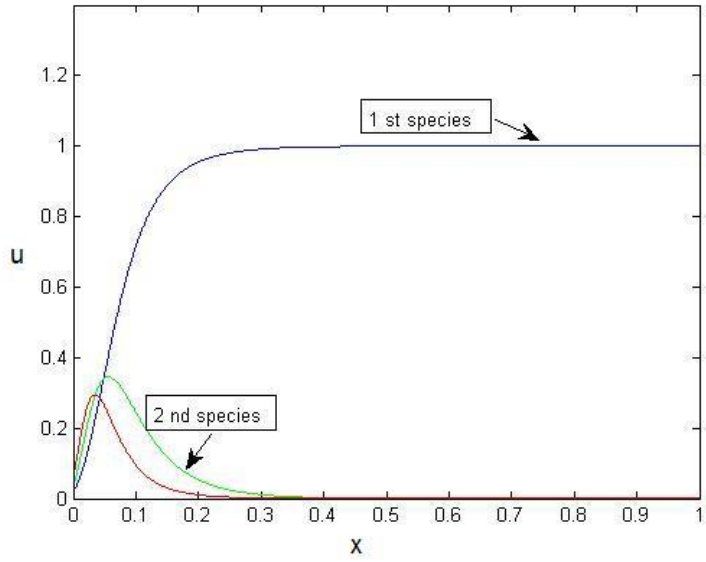

Figure 4.21: Spatial profile of coexistence state for Non-cyclic Case (a), for $q = 1.4$, $r_1 = 1$, $r_2 = 1.2$, $r_3 = 1.5$, $\alpha = 1.2$ and $\beta = 0.5$.

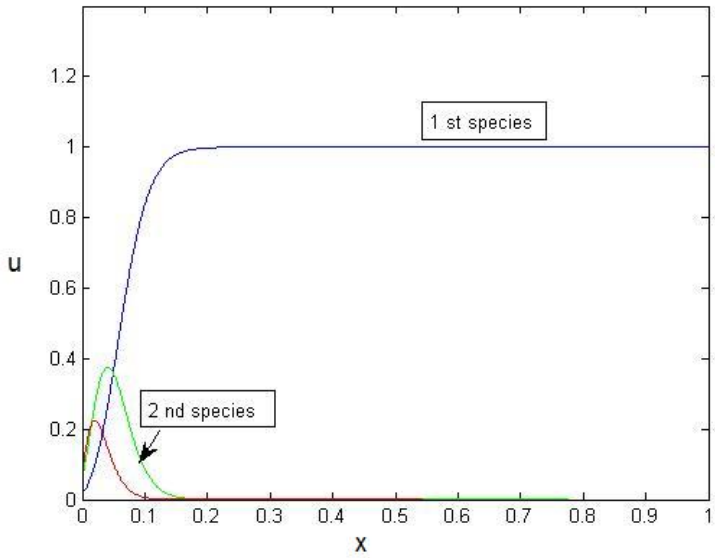

Figure 4.22: Spatial profile of coexistence state for Non-cyclic Case (b), for $q = 1.4$, $r_1 = 1$, $r_2 = 1.4$, $r_3 = 2.2$, $\alpha = 1.7$ and $\beta = 0.5$.

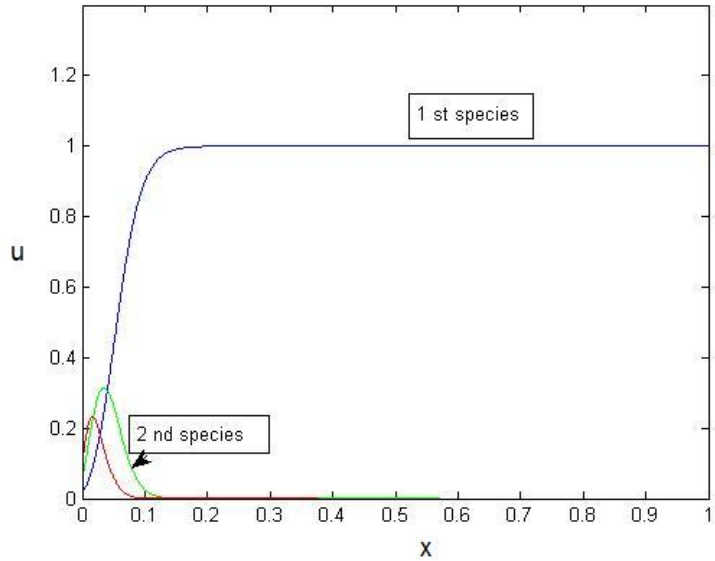

Figure 4.23: Spatial profile of coexistence state for Non-cyclic Case (c), for $q = 1.4$, $r_1 = 1$, $r_2 = 1.5$, $r_3 = 2.7$, $\alpha = 2.0$ and $\beta = 0.49$.

Chapter 5

Conclusions and Biological implications

We will now summarize our work on the dynamics of single species and competition of two or three species in an advective environment, emphasizing the biological implications. We also outline possible topics for future research coming out of this thesis.

In Chapter 2, we considered a reaction-advection-diffusion equation with logistic growth term on a bounded domain with Danckwerts' boundary conditions. We proved the existence, uniqueness and stability of a positive steady state for domain lengths above a critical threshold. Below this threshold, the zero steady state is stable. In particular, a transcritical bifurcation occurs at this threshold. The positive steady state solution is an increasing function of the spatial variable. For large enough advection, the solution has an inflection point; we gave an approximate formula for the distance of this inflection point from the upstream boundary. We also showed that the solution is a decreasing function of advection speed. From a mathematical point of view, the analysis of the single species equation is now relatively complete.

These results complement and contrast the results on reaction-diffusion equations

without advection, but with hostile boundary conditions; see for example [25]. Those models also exhibit a transcritical bifurcation at the critical domain size. Loss of individuals in that case is entirely due to diffusion, while in our case, it is purely due to advection. Also, the positive steady state in those models has no inflection point.

While this work focuses on mathematical analysis, our model is inspired by the biological question of population dynamics in advective environments, such as streams and rivers. Speirs and Gurney [47] first applied a linear analogue of our model (albeit with slightly different boundary conditions) to study the persistence conditions of plankton and insects in small streams in Southeast England. They demonstrated that, under certain conditions, diffusive movement of individuals can counterbalance the loss of individuals through directed movement with the water and thereby lead to population persistence.

For example, their model explains the absence of plankton organisms in Broadstone Stream (Southeast England), which is relatively short and shallow with significant advection. The authors argue that, due to its shallowness and the nature of plankton, the organisms would have to be present throughout the water column, and would be subjected to average advection, which exceeds the critical value for any realistic growth rate and diffusivity of plankton. On the other hand, stoneflies are actually found in the creek. Their nymphs are primarily benthic organisms, and enter the stream for only 0.01% of time. Therefore, they experience an *effective* advection speed that is reduced by a factor of 10^4; well below the critical advection value for this species. Thus, even though the timescale of the growth dynamics is typically much slower than that of the advective movement, the latter is significantly smaller for predominantly benthic species and is actually comparable with the former.

Stoneflies have winged adult stages that can easily move upstream for egg-deposition. It is unclear whether this movement can be accurately captured by the diffusion operator. Potentially more realistic could be a discrete-time model with a dispersal kernel as in [31]. The reaction-advection-diffusion approach does, however,

seem appropriate for many benthic species that never emerge from the water, such as, *Dreissena polymorpha* (zebra mussels), meroplanktonic copepod (*Caullana canadensis*), and mysid shrimp (*Neomysis integer*), where a similar reduction of the actual advection speed occurs. Benthic algae can be considered within this framework as well. Some "best guesses" for parameter values were given in [30]

Our model makes some testable hypotheses. Is it true that the abundance of these organisms increases downstream from an insurmountable barrier? And does the location of the inflection point (2.8.3) predict the spatial scale over which the influence of this upstream barrier is present?

The reduction of population density at the upstream end can also be a mechanism for coexistence of two competing species that would not coexist in the absence of advection. A special case of this mechanism has been demonstrated numerically in [30]. The study of species interaction in habitats with a unidirectional flow is a new and interesting area. In Chapter 3, we studied Lotka-Volterra competition of two species in an advective environment, combining mutual invasibility analysis via variational formulas with numerics and a nonspatial approximation. We assume that both species have the same motility, and reduce the system to a spatially implicit model. We built various bifurcation diagrams for mutual invasion using both numerics and the nonspatial approximation, and used them to classify the possible scenarios as advection increases. In particular, we have established that if, in the absence of advection, Species 1 outcompetes the faster growing Species 2, the increase in advection will eventually reverse the outcome, with the system either going through coexistence of the two species or through the founder control situation.

In Chapter 4, we extended the model to the case of three competitors, and used nonspatial approximation to describe the effect of advection on the competition outcome. In the case of three competitors, we concentrated on two special cases (cyclic and non-cyclic arrangement), and classified the possible scenarios as we increase advection. Change in advection can cause transition between various stable steady

states: single species domination, coexistence of two species, coexistence of three species, heteroclinic cycle (alternating dominations by each of the three species), and a limit cycle.

In both two and three species cases, the nonspatial approximation allows one to estimate the critical values of advection corresponding to various bifurcations. Numerical simulations have also shed some light on the spatial arrangements in the case of coexistence, in terms of which species occupies the upstream or downstream region. In the three species case, for certain values of advection, species can coexist in the form of alternating patches dominated by a single species, a phenomenon which would be interesting to observe in nature.

We can make a general observation that high advection makes the growth rate the most important factor in competition, whereas in the case of low advection, competition outcome is decided mostly by the species interaction. For example, in cyclic case I of three-species competition, advection does not change the outcome in the two species subsystem 1-3, since Species 1 has the higher growth rate and is stronger than Species 3 (in terms of interspecific coefficients). However, the outcomes in the subsystems 1-2 and 2-3 are both changed by advection. When advection is high enough, only Species 1 remains, as the species with the highest growth rate among the three.

The main practical conclusion that can be derived from our study of competition in an advective environment is that human activity that affects the flow speed (building dams, diverting water for agricultural use) can change the ecological balance by giving some species a competitive advantage over others.

The techniques used to study the nonspatial approximation of two- and three-species Lotka-Volterra models with advection can be potentially applied to describe various nonspatial competition models with an additional linear "death term" λu_i, where the coefficient $\lambda < 0$ is the same for all the species. An example of such a setting would be competition of two or three similar species subject to "uniform"

harvesting.

Our analysis of two- and three-species competition in an advective environment is not as complete as in the single species case, but it opens up a variety of interesting topics. A natural question coming out of our work on competition of two species in an advective environment is the role of diffusivity. What if the two species have different diffusivity (motility)? Will a more motile species have an advantage? This type of question is closely related to the study of evolution of dispersal [14]. One repeatedly occurring result in reaction-diffusion models for evolution of dispersal is that slower dispersal is advantageous [18]. In our models with advection, it is clear that a certain amount of dispersal is necessary for a population to persist (e.g. see Remark 2.2.2). Hence, we expect that slower dispersal is not always advantageous. The tools and techniques developed in Chapter 3 can be applied in future work to tackle the question of optimal dispersal in advective environments.

On the other hand, there are some challenging questions arising from the spatial PDE models describing Lotka-Volterra competition in advective environment. One of them is to analyze the dependence of the principal eigenvalues in the mutual invasion conditions (for the two-species model) on advection. So far, this dependence has been described using numerics and nonspatial approximation. Another question is to obtain sufficient and/or necessary conditions for persistence and permanence of the three-species model. This question has been already studied in [10] and [11] in the non-advective spatial case with hostile boundary conditions, using the average Lyapunov function technique. It remains to see whether this technique can be extended to the reaction-diffusion-advection case here.

Another possible direction in which we could extend our work on single species and competition is to incorporate heterogeneity of the habitat in our models. Two types of heterogeneity seem particularly appropriate for river ecosystems. Strong spatial heterogeneity on small spatial scales in the form of alternating patches of different habitat quality could represent a pool-riffle structure in a river. Corresponding

non-advective models were first studied by Shigesada et al. (see [21], [22], [43]) and in rivers by Lutscher et al. [29]. Spatial heterogeneity can create niches for various species and thereby greatly facilitate coexistence of competitors; see [13], [42]. Rivers also exhibit more gradual heterogeneity on large spatial scales. For example, water temperature and nutrient load typically increase downstream. This scenario has so far only been explored numerically and is a wide open field for future studies.

Bibliography

[1] D.G. Aronson. The role of diffusion in mathematical population biology: Skellam revisited. In S.A. Levin, editor, *Mathematics in Biology and Medicine*, pages 2–6. Lect. Notes on Biomath., 57, Springer, 1983.

[2] J. E. Bailey and D. F. Ollis. *Biochemical Engineering Fundamentals*. McGraw-Hill, 1986.

[3] M. Ballyk, Le Dung, D. A. Jones, and H. Smith. Effects of random motility on microbial growth and competition in a flow reactor. *SIAM J. Appl. Math.*, 59(2):573–596, 1998.

[4] M. Ballyk and H. Smith. A flow reactor with wall growth. In Mary Ann Horn, editor, *Mathematical models in medical and health science*, pages 17–28. Nashville, Vanderbilt University Press, 1998.

[5] M. Ballyk and H. Smith. A model of microbial growth in a plug flow reactor with wall attachment. *Math. Biosci.*, 158:95–126, 1999.

[6] H. Berestycki, O. Diekmann, C.J. Nagelkerke, and P.A. Zegeling. Can a species keep pace with a shifting climate? *Bulletin of Mathematical Biology*, 71:399–429, 2009.

[7] G. Birkhoff and G.-C. Rota. *Ordinary differential equations*. Waltham, Mass., Blaisdell Pub. Co., 1969.

[8] N.F. Britton. *Reaction–Diffusion Equations and Their Applications to Biology*. Academic Press, London, 1986.

[9] R. S. Cantrell and C. Cosner. Spatial heterogeneity and critical patch size: Area effects via diffusion in closed environments. *J. theor. Biol.*, 209:161–171, 2001.

[10] R. S. Cantrell and C. Cosner. *Spatial Ecology via Reaction-Diffusion Equations*. Mathematical and Computational Biology. Wiley, 2003.

[11] R. S. Cantrell, C. Cosner, and V. Hutson. Permanence in some diffusive lotka-volterra models for three interacting species. *Dynamic Systems and Application*, 2:505–530, 1993.

[12] C. Cosner. Reaction-diffusion equations and ecological modeling. *Tutorials in Mathematical Biosciences IV, Lecture Notes in Mathematics*, 1922:77–115, 2008.

[13] G.C. Cruywagen, P. Kareiva, M.A. Lewis, and J.D. Murray. Competition in a spatially heterogeneous environment: Modelling the risk of spread of a genetically engineered population. *Theor. Popul. Biol.*, 49(1):1–38, 1996.

[14] J. Dockery, V. Hutson, K. Mischaikow, and M. Pernarowski. The evolution of slow dispersal rates: a reaction-diffusion model. *J. Math. Biol.*, 37:61–83, 1998.

[15] R.A. Fisher. The advance of advantageous genes. *Ann. Eugenics*, 7:355–369, 1937.

[16] B. Gaylord and S.D. Gaines. Temperature or Transport? Range limits in marine species mediated solely by flow. *Am. Nat.*, 155:769–789, 2000.

[17] K.P. Hadeler and M.A. Lewis. Spatial dynamics of the diffusive logistic equation with sedentary component. *Canadian Applied Math. Quarterly*, 10:473–500, 2002.

[18] A. Hastings, K. Cuddington, K. Davies, C. Dugaw, S. Elmendorf, A. Freestone, S. Narrison, M. Holland, J. Lambrionos, U. Malvadkar, B. Melbourne, K. Moore, C. Taylor, and D. Thomson. The spatial spread of invasions: new developments in theory and evidence. *Ecology Letters*, 8:91–101, 2005.

[19] J. Hofbauer and K. Sigmund. *Evolutionary Games and Population Dynamics*. Cambridge University Press, 1998.

[20] J. Huisman, M. Arrayás, U. Ebert, and B. Sommeijer. How do sinking phytoplankton species manage to persist. *Am. Nat.*, 159:245–254, 2002.

[21] N. Kinezaki, K. Kawasaki, and N. Shigesada. Spatial dynamics of invasion in sinusoidally varying environments. *Pop. Ecol.*, 48:263–270, 2006.

[22] N. Kinezaki, K. Kawasaki, F. Takasu, and N. Shigesada. Modeling biological invasions into periodically fragmented environments. *Theor. Pop. Biol.*, 64:291–302, 2003.

[23] K. Kishimoto. The diffusive Lotka-Volterra system with three species can have a stable non-constant equlibrium solution. *J. Math. Biol.*, 16:103–112, 1982.

[24] T. Kolokolnikov, C. Ou, and Y. Yuan. Profiles of self-shading, sinking phytoplankton with finite depth. *J. Math. Biol.*, 59(1):105–122, 2009.

[25] M. Kot. *Elements of Mathematical Ecology*. Cambridge Univ. Press, Cambridge, 2001.

[26] M.A. Lewis, T. Hillen, and F. Lutscher. Spatial dynamics in ecology. *Mathematical Biology; Editors: M.A. Lewis, J. Keener, P. Maini and M. Chaplain IAS/Park City Mathematics Series, Volume 14*, 2009.

[27] M.A. Lewis and G. Schmitz. Biological invasion of an organism with separate mobile and stationary states: Modeling and analysis. *Forma*, 11:1–25, 1996.

[28] A.J. Lotka. *Elements of Physical Biology*. Williams and Wilkins, 1925.

[29] F. Lutscher, M.A. Lewis, and E. McCauley. The effects of heterogeneity on population persistence and invasion in rivers. *Bull. Math. Biol.*, 68(8):2129–2160, 2006.

[30] F. Lutscher, E. McCauley, and M.A. Lewis. Spatial patterns and coexistence mechanisms in rivers. *Theor. Pop. Biol.*, 71(3):267–277, 2007.

[31] F. Lutscher, R.M. Nisbet, and E. Pachepsky. Population persistence in the face of advection. *Theoretical Ecology*, 3:271–284, 2010.

[32] F. Lutscher, E. Pachepsky, and M.A. Lewis. The effect of dispersal patterns on stream populations. *SIAM Rev.*, 47(4):749–772, 2005.

[33] R. McOwen. *Partial Differential Equations*. Prentice Hall, 1996.

[34] K. Müller. Investigations on the organic drift in north swedish streams. Technical Report 34, Institute of Freshwater Research, Drottningholm, 1954.

[35] K. Müller. The colonization cycle of freshwater insects. *Oecologica*, 53:202–207, 1982.

[36] J. D. Murray. *Mathematical Biology II: Spatial Models and Biomedical Applications*. Springer-Verlag, Berlin, 2002.

[37] A. Okubo and S. A. Levine. *Diffusion and Ecological Problems: Modern Perspectives*. Springer, New York, NY, USA, 2001.

[38] E. Pachepsky, F. Lutscher, R. Nisbet, and M. A. Lewis. Persistence, spread and the drift paradox. *Theor. Pop. Biol.*, 67:61–73, 2005.

[39] L. Perko. *Differential Equations and Dynamical Systems*. Springer-Verlag, 2000.

[40] A.B. Potapov and M.A. Lewis. Climate and competition: The effect of moving range boundaries on habitat invasibility. *Bull. Math. Biol.*, 66(5):975–1008, 2004.

[41] M. Renardy and R.C. Rogers. *An Introduction to Partial Differential Equations*. Springer, New York, 1993.

[42] Y. Samia and F. Lutscher. Coexistence and spread of competitors in heterogeneous landscapes. *Bull. Math. Biol.*, 72:2089–2112, 2010.

[43] N. Shigesada, K. Kawasaki, and E. Teramoto. Traveling periodic waves in heterogeneous environments. *Theor. Popul. Biol.*, 30:143–160, 1986.

[44] N. Shigesada and A. Okubo. Analysis of the self-shading effect on algal vertical distribution in natural waters. *J. Math. Biol.*, 12:311–326, 1981.

[45] H.L. Smith. *Monotone Dynamical Systems*. American Mathematical Society, 1995.

[46] J. Smoller. *Shock Waves and Reaction–Diffusion Equations*. Springer, 1983.

[47] D.C. Speirs and W.S.C. Gurney. Population persistence in rivers and estuaries. *Ecology*, 82(5):1219–1237, 2001.

[48] J. A. Vano, J. C. Wildenberg, M. B. Anderson, J. K. Noel, and J. C. Sprott. Chaos in low-dimensional Lotka-Volterra models of competition. *Nonlinearity*, 19(10):1–28, 2006.

[49] V. Volterra. Variazionie fluttuazioni del numero d'individui in specie animali conviventi. *Mem. Acad. Lincei.*, 2:31–113, 1926.

[50] R.F Waters. The drift of stream insects. *Annu. Rev. Entomol.*, 17:253–272, 1972.